MRI ARTIFACTS AND REDUCTION TECHNIQUES

PAITOON MAPRAKOB

A THESIS SUBMITTED IN PARTIAL FULFILLMENT OF THE REQUIREMENTS FOR THE DEGREE OF MASTER OF SCIENCE (RADIOLOGICAL SCIENCE)
FACULTY OF GRADUATE STUDIES
MAHIDOL UNIVERSITY
2000

ISBN 974-664-426-7

Thesis
entited

MRI ARTIFACTS AND REDUCTION TECHNIQUES

.....
Mr. Paitoon Maprakob,
Candidate

.....
Asst. Prof. Pirash Saiviroonporn, Ph.D.
Major-advisor

.....
Assoc. Prof. Manus Mongkolsuk, M.Sc.
Co-advisor

.....
Prof. Liangchai Limlowongse, Ph.D.
Dean
Faculty of Graduate Studies

.....
Prof. Sutee Na Songkhla,M.D.
Chairman
Master of science Program in
Radiological Science
Faculty of Medicine, Siriraj Hospital

Thesis
entited

MRI ARTIFACTS AND REDUCTION TECHNIQUES

was submitted to Faculty of Graduate Studies, Mahidol University
for the degree of Master of Science (Radiological Science)

On
June 29, 2000

Mr. Paitoon Maprakob,
Candidate

Asst. Prof. Pirash Saiviroonporn, Ph.D.
Chairman

Assoc. Prof. Manus Mongkolsuk, M.Sc.
Member

Asst. Prof. Patana Puwanich, Ph.D.
Member

Prof. Liangchai Limlowongse, Ph.D.
Dean
Faculty of Graduate Studies

Prof. Chanika Tuchinda,
M.D., M.S., FAAP.
Dean
Faculty of Medicine, Siriraj Hospital

ACKNOWLEDGEMENTS

At this time, I would like to thank the following persons for their valuable guidance and support in the preparation. First, I would like to thank my adviser, Assistant Professor Dr.Pirash Saiviroonporn for knowledge required to completing such the thesis. I am sure that without his help I would not have been able to accomplish this task.

Next, I would like to express my sincere gratitude to my co-adviser, Associate.Professor.Manus Mongkolsuk, for his valuable guidance and encouragement which make my success become true. I am extremely thankful to Assistant Professor Dr. Patana Puwanich.for his being the member of my thesis candidate.

Special thanks are given to Assistant.Professor.Chirawat Utamakul for his assistance in proving English on some part, as well as Mr.Arjin Rittikumjorn and Mr.Pratuan Maprakob for their advice about the use of computer. Finally, I would like to thank my family for their continued support. I can not reach to this goal without them.

Paitoon Maprakob.

4037376 SIRS/M: MAJOR: RADIOLOGICAL SCIENCE; M.Sc. (RADIOLOGICAL SCIENCE)
KEYWORD : MRI ARTIFACTS, REDUCTION TECHNIQUES
PAITOON MAPRAKOB: MRI ARIFACTS AND REDUCTION TECHNIQUES. THESIS ADVISORS: PAIRASH SAIVIROONPORN, Ph.D., MANUS MONGKOLSUK, M.Sc. 250p.
ISBN 974-664-426-7

The image quality is very important for Magnetic Resonance Imaging (MRI). There are several factors that can degrade image quality. One of these factors is the artifacts. MRI artifacts are irregularly noted on MR image, rather than an anatomical or physiological abnormality. These artifacts may occur during each of scanning process, from data acquisition through image display. Various artifacts are associated with MR scanning. The objectives of this study are to extend present knowledge and to reveal the causes or sources of MRI artifacts as well as to select and use appropriate reduction techniques for some artifacts. The data sources of study are from literature reviews. The principals including basic physics such as spin physics, imaging principles, Fourier transform imaging, imaging pulse sequences techniques and imaging hardware and advance imaging techniques as well as practical considerations in MR imaging were reviewed to gain theoretical background. Then the selected relevant articles about any MRI artifacts and their reduction techniques were studied and analyzed.

The results of study are revealed that the MRI artifacts are caused mainly from 3 sources 1). the instrument 2). data acquisitions or imaging techniques and 3). the patient's physiologic motion. Reduction of these artifacts can be obtained by employing an appropriate hardware for instrument-related artifacts, suitable software for data acquisition-related artifacts and appropriate techniques for the reduction of motion artifacts.

However, at the present several artifacts remain unresolved and problematic. These results suggest further development of advanced reduction techniques that is necessarily for the better correction or elimination of these MRI artifacts.

403737 SIRS/M: สาขาวิชา: วิทยาศาสตร์รังสี: วทม (วิทยาศาสตร์รังสี)

ไพฑูล มาประกอบ : สิ่งแปลกปลอมที่เกิดขึ้นจากการสร้างภาพกำทอนแม่เหล็กและเทคนิคการทำให้สิ่งแปลกปลอมลดลง (MRI Artifacts and reduction techniques): คณะกรรมการควบคุมวิทยานิพนธ์ :ไพรัช สายวิรุณพร Ph.D , มนัส มงคลสุข M.Sc. 250 หน้า ISBN 974-664-426-7

คุณภาพภาพที่ได้จากการสร้างภาพกำทอนแม่เหล็กเป็นสิ่งสำคัญและมีปัจจัยที่เกี่ยวข้องหลายปัจจัย สิ่งแปลกปลอมที่เกิดขึ้นจากการสร้างภาพกำทอนแม่เหล็กเป็นปัจจัยหนึ่งที่ทำให้คุณภาพของภาพลดลง วิทยานิพนธ์นี้มีวัตถุประสงค์เพื่อศึกษาเพิ่มเติมและขยายความเข้าใจเกี่ยวกับสาเหตุกลไกและแหล่งกำเนิด รวมทั้งการเลือกใช้เทคนิคที่เหมาะสมในการทำให้สิ่งแปลกปลอมเหล่านี้ลดลงการศึกษาใช้วิธีค้นคว้าวรรณกรรมที่เกี่ยวข้องเริ่มต้นจากการทำความเข้าใจฟิสิกซ์พื้นฐานประกอบด้วยฟิสิกซ์เกี่ยวกับการสปิน หลักการสร้างภาพเบื้องต้น หลักการสร้างภาพจากการแปลงฟูเรียร์ เทคนิคการสร้างภาพและการลำดับพลัสส์เบื้องต้น ภาพรวมเกี่ยวกับฮาร์ดแวร์ เทคนิคการสร้างภาพที่ก้าวหน้าและข้อพิจารณาถึงปัจจัยที่มีผลต่อคุณภาพของภาพ อาทิเช่นความเปรียบต่าง (Contrast) อัตราส่วนระหว่างสัญญาณต่อสัญญาณรบกวน และความสามารถในการแยกแยะรายละเอียดภาพ เหตุจำเป็นที่ต้องกล่าวถึงความรู้พื้นฐานเหล่านี้เนื่องจากการศึกษาเกี่ยวกับ MRI ต้องใช้องค์ความรู้ทางด้านฟิสิกส์เป็นอย่างมาก

ผลการศึกษาสิ่งแปลกปลอมที่เกิดขึ้นแบ่งตามแหล่งกำเนิด 3 แหล่งใหญ่ด้วยกันคือ 1) เกิดจากเครื่องมือ 2) เกิดจากเทคนิคการสร้างภาพและการเก็บข้อมูลภาพ 3) เกิดจากการเคลื่อนไหวจากตัวผู้ป่วย สำหรับเทคนิคการทำให้ลดลงนั้นมีความเกี่ยวเนื่องกับสิ่งแปลกปลอมที่เกิดขึ้นคือพัฒนาฮาร์ดแวร์เพื่อลดสิ่งแปลกปลอมที่เกิดจากเครื่องมือพัฒนาซอฟแวร์เพื่อลดสิ่งแปลกปลอมที่เกิดจากหลักการสร้างภาพและการเก็บข้อมูลภาพ ส่วนสิ่งแปลกปลอมที่เกิดจากการเคลื่อนไหวจากตัวผู้ป่วยพัฒนาเทคนิคที่เหมาะสมในการติดตามเก็บข้อมูล (gating) ให้สอดคล้องกับการเคลื่อนไหวนั้นๆ

แต่อย่างไรก็ตามสิ่งแปลกปลอมบางตัวที่เกิดขึ้นสามารถกำจัดและสามารถทำให้ลดลงและมีบางตัวที่ยังเป็นปัญหาดังนั้นจึงต้องมีการพัฒนาปรับปรุงเทคนิคที่ก้าวหน้าเพื่อลดสิ่งแปลกปลอมที่มีผลต่อคุณภาพของภาพให้หมดไป

CONTENTS

CONTENTS (continue)

CONTENTS (continue)

CONTENTS (continue)

CONTENTS (continue)

CONTENTS (continue)

LIST OF TABLES

LIST OF FIGURES

LIST OF FIGURES (continue)

LIST OF FIGURES (continue)

LIST OF FIGURES (continue)

LIST OF FIGURES (continue)

LIST OF FIGURES (continue)

LIST OF FIGURES (continue)

LIST OF FIGURES (continue)

LIST OF FIGURES (continue)

LIST OF FIGURES (continue)

LIST OF ABBREVIATIONS

A	Anterior
A°	Angstrom (10^{-10} meters)
AP	Array Processor
B_o	Static magnetic field
B_1	The radio Frequency magnetic field
C	Contrast
CF	Center Frequency
ChemSat	Chemical shift Saturation
CSF	Cerebral Spinal Fluid
CSMEMP	Contiguous Slice Multi-Echo
CW	Continuous wave
E	Energy
ECG	Electrocardiogram
ED	Extended Dynamic Range
EG	ECG Gated
EG	Electrode Gated or Electrocardiac Gating
FC	Flow Compensation
FID	Free Induction Decay for GRE for SPGR for SSFP
FOV	Field of View
FT	Fourier transform
G_{BP}	Bipolar magnetic field gradient

LIST OF ABBREVIATIONS (continue)

G_f	Frequency encoding gradient
G_i	Field gradient in the i direction
G♦	Phase encoding gradient
$G♦_{max}$	Maximum value of phase encoding gradient.
G_s	Slice selection gradient
GRASS	Gradient Recalled Acquisition
GRE	Gradient Echo
GRE	Gradient Recalled Echo
GRE/(angle)	User-Selected Flip Angle
Gx	Logical Frequency Encoding
Gy	Logical Phase Encoding
Gz	Logical Slice Selection
h	Planck's constant
Hz	Hertz
I	Inferior
IFT	Inverse Fourier Transform
IM	Imaginary part of a complex number
IR	Inversion Recovery
J	Joule
K	Killo (10^3)
KHz	Kilohertz
L	left

LIST OF ABBREVIATIONS (continue)

m	milli (10^{-3})
mm	Millimeter
M_0	Equilibrium magnetization
M_x	X component of magnetization
$M_{x'}$	X' component of magnetization
M_y	Y component of magnetization
$M_{y'}$	Y' component of magnetization
M_z	Z component of magnetization
M_{xy}	Transverse component of magnetization
MR	Magnetic Resonance
MRA	Magnetic resonance angiography
MRI	Magnetic resonance imaging
MS	Multiple Sclerosis
Msec	Milliseconds
Multi	Multiple Slices or Acquisitions
Mxy	Transverse Magnetization
Mz	Magnetization
N^+	Spin population in low energy state
N^-	Spin population in high energy state
NEX	Number of Excitations
NF	No Frequency Wrap
NMR	Nuclear magnetic resonance

LIST OF ABBREVIATIONS (continue)

NP	No Phase Wrap
Np	Number of Phase Encodings
NPW	NO Phase Wrap
Ns	Number of Slice Encodings
NPW	No Phase Wrap
Ns	Number of Slice Encodings
P	Posterior
PG	Peripheral Gated
PG	Peripherally Gated
PM	Phase Offset Multi-Planar
POMP	Phase Offset Multi-planar
ppm	Parts per million
R	Right
RE	Real part of a complex number
RF	Radio frequency
R/L	Right/Left
RC	Respiratory Compensation
RF	Radio Frequency
ROI	Region of Interest
R-R	Interval Between Two QRS
RR	R-R Interval
S	Superior

LIST OF ABBREVIATIONS (continue)

Sec	Second
SAR	Specific Absorption Rate
SE	Spin Echo
Sinc	Sin(x)/x
SNR	Signal-to-Noise Ratio
SPF	Swap Phase and Frequency
SPGR	Spoiled Grass
SPGR/(flip angle)	User-Selected Flip Angle
SSFP	Steady State Free Precession
SSFP/(flip angle)	User-Selected Flip Angle
ST	Pre-Saturation
ST	Saturation Parameters (SAT)
ST/F	Fat Saturation or Suppression
ST/W	Water Saturation or Suppression
T	Temperature
T	Tesal
T_1	Spin-lattice relaxation time
T_2	Spin-spin relaxation time
T_2*	T Star
$T_{2inhomo}$	Inhomogeneous T_2
TE	Echo Time
Thk	Slice thickness

LIST OF ABBREVIATIONS (continue)

TG	Transmit Gain
TI	Inversion Time
TR	Repetition Time
Ts	Time Sequence
VB	Variable Bandwidth
VE	Variable Echo
VEMP	Variable Echo Multi-Planar
X	Axis in laboratory coordinate system
X'	Rotating frame X axis
Y	Axis in laboratory coordinate system
Y'	Rotating frame Y axis
Z	Axis in laboratory coordinate system

LIST OF ABBREVIATIONS (continue)

TG	Transmit Gain
TI	Inversion Time
TR	Repetition Time
Ts	Time Sequence
VB	Variable Bandwidth
VE	Variable Echo
VEMP	Variable Echo Multi-Planar
X	Axis in laboratory coordinate system
X'	Rotating frame X axis
Y	Axis in laboratory coordinate system
Y'	Rotating frame Y axis
Z	Axis in laboratory coordinate system

Chapter I

Introduction

Magnetic Resonance Imaging (MRI) is currently a conventional medical diagnostic tool, used for acquiring cross-sectional image of patient's anatomy. MRI represents a continuing revolution in medical technology and provides detailed images of the human body with unprecedented soft tissue contrast (1). Therefore, the requirements of the image quality including spatial resolution, contrast, signal to noise ratio and reducing artifacts are the most importance (2).

The image quality can be divided into 2 major controlling factors. The first factor is subsystem design and maintenance such as engineering and manufacturing quality and the second one is operator controlled variable such as contrast, signal to noise ratio, spatial resolution, artifacts reduction and scan time. Many previously mentioned factors influent to the image quality. Any MRI artifacts are ones of these factors. The image quality may degrade by artifacts(3).

MRI artifacts are irregular noted on MR image, rather than an anatomical or physiological abnormality (4). These artifacts may occur during each of scanning process, from data acquisition through image display (5). A various artifacts are associated with MR scanning (5) and multiple causes (6).

There are various causes, influenced artifacts during MR scanning process (7). Physics, clinic and techniques are among artifacts causes (8). Physical artifacts are generated by inherent physics of MR scanning process, such as chemical shift artifact

(8), T2* effect artifact (9, 10, 11, 12). Patient's body generates clinical artifact or pathology, such as motion artifacts (13, 14, 15, 16, 17), flow artifacts (18, 19, 20). Technical artifacts are generated by malfunction of the system-included hardware or software, such as main magnetic instability artifacts (21), truncation of artifact (22), zipper artifacts (23) and zero-fill artifact (24).

These artifacts mentioned above are multiple visual appearances (2, 25, and 26). On the top of that some artifacts could simulate pathologic condition (27). Then, it is imperative for MRI technologists to understand the principles behind the various types of artifacts and find the possible ways to reduce their effect (28).

We recognize artifacts in such a way that hidden artifacts lead to diagnostic error, which suggest wrong pathologic condition. In addition, recognizing that certain artifacts can indicate particular problems, in order to proper service or repair can be started before major problem occur (7).

The recognition of artifact lead to the image quality improvements depending on MRI technologist's role. Since, the MRI technologists is expected to operate independently and making decision based on clinical condition, symptom and more important what is visualized on the monitor should be notified (28). MRI technologists should learn basic properties and applications of MRI techniques available from existing resources.

The content is varying from basic to advance and also varying in the branching subjects among many textbook (28, 29, 30, 2, 6,). The development of its leading edge MRI techniques or pulse sequences which subsequently resulting into fast imaging technique such as echo-planar imaging (EPI) (1) may lead to new artifacts opportunity (31) such as N/2 ghosts (1).

To avoid difficulty, acknowledge should be put altogether, especial the balance between basic properties and applications of MRI techniques (25). Consequently, new artifacts collection and classification would settle MRI artifact knowledge to the future.

Objectives of this thesis

The objectives of this thesis are

1) To extend the understanding and be available the causes or sources of MRI artifacts
2) To select and use the appropriate reduction techniques for some of artifacts

Literatures review

The complexity of MRI has unfortunately brought with it a plethora of new imaging artifacts. Luckily, many can be interpreted easily and do not interfere with diagnosis. However, the addition of each new imaging technique or RF pulse sequence brings the possibility of new artifacts. An understanding of the mechanisms those causes the artifacts can lead to methods for reduce them.

A general pattern to present MRI artifacts (6): the visual characteristics of an artifact are described, then the cause or origin of the artifact is demonstrated, and finally methods that can be used to reduce or prevent such artifacts in the imaging process are discussed.

The visual characteristics concentrate on visual appearance. Artifacts are identified using appearance on image display and explained by visual notification. The artifacts would be; ghosts (blurring and unsharpened), wraparound (aliasing), ripples, straight line, false contour, shading, geometric distortions.

We, however, concentrate on hardware or software and techniques that affect causes or origins of artifacts. We should understand how artifacts are produced. The following artifacts are examples listed by its causes: main magnetic field inhomogeneity artifacts, susceptibility artifacts, data acquisition and gradient artifacts, motion artifacts, flow artifacts, pulse sequences relating artifacts. As we could see that, this process emphasizes mainly in sequence.

Artifacts can be reduced when we know the causes and mechanisms behind the various types. Then, various methods, that can be used to reduce or prevent such artifacts in the imaging process, will be presented. For example, there are many methods to reduce or prevent motion artifact, such as gating, phase-reordering method, varying TR and NEX, signal averaging, reducing the signal intensity of the moving tissue that is the source of ghost artifact, gradient reorientation, motion compensation using gradient rephasing, presaturation, short-TE, fast sequences, post processing advances and etc.

To identify which method should be carried out is depending on which groups to be attended. Three methods are presented in the content of MRI artifacts; 1) causes or origin, 2) visual appearances, 3) both causes and visual appearances.

First method, Woodward and Friemarch (28) explained artifacts by causes and origin. They divide artifacts causes into 3 categories: 1) hardware or mechanics, 2) physiology, 3) inherent physics. However, Markize and Aquillia (7) split physiology

category into 2 subcategories: 1) physiology, 2) artifacts resulting from the patient. Patient's body alone explains the latter, not including physiology. Stark and Bradley (6) have categorized artifacts by causes as hardware, RF pulse, static and gradient field, and motion artifact, sequence and reconstruction techniques. Edelman and colleagues (1) divide artifacts in to 6 categories resembling to Stark and Bradley but different from in the content detail. Most of researches are concentrated on the cause or origin and mechanism (32). It is appropriate for MRI technologists to study artifacts. Since all MRI technologists should review all possible causes behind them.

Second method, medical personals such as radiologists prefer to visual appearance. As Lufkin (26) explain artifacts by visual appearances. He divides in to 5 categories: edge artifact, chemical shift misregistration error, truncation artifact, and magnetic field distortion, aliasing artifact. Young (33) explain artifacts by visual appearance. He divides in to 6 categories; motion artifact, alising or wraparound artifact, metallic artifacts, chemical shift artifact, radiofrequency field artifacts and other MRI artifacts. Stark and Bradley (2) have categorized by visual appearance as aliasing (wraparound, edge rinning), truncation, black boundaries, central artifact, error in the data, magnetic field perturbation, chemical shift misregistration and ghosts artifact.

They prefer calling the names of artifacts to the sources or origin and mechanism. Furthermore, artifact's names are subjected to visual appearance. Reiderer and colleagues (25) have categorized by visual appearance as ghosts, wraparound, ripples, straight lines, false contours, shading and geometric distortion.

Since, the first two methods contain either benefit or shortcoming; the third method is employed, taking advantage of the first two methods. As Bellon and

colleagues (5) have categorized artifacts by cause as sequence, reconstruction algorithm, patient and system related. In their thorough and comprehensive review article, Henkelman and Bronskill (34) classified artifact based on both their appearance and causes. This work is intended to serve as a complete set of MRI artifacts' studies provide explanations geared to MRI technologist involved in MR scanning process.

As we discuss earlier, artifacts studying methods are arbitrary and incomplete. Since, these are fast progress in this area. New techniques or pulse sequences development are also emerging all the ways, which may generate new form of artifacts.

The work in this study, we consolidate the knowledge about artifacts, especially the balance between basic properties and applications of MRI techniques. We then investigate both causes and visual appearances method based on the work by Edelman and colleagues (1). In such a way that their study use more detail artifact's categories. In addition, they also add fast imaging and magnetic resonance angiography technique to existing with of artifacts. These two techniques are consistent with to state-of-the-art MRI technology.

This thesis is organized into 11 chapters as follows:

Chapter 2 Introduction of MRI

Chapter 3 reviews the theoretical background of basics MRI about spin physic.

Chapter 4 reviews the theoretical background of basics MRI about imaging principles.

Chapter 5 reviews the theoretical background of basics MRI about Fourier transform imaging principles.

Chapter 6 reviews the theoretical background of basics MRI about basic imaging techniques.

Chapter 7 reviews about imaging hardware.

Chapter 8 reviews about advanced imaging techniques.

Chapter 9 Practical considerations for acquiring or interpreting MR images, including image contrast, signal-to-noise ratio, spatial resolution

Chapter 10 describes the cause and mechanism of artifacts and artifact and reduction techniques. In this chapter, we can divide into 7 categories. Each category including define artifact's names, describe artifact's causes and mechanism, suggestion reduction techniques and solution, comment and awareness, selected artifacts image example.

Chapter 11 includes the conclusions and recommendation for future research.

CHAPTER II

MRI INTRODUCTION

2.1 Alternative names and Definition

Alternative names

Magnetic Resonance Imaging or Nuclear Magnetic Resonance (NMR)(4).

Definition (4)

A non-invasive procedures that use magnets and radio waves to produce a picture of inside of the body area under investigation.

The MR images are obtained by placing the patient or area of interest within a powerful, highly uniform, static magnetic field. Magnetized protons (hydrogen nuclei) (2) within the patient align like small magnets in this field. Radio-frequency pulses are then utilized to create an oscillating magnetic field perpendicular to the main field, from which the nuclei absorb energy and move out of alignment with the static field, in a state of excitation. As the nuclei return from excitation to the equilibrium state, a signal induced in the receiver coil of the instrument by the nuclear magnetization can then be transformed by a series of algorithms into diagnostic images. Images based on different tissue characteristics can be obtained by varying the number and sequence of pulsed radio-frequency fields in order to take advantage of magnetic relaxation properties of the tissues. Magnetic resonance images differ from those produced by x-rays: the latter are associated with absorption of x-ray energy, while MR images are based on proton density and proton relaxation dynamics. These vary according to the

tissue under examination and reflect its physical and chemical properties. This thesis presents some comprehensive theory of the basic principles of MRI.

The purpose of chapter 2-9 is to explore basic phenomenon associated with physical principles of nuclear magnetic resonance and to relate these to the MRI artifacts and MRI artifact reduction techniques. Due to the understanding the causes, mechanism and how to resolved these artifacts you must understand to the basic principles of MRI.

2.2 Nucleus Property Responsible for MRI (2,6)

Nuclei possess two type of particle; neutron, which are electrically neutral, and protons, which are electrically positive, Electron, on the other hand, are electrically negative. In the nucleus, both types of particles, positively charged protons and neutrons, are called nucleons (figure 2-1). The nucleus of an atom must contain an uneven number of protons in order to be affected by a magnetic field. The simplest atom to contain an odd number of protons is the hydrogen which contains just one proton. Presently, all clinical applications of MRI utilize the hydrogen nucleus. Within each cell there are water molecules. Here are some of the water molecules. Each water molecule has one oxygen and two hydrogen atoms. If we zoom into one of the hydrogens past the electron cloud we see a nucleus comprised of a single proton. The proton possesses a property called spin which:

1.can be thought of as a small magnetic field (figure 2-2), and

2.will cause the nucleus to produce an NMR signal.

Not all nuclei possess the property called spin. A list of these nuclei will be presented in next chapter on spin physics.

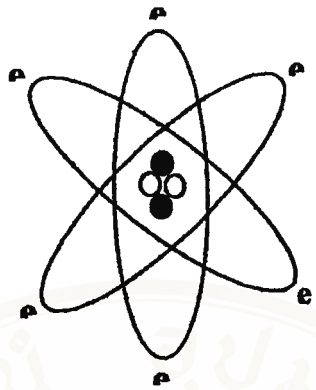

Figure 2-1 The atomic structure.

Figure 2-2 A spinning charged hydrogen nucleus (i.e, proton) generating a magnetic field. For this reason, these particles have like tiny bar magnets and have north and south poles.

CHAPTER III

SPIN PHYSICS

3.1 Spin (1,2,6)

A basic characteristic of protons is that of spin. In addition to a proton, a hydrogen nucleus contains a positive charge. From physics we know that a spinning charge creates a magnetic field. Located in a random direction, each proton's magnetic field will cancel the other out. However, when a patient is placed in a magnetic field, the proton becomes orientated either parallel or anti-parallel to the magnetic field (figure3-1). Parallel creates a low energy state and anti-parallel creates a high-energy state (figure 3-2). More protons will be aligned in the low energy than in the high-energy state. Because of this, there will be a net magnetic moment when all charges are in a single direction in the low energy or parallel direction of the magnetic field.

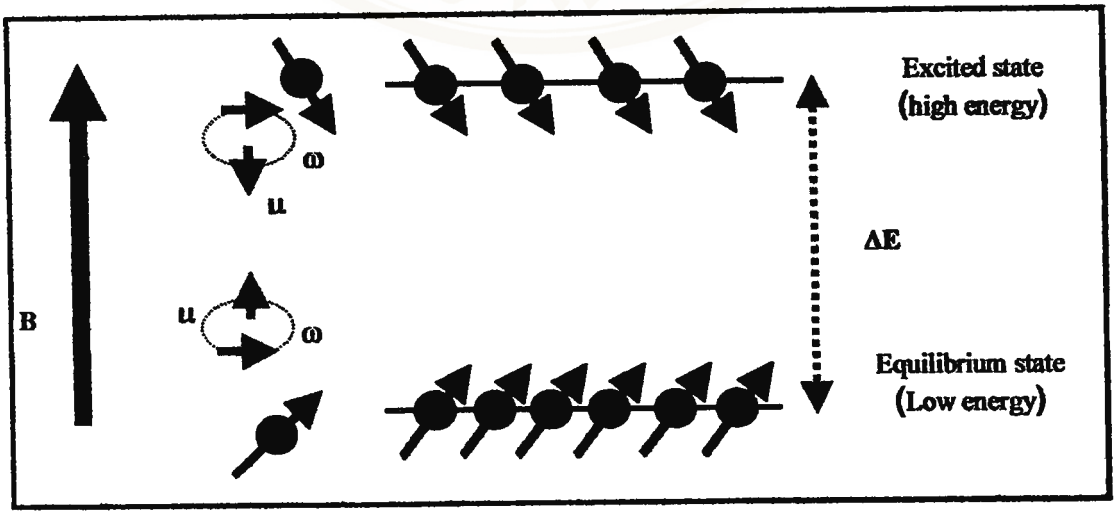

Figure 3-1 The population of proton when it aligned in the external magnetic field, Bo.(see detail in text)

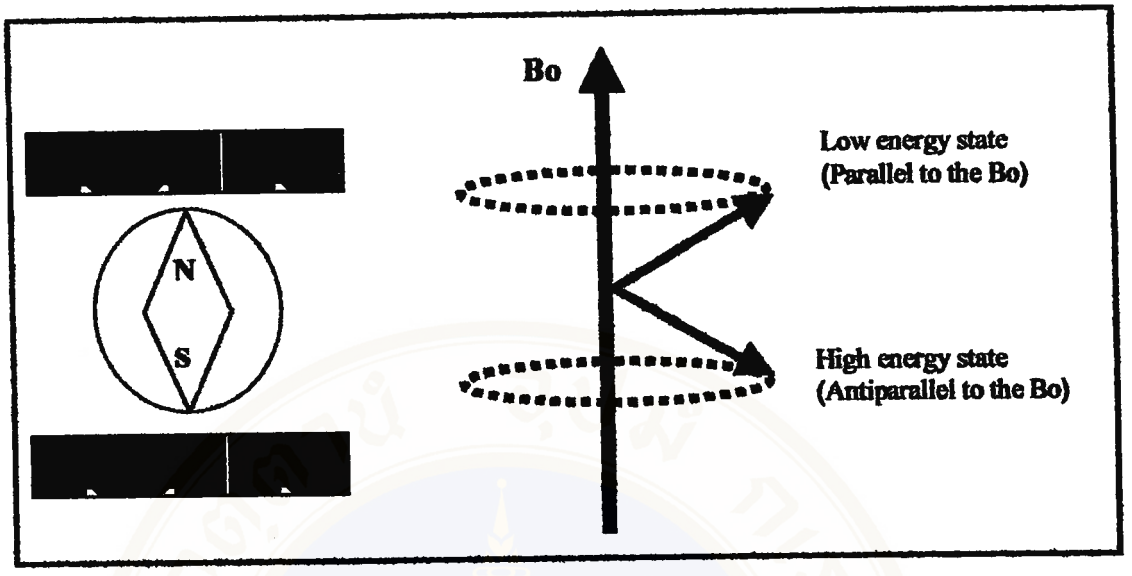

Figure 3-2 The diagram of one proton when it is aligned in the external magnetic field, Bo.

3.2 Properties of Spin (1,2,6)

When placed in a external magnetic field of strength B_0, a particle with a net spin may absorb a photon, the frequency,ω, of which depends on its gyromagnetic ratio,γ. The relationship between B_0, ω and γ is represented by this equation.

$$\omega = \gamma B_0 \qquad \text{(E.q. 3-1)}$$

In equation 3-1, the ω is the larmor frequency, γ is the gyromagnetic constant, B_o is the external magnetic field in unit Tesla. For hydrogen $\gamma = 42.58$ MHz / T.

3.3 Nuclei with Spin (1,2,6)

Just about every element in the periodic table can have an isotope with a net nuclear spin. NMR can only be performed on isotopes whose natural abundance is high enough to be detected. Some of these nuclei which are of interest in MRI are listed in the table below.

Nuclei	Unpaired protons	Unpaired neutrons	Net spin	γ(MHz/T)
^{1}H	1	0	1/2	42.58
^{2}H	1	1	1	6.54
^{31}P	0	1	1/2	17.25
^{23}Na	0	1	3/2	11.27
^{14}N	1	1	1	3.08
^{13}C	0	1	1/2	10.71
^{19}F	0	1	1/2	40.08

Table3-1 Type of nuclei which these nuclei are of interested in MRI.

3.4 Energy Levels (1,2,6)

To understand how particles with spin behave in a magnetic field, consider a proton. This proton has the property called spin. Think of this property as a magnetic moment, causing the proton to behave like a tiny magnet with a north and south pole. When the proton is placed in an external magnetic field, the particle aligns itself with the external field, just like a magnet would. There is a low energy configuration or state where the poles are aligned S to N and a high-energy state N to S (figure 3-2).

3.5 Transitions (1,2,6)

This particle can undergo a transition between the two energy states by the absorption of a photon. A particle in the lower energy state absorbs a photon and ends

up in the upper energy state. The energy of this photon must exactly match the energy difference between the two states (figure 3-3). The energy, E, of a photon is related to its frequency, ω, by Plank's constant ($h = 6.626 \times 10^{-34}$ J s).

$$E = h\omega \qquad \text{(E.q.3-2)}$$

In equation 3-2 E is the difference between protons in lower energy state and protons in high-energy state (figure3-3). In NMR and MRI, the quantity ω is called the resonance frequency and the Larmor frequency.

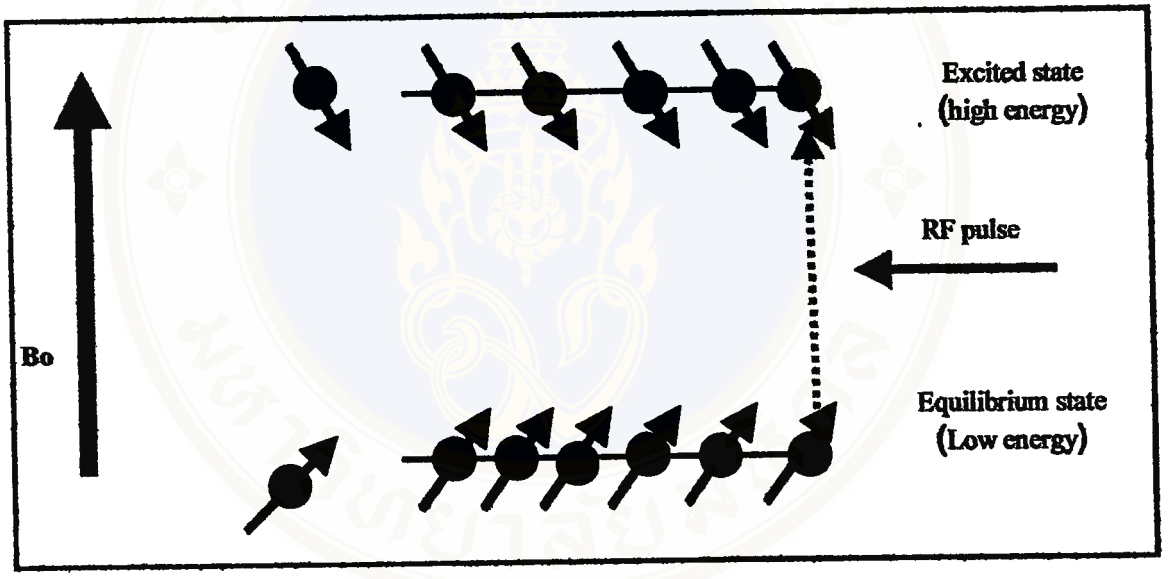

Figure3-3 The energy different between high and low energy state when the group of proton located in the Bo when we sent the RF pulse with the energy match to the energy different it make resonance.

3.6 Energy Level Diagrams (2,6)

The energy of the two spin states can be represented by an energy level diagram We saw that $\omega = \gamma B_0$ and $E = h\omega$, therefore the energy of the photon needed to cause a transition between the two spin states is

$$E = h\,\omega$$

When the energy of the photon matches the energy difference between the two spin states an absorption of energy occurs. In the NMR experiment, the frequency of the photon is in the radio frequency (RF) range. In NMR spectroscopy, ω is between 60 and 800 MHz for hydrogen nuclei. In clinical MRI, ω is typically between 15 and 80 MHz for hydrogen imaging.

3.7 CW NMR Experiment (2,6)

The simplest NMR experiment is the continuous wave (CW) experiment. There are two ways of performing this experiment. In the first, a constant frequency, which is continuously on, probes the energy levels while the magnetic field is varied (in the figure 3-4 is represented by ΔE_1, ΔE_2, ΔE_3). The energy of this frequency is represented by the dot line in the energy level diagram (figure3-4). The CW experiment can also be performed with a constant magnetic field and a frequency which is varied (figure 3-5 is represented by dot line). The magnitude of the constant magnetic field is represented by the position of the vertical dot line in the energy level diagram (figure 3-5).

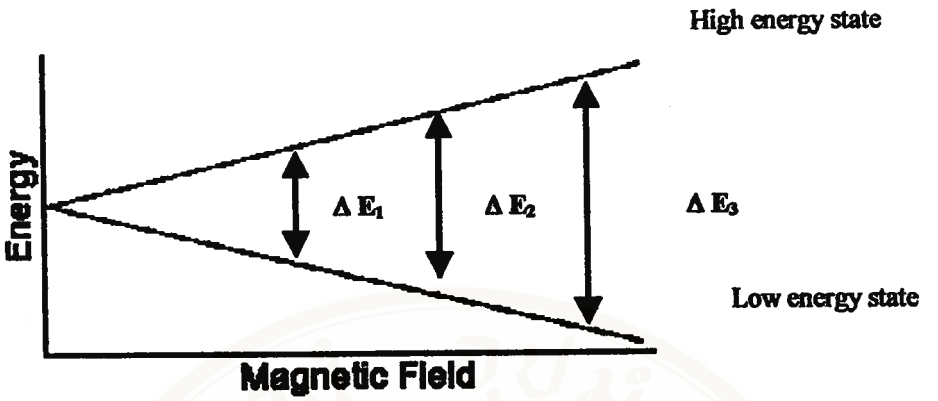

Figure3-4 The energy different between high and low energy state when the varying

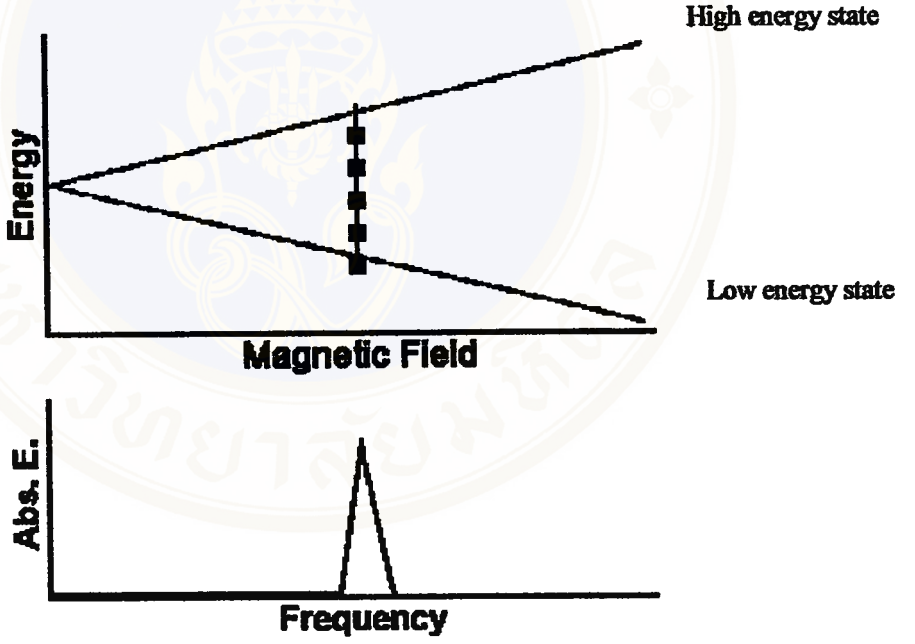

Figure3-5 The magnitude of constant magnetic field by position of dot line in the energy level diagram.

3.8 Boltzmann Statistics (1,2,6,38)

When a group of spins are placed in a magnetic field they align in one of the two possible orientations. At room temperature the number of spins in the lower energy level N^+ slightly outnumber the number in the upper level N^-. Boltzmann statistics tells us that

$$N^-/N^+ = e^{-E/kT} \qquad \text{(E.q.3-3)}$$

In Eq. 3-3. E is the energy difference between the spin states, k is Boltzmann's constant 1.3805×10^{-23} J/Kelvin, and T is the temperature in Kelvin. As the temperature decreases so does the ratio N- /N+. As the temperature increases the ratio approaches one. The signal in NMR spectroscopy is proportional to the population difference between the states. NMR is a rather sensitive spectroscopy since it is capable of detecting these very small population differences. It is the resonance, or exchange of energy at a specific frequency between the spins and the spectrometer, which gives NMR its sensitivity.

3.9 Spin Packets (1,2,6,38)

It is clumsy to describe NMR on a microscopic scale. A macroscopic picture is more convenient. The first step in developing the macroscopic picture is to define the spin packet. A spin packet is a group of spins experiencing the same magnetic field strength. In this example, the spins within each grid section represent a spin packet (figure3-6). At any instant in time the magnetic field due to the spins in each spin packet can be represented by a magnetization vector (figure3-7). The size of each vector is proportional to $(N^+ - N^-)$. The sum of all the magnetization vectors from all spin packets is the net magnetization. In order to describe pulsed NMR is necessary

from here on to talk in terms of the net magnetization (figure3-8). Adapting the conventional NMR coordinate system, the external magnetic field is along the Z axis, and the net magnetization vector are along the Z axis (figure3-9).

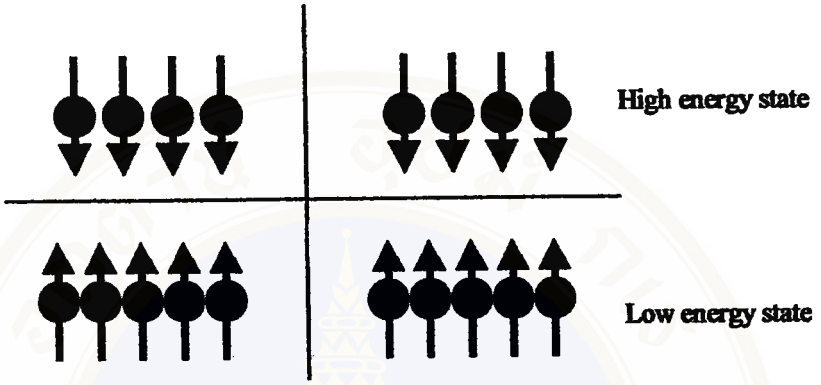

Figure3-6 The group of spin experiencing the same magnetic field strength.

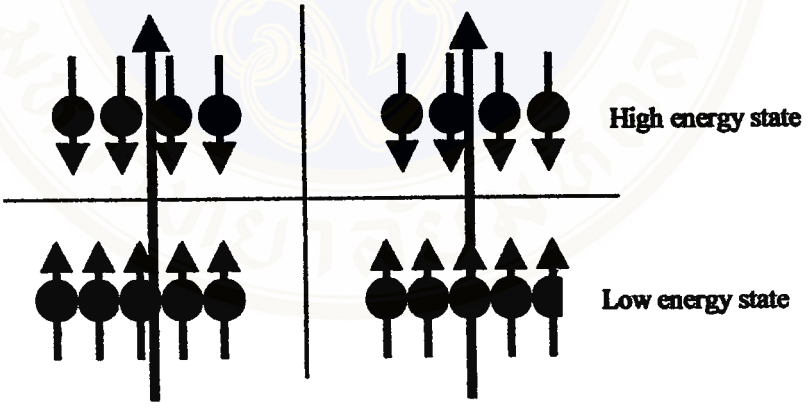

Figure3-7 The net magnetization which it occurred from each spin packet.

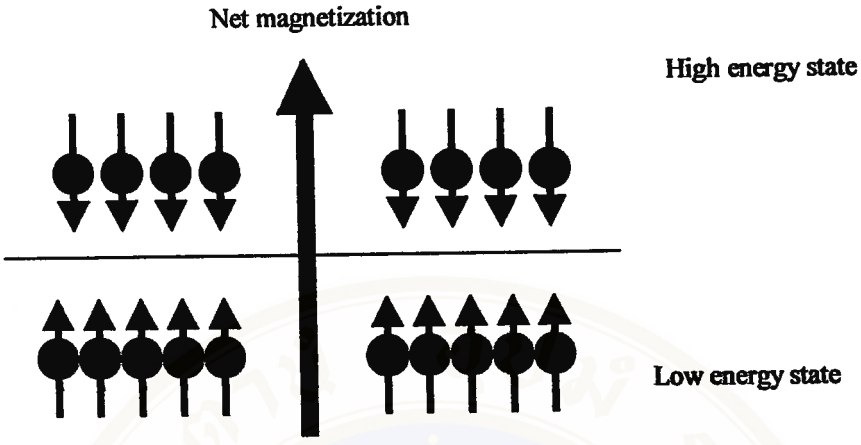

Figure3-8. The net magnetization which it is occurred form every each spin packets.

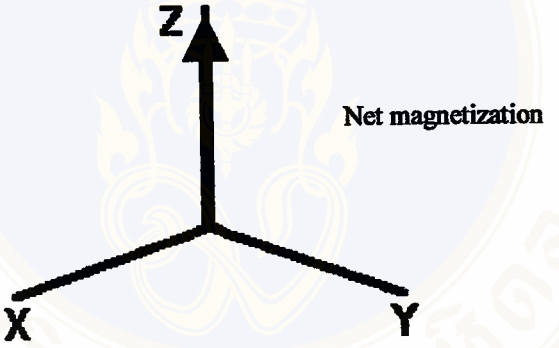

Figur3-9 The net magnetization is aligned in the rotating reference frame.

3.10 T1 Processes (1,2,6,38)

At equilibrium, the position of the net magnetization vector lies along the direction of the applied magnetic field Bo and is called the equilibrium magnetization M_o. In this configuration the Z component of magnetization M_Z equals M_o. M_Z is referred to as the longitudinal magnetization. There is no transverse (M_X or M_Y) magnetization in the xy plane (figure3-10). It is possible to change the net

magnetization by exposing the nuclear spin system to energy of a frequency equal to the energy difference between the spin states. If enough energy is put into the system, it is possible to saturate the spin system and make M_Z=0(figure3-11). The time constant which describes how M_Z returns to its equilibrium value is called the spin lattice relaxation time (T_1). The equation governing this behavior as a function of the time t after its displacement is (figure3-12):

$$M_z = M_o (1 - e^{-t/T_1}) \qquad \text{(E.q3-4)}$$

In Eq 3-4. Mz is the longitudinal magnetization, Mo is the magnetization which it is in the equilibrium state, t is the time after magnetization displacement

T_1 is therefore defined as the time required to change the Z component of magnetization by a factor of e (figure3-13). If the net magnetization is displaced to along the -Z axis it will gradually return to its equilibrium position along the +Z axis at a rate governed by T1 (figure3-14). The equation governing this behavior as a function of the time t after its displacement is (figure3-15):

$$M_z = M_o (1 - 2e^{-t/T_1}) \qquad \text{(E.q.3-5)}$$

The spin-lattice relaxation time (T1) is the time to reduce the difference between the longitudinal magnetization (M_Z) and its equilibrium value by a factor of e.

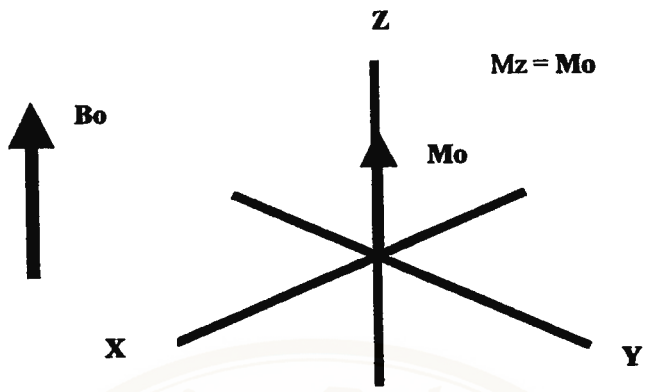

Figure 3-10 The long magnetization, M_Z equal to equilibrium magnetization ,Mo (Mz=Mo)

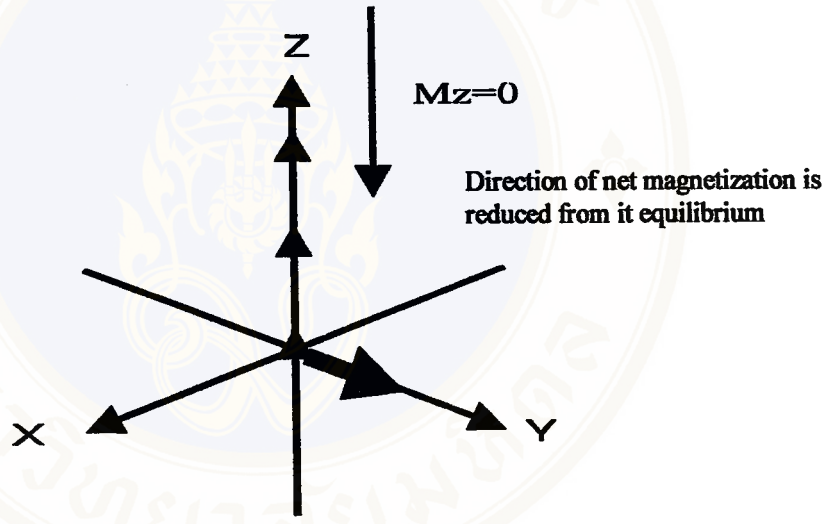

Figure3-11 The long magnetization, Mz equal to equilibrium magnetization,Mo when it exposed by RF energy

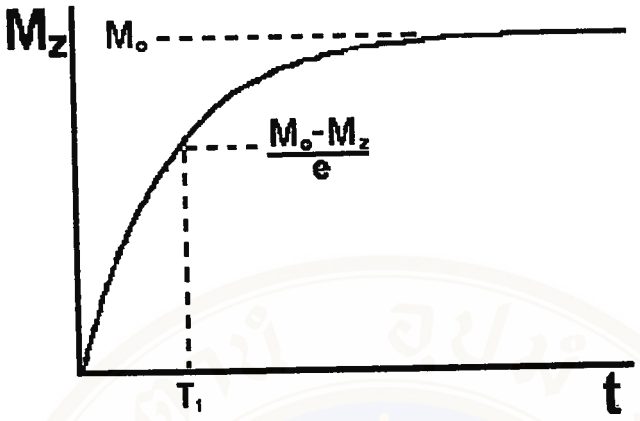

Figure3-12 The longitudinal magnetization regrowth to equilibrium state by a factor e.

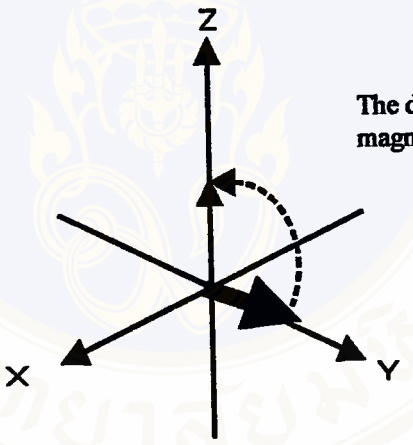

The displacement the long magnetization from transverse axis

Figure3-13 The long magnetization regrowth from the transverse plane in to equilibrium state

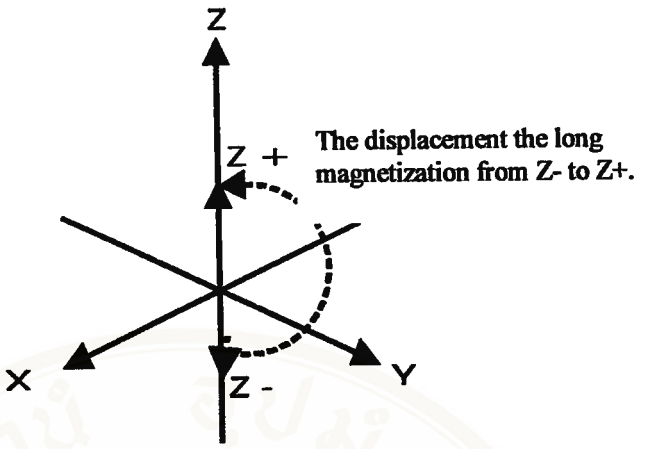

Figure3-14 The displacement the long magnetization from Z- to Z+, the duration time between Z- to Z+ is called inversion recovery time.

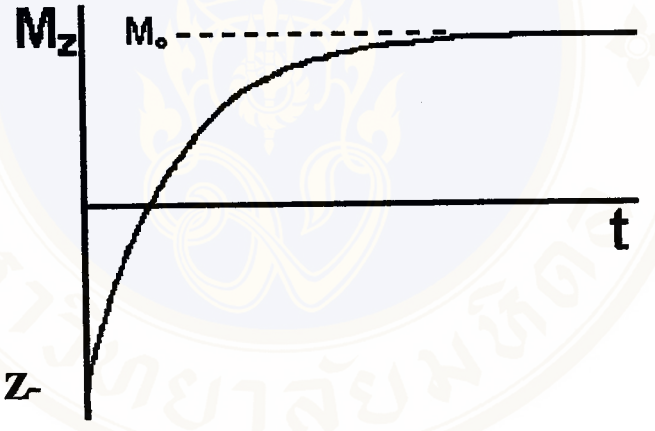

Figure3-15 The regrowth of the long magnetization from Z- to Z+ to equilibrium state by a factor e.

3.11 Precession (1,2,6,38)

If the net magnetization is displaced to a position in the XY plane (figure3-16). It will rotate about the Z axis at a frequency equal to the frequency of the photon which would cause a transition between the two energy levels of the spin. This frequency is called the Larmor frequency (figure3-17).

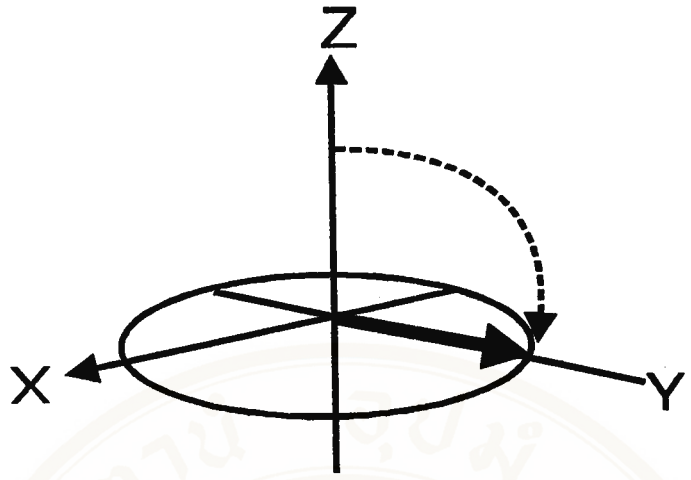

Figure3-16 The long magnetization is fliped into the transverse plane (XY plane)

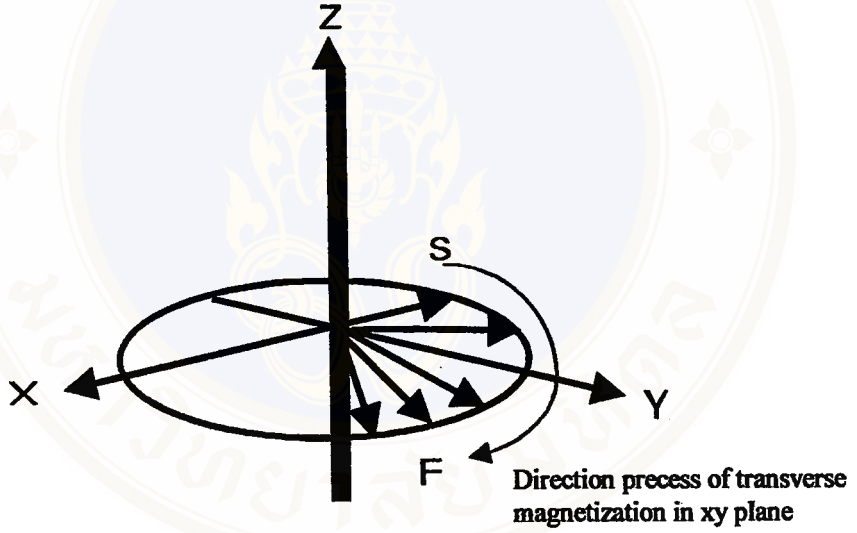

Figure3.17 The transverse magnetization in the transverse plane precession at Larmor frequency but it is not the same rate and its own larmor frquency.

3.12 T2 Processes (1,2,6,38)

In addition to the rotation this vector starts to dephase because each of the spin packets is experiencing a slightly different magnetic field and rotates at its own Larmor frequency. The longer the elapsed time, the greater the phase difference. Here the net magnetization vector is initially along +Y. For this and all dephasing examples

think of this vector as the overlap of several thinner vectors from the individual spin packets. The time constant which describes the behavior of the transverse magnetization, M_{XY}, is called the spin-spin relaxation time, T_2 (figure3-18).

$$M_{XY} = Moe^{-t/T2} \qquad \text{(E.q3.6)}$$

In Eq 3.6. M_{xy} is the transverse magnetization, T_2 is the spin-spin relaxation time or transverse relaxation time.

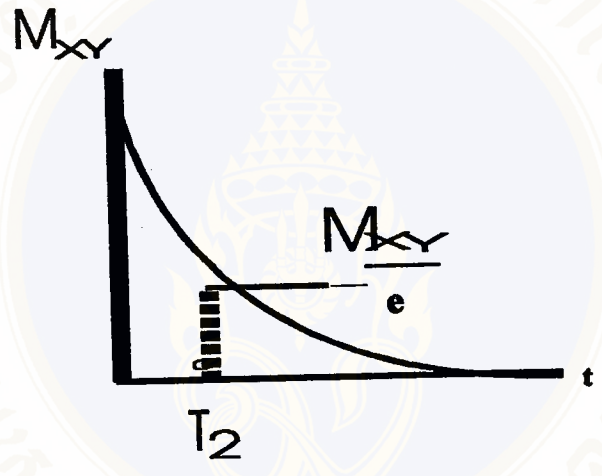

Figure3-18 The transverse magnetization which it is demonstrate the decay by a factor e.

T2 is always less than T1. The net magnetization in the plane goes to zero and then the longitudinal magnetization grows in until we have M_o along Z (figure3-19). Any transverse magnetization behaves the same way (figure3-20). The transverse component rotates about the direction of applied magnetization and dephases. T1 governs the rate of recovery of the longitudinal magnetization. In summary, the spin-spin relaxation time, T2, is the time to reduce the transverse magnetization by a factor of e. In the previous sequence, T_2 and T_1 processes are shown separately for clarity. That is the magnetization vectors fill the XY plane completely before growing back

up along the Z axis. Actually, both processes occur simultaneously with the only restriction that T2 is less than or equal to T1.

Two factors contribute to the decay of transverse magnetization.

1) Pure T2 due to molecular interactions.

2) Inhomogeneous T2 from variations in Bo.

The combination of these two factors is what actually results in the decay of transverse magnetization. The combined time constant is called T2 star and is given the symbol T2*. The relationship between the T2 from molecular processes and that from inhomogeneities in the magnetic field is as follows.

$$1/T_{2^*} = 1/T_2 + 1/T_{2inhomo} \qquad \text{(E.q.3.7)}$$

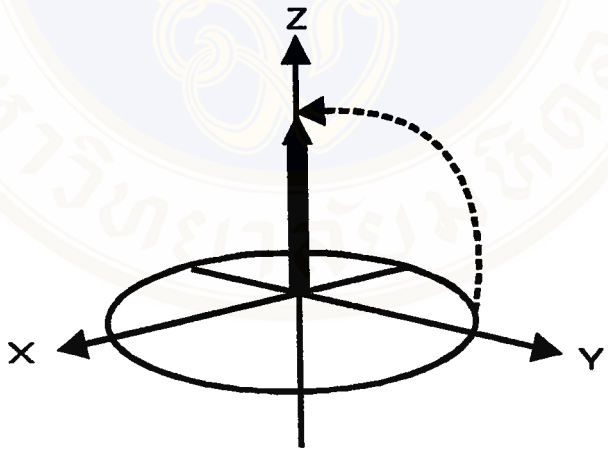

Figure3-19 The direction the long magnetization from the transverse plane.

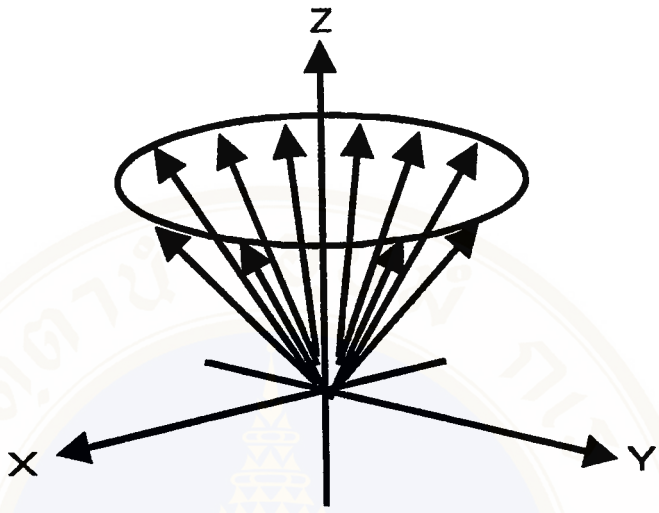

Figure3-20 The long magnetization behave precession at the same way.

3.13 Rotating Frame of Reference (1,2,6,38)

We have just seen the behavior of spins in the laboratory frame of reference. It is convenient to define a rotating frame of reference which rotates about the Z axis at the Larmor frequency. We distinguish this coordinate system from the laboratory system by primes on the X and Y axes, X'Y'(figure3-21).

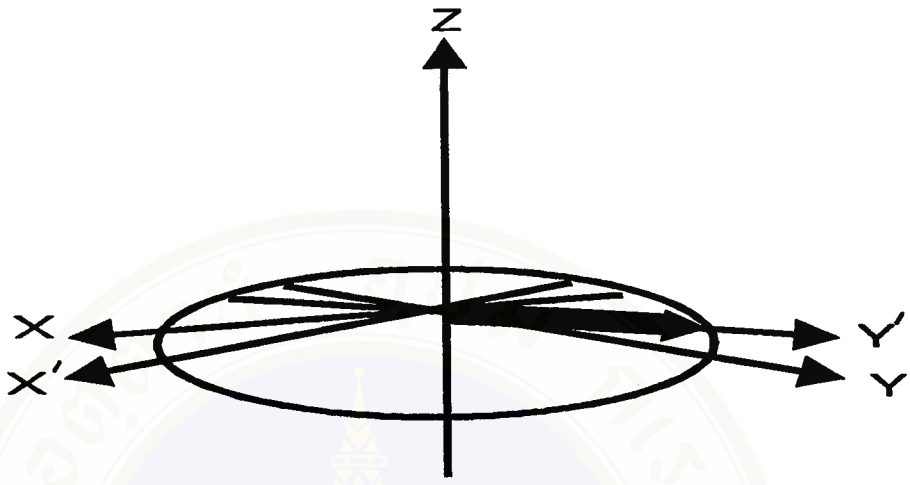

Figure3-21 The transverse magnetization in the laboratory frame on the X,Y and X', Y'

A magnetization vector with Larmor frequency in a frame of reference rotating about the Z axis at frequency will appear to be stationary. In the rotating frame, relaxation of M_Z magnetization to its equilibrium value looks the same as it did in the laboratory frame (figure3-22). A transverse magnetization vector rotating about the Z axis at the same velocity as the rotating frame will appear stationary in the rotating frame (figure3-23). A magnetization vector traveling faster than the rotating frames will rotate clockwise about the Z axis (figure3-24). A magnetization vector traveling slower than the rotating frame will rotate counter clockwise about the Z axis. (figure3-25). In a sample there are spin packets traveling faster and slower than the rotating frame. As a consequence, when the mean frequency of the sample is equal to the rotating frame, the dephasing of $M_{XY'}$ looks like on the figure3-26.

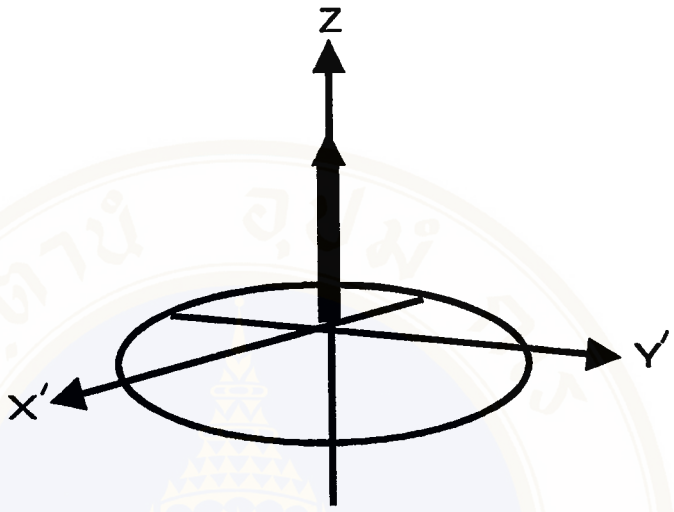

Figure3-22 The magnetization vector with Larmor frequency in a frame of reference rotating about the Z axis at frequency will appear to be stationary.

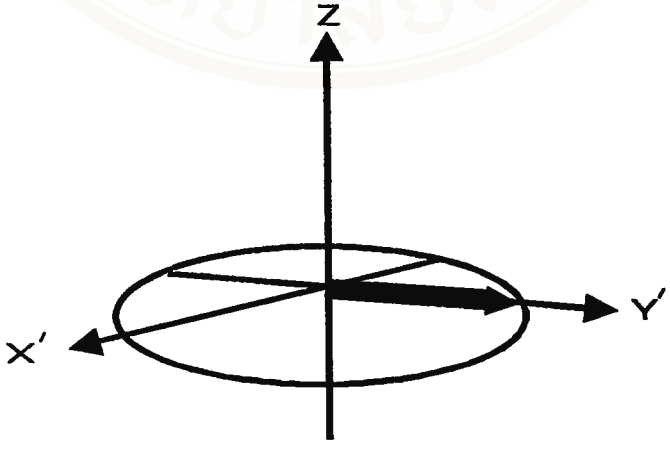

Figure3-23 The transverse magnetization vector rotating about the Z axis at the same velocity as the rotating frame will appear stationary in the rotating frame.

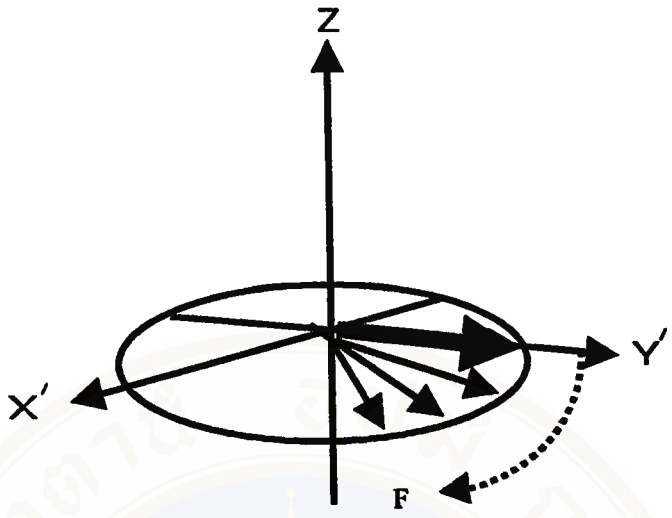

Figure3-24 The magnetization vector traveling faster than the rotating frames will rotate clockwise about the Z axis.

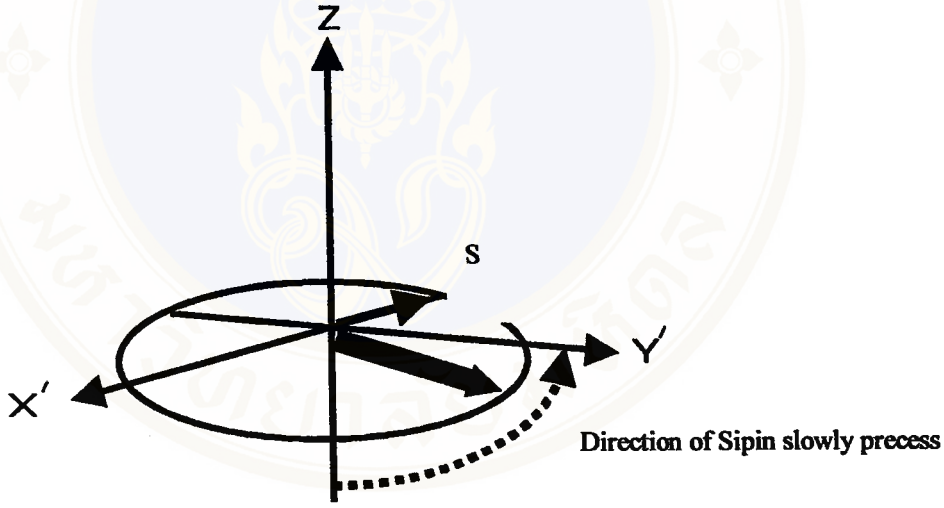

Figure3-25 represented the magnetization vector traveling slower than the rotating frame will rotate counter clockwise about the Z axis.

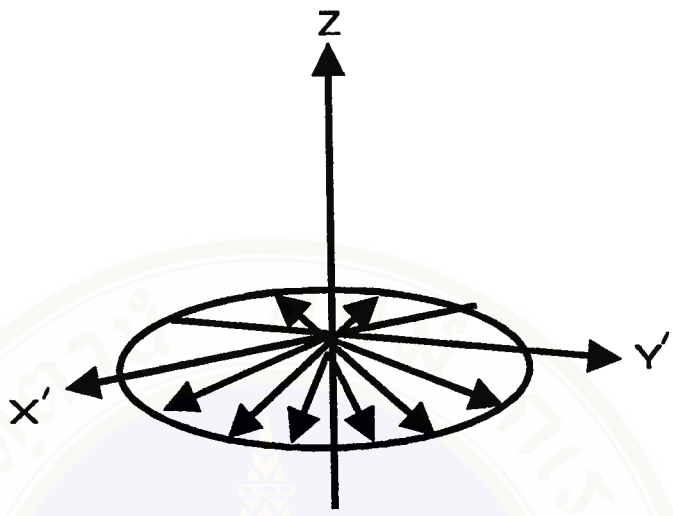

Figure3-26 There are spin packets traveling faster and slower than the rotating frame.As a consequence, when the mean frequency of the sample is equal to the rotating frame, the dephasing of $M_{X'Y'}$.

3.14 Pulsed Magnetic Fields (1,2,6,38)

A coil of wire placed around the X axis will provide a magnetic field along the X axis when a direct current is passed through the coil (figure3-27). An alternating current will produce a magnetic alternating in direction X' (figure3-28). In a frame of reference rotating about the Z axis at a frequency equal to that of the alternating current, the magnetic field along the X' axis will be constant, just as in the direct current case in the laboratory frame (figure3-29). This is the same as moving the coil about the rotating frame coordinate system at the Larmor frequency. In magnetic resonance, the magnetic field created by the coil passing an alternating current at the Larmor frequency is called the B_1 magnetic field. When the alternating current

through the coil is turned on and off, it creates a B_1 magnetic field along the X' axis. The spins respond to this pulse in such a way as to cause the net magnetization vector to rotate about the direction of the applied B_1 field. The rotation angle θ, depends on the length of time the field is on, τ, and its magnitude B_1.

$$\theta = 2\pi\gamma\tau B_1. \qquad \text{(E.q.3.8)}$$

In our examples, τ will be assumed to be much less than T1 and T2. A 90° pulse is one which rotates the magnetization vector clockwise by 90 degrees about the X' axis. A 90° pulse rotates the equilibrium magnetization down to the Y' axis. (figure3-30) In the laboratory frame the equilibrium magnetization spirals down around the Z axis to the XY plane(figure3-31). You can see why the rotating frame of reference is helpful in describing the behavior of magnetization in response to a pulsed magnetic field.

A 180° pulse will rotate the magnetization vector by 180 degrees. A 180° pulse rotates the equilibrium magnetization down to along the -Z axis. The net magnetization at any orientation will behave according to the rotation equation. For example, a net magnetization vector along the Y' axis will end up along the -Y' axis when acted upon by a 180° pulse of B_1 along the X' axis (figure3-33). A net magnetization vector between X' and Y' will end up between X' and Y' after the application of a 180° pulse of B_1 applied along the X' axis (figure3-34). A rotation matrix can also be used to predict the result of a rotation. Here is the rotation angle about the X' axis, [X', Y', Z'] is the initial location of the vector, and [X", Y", Z"] the location of the vector after the rotation (figure3-35).

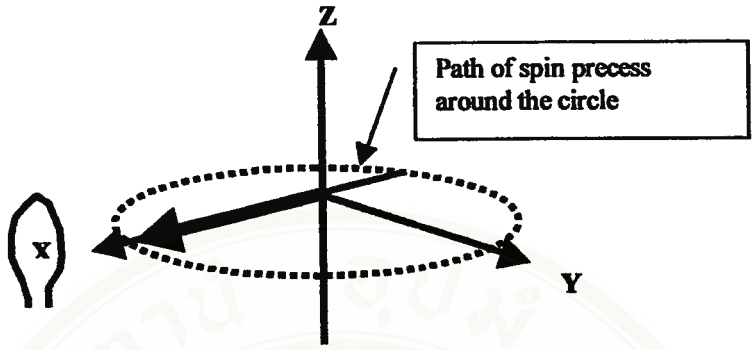

Figure3-27 A coil of wire placed around the X axis will provide a magnetic field along the X axis when a direct current is passed through the coil

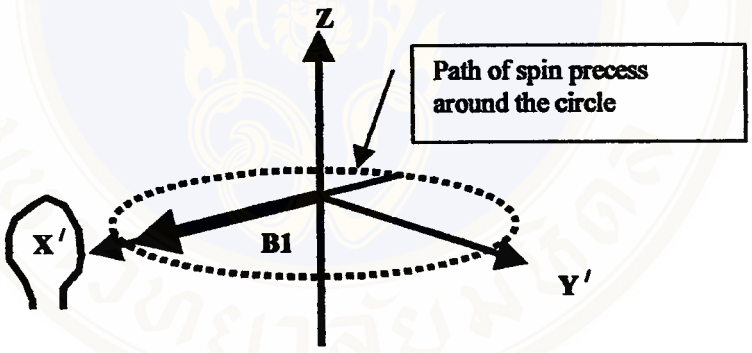

Figure3-28 An alternating current will produce a magnetic alternating in direction X'.

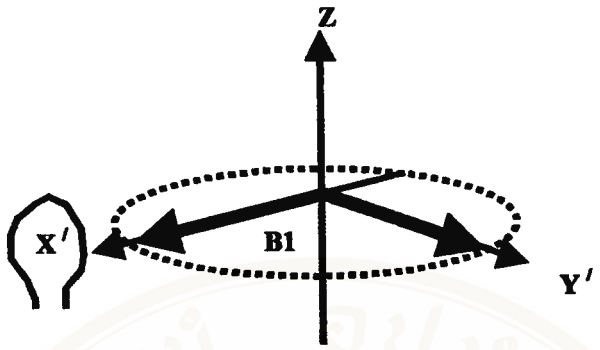

Figure3-29 The frame of reference rotating about the Z axis at a frequency equal to that of the alternating current, the magnetic field along the X' axis will be constant, just as in the direct current case in the laboratory frame.

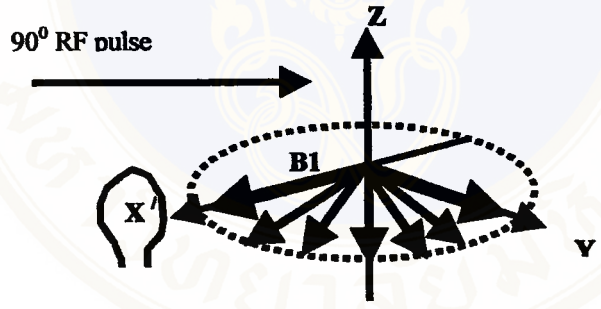

Figure3.30 represented a 90° pulse is one which rotates the magnetization vector clockwise by 90 degrees about the X' axis. A 90° pulse rotates the equilibrium magnetization down to the Y' axis.

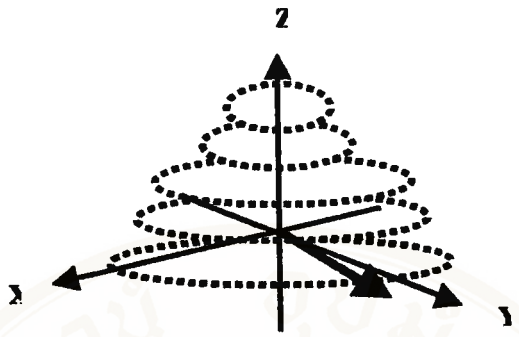

Figure3-31 In the laboratory frame the equilibrium magnetization spirals down around the Z axis to the XY plane.

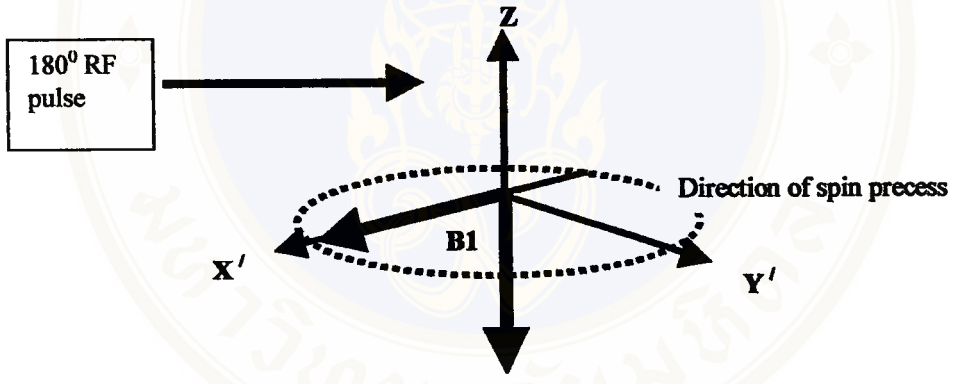

Figure3-32 A 180° pulse rotates the equilibrium magnetization down to along the -Z axis.

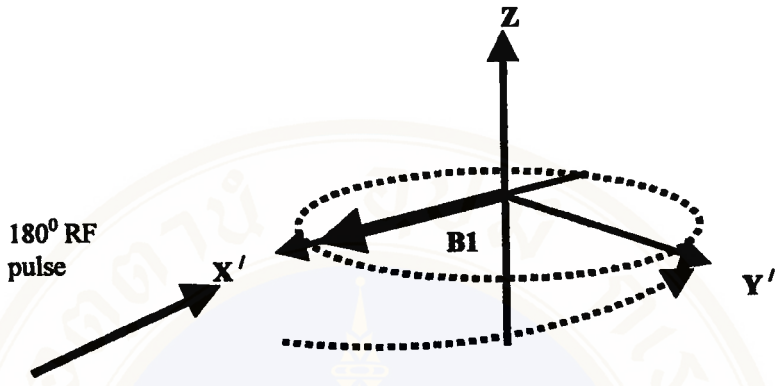

Figure3-33 A net magnetization vector along the Y' axis will end up along the -Y' axis when acted upon by a 180° pulse of B_1 along the X' axis.

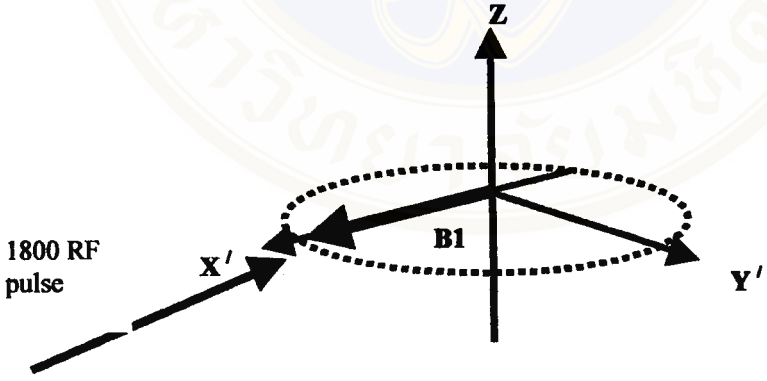

Figure3-34 A net magnetization vector between X' and Y' will end up between X' and Y' after the application of a 180° pulse of B_1 applied along the X' axis.

$$\begin{bmatrix} X'' \\ Y'' \\ Z'' \end{bmatrix} = \begin{bmatrix} 1 & 0 & 0 \\ 0 & Cos\theta & Sin\theta \\ 0 & -Sin\theta & Cos\theta \end{bmatrix} \begin{bmatrix} X' \\ Y' \\ Z \end{bmatrix}$$

Figure3-35 The rotation angle or flip angle about the X' axis, [X', Y', Z] is the initial location of the vector, and [X", Y", Z"] the location of the vector after the rotation.

3.15 Spin Relaxation (2,4,6,26,33)

Motions in solution which result in time varying magnetic fields cause spin relaxation. Time varying fields at the Larmor frequency cause transitions between the spin states and hence a change in M_Z. The figure 3-36 depicts the field at the one hydrogen on the water molecule as it rotates the external field Bo and a magnetic field from the another hydrogen. Note that the field experienced at the green hydrogen is sinusoidal. There is a distribution of rotation frequencies in a sample of molecules. Only frequencies at the Larmor frequency effect T1. Since the Larmor frequency is proportional to Bo, T1 will therefore vary as a function of magnetic field strength (figure3-37). In general, T1 is inversely proportional to the number of molecular motions at the Larmor frequency. The frequency distribution depends on the temperature and viscosity of the solution.

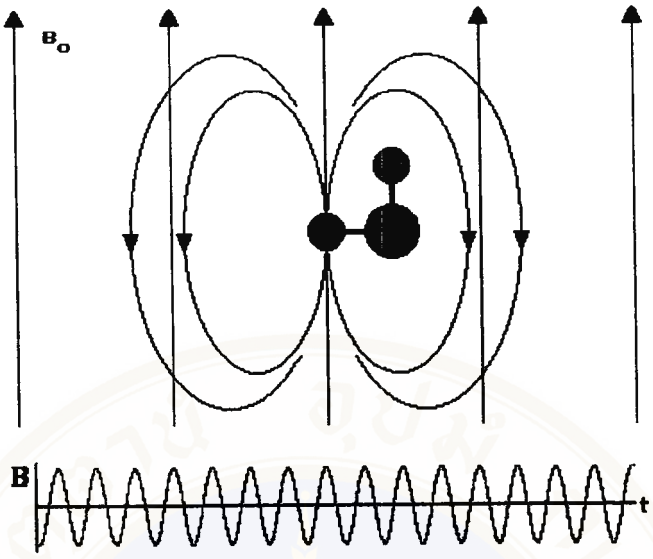

Figure 3-36 represent the field at the one hydrogen on the water molecule as it rotates the external field Bo and a magnetic field from the another hydrogen.

Figure 3-37 T_1 will vary as a function of magnetic field strength because of Larmor frequency is proportional Bo.

Therefore T_1 will vary as a function of temperature (figure3-38). At the Larmor frequency indicated by o T_1 (280 K) < T_1 (340 K). The temperature of the human body does not vary by enough to cause a significant influence on T_1. The viscosity does however vary significantly from tissue to tissue and influences T_1 as is seen in

the following molecular motion plot (figure3-39). Fluctuating fields which perturb the energy levels of the spin states cause the transverse magnetization to dephase. The number of molecular motions less than and equal to the Larmor frequency is inversely proportional to T_1. In general, relaxation times get longer as Bo increases because there are fewer relaxation causing frequency components present in the random motions of the molecules.

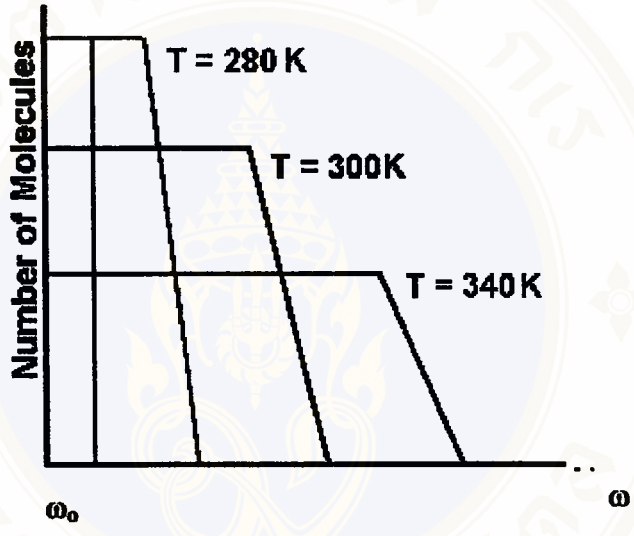

Figure3-38 represented T_1 will vary as a function of temperature (see more detail in text).

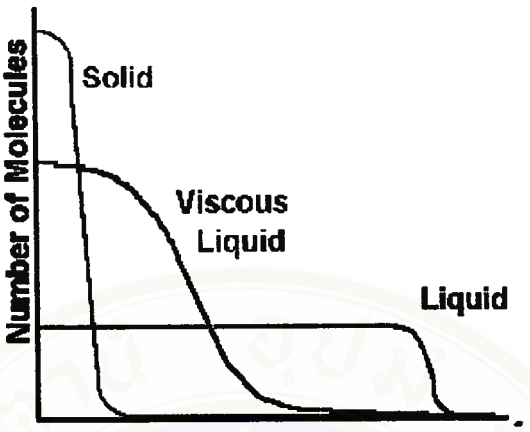

Figure3-39 The viscosity does vary significantly from tissue to tissue and influences T1 as is seen in the following molecular motion plot(see more detail).

CHAPTER IV

IMAGING PRINCIPLES

4.1 Introduction

The last chapter that magnetic resonance imaging is an imaging modality which is primarily used to construct pictures of the NMR signal from the hydrogen atoms in an object. In medical MRI, radiologists are most interested in looking at the NMR signal from water and fat, the major hydrogen containing components of the human body. The principle behind all magnetic resonance imaging is the resonance equation, which shows that the resonance frequency ω of a spin is proportional to the magnetic field, Bo, it is experiencing.

$$\omega = \gamma Bo$$

Recall from the spin physics chapter that γ is the gyromagnetic ratio. For example, assume that a human head contains only three small distinct regions where there is hydrogen spin density (figure4-1). In reality the entire head would contain signal. When these regions of spin are experiencing the same general magnetic field strength, there is only one peak in the NMR spectrum (figure4-2).

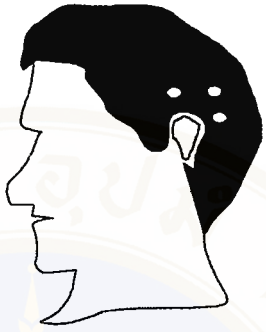

Figure4-1The three protons (are represented by dot) contain in human head.

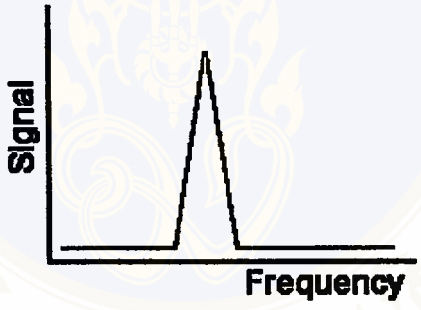

Figure4-2 The frequency of MR signal which it come from the three proton in the figure 4-1, when it aligned in the same magnetic field (see detail in text).

4.2 Magnetic Field Gradient (1,2,6,33,38,39)

If each of the regions of spin was to experience a unique magnetic field we would be able to image their positions. A gradient in the magnetic field is what will allow us to accomplish this. A magnetic field gradient is a variation in the magnetic field with respect to position. A one-dimensional magnetic field gradient is a variation with respect to one direction, while a two-dimensional gradient is a variation with

respect to two. The most useful type of gradient in magnetic resonance imaging is a one-dimensional linear magnetic field gradient. A one-dimensional magnetic field gradient along the x axis in a magnetic field, Bo, indicates that the magnetic field is increasing in the x direction. Here the length of the vectors represent the magnitude of the magnetic field(figure4-3). The symbols for a magnetic field gradient in the x, y, and z directions are G_x, G_y, and G_z.

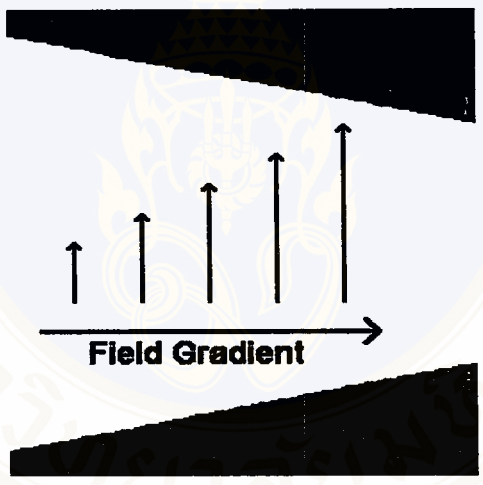

Figure4.3 The linear magnetic field gradient in the external magnetic field, Bo

4.3 Frequency Encoding (1,2,6,33,38,39)

The point in the center of the magnet where (x,y,z) =0,0,0 is called the isocenter of the magnet. The magnetic field at the isocenter is B_o and the resonant frequency is ω_o (figure4-4). If a linear magnetic field gradient is applied to our hypothetical head with three spin containing regions, the three regions experience different magnetic fields (figure4-5). The result is an NMR spectrum with more than

one signal. The amplitude of the signal is proportional to the number of spins in a plane perpendicular to the gradient. This procedure is called frequency encoding and causes the resonance frequency to be proportional to the position of the spin.

$$\omega = \gamma\ (Bo + x\ Gx) = \omega o + \gamma\ x\ Gx \qquad \text{(E.q.4.1)}$$

$$x = (\omega - \omega o) / (\gamma Gx) \qquad \text{(E.q.4.2)}$$

This principle forms the basis behind all magnetic resonance imaging. To demonstrate how an image might be generated from the NMR spectra, the backprojection method of imaging is presented in the next section.

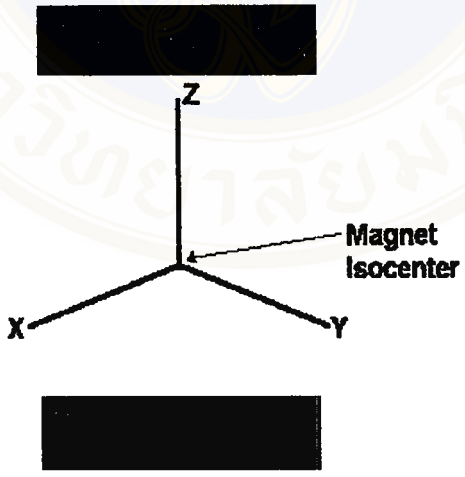

Figure4.4 The isocenter point in the rotating frame. At this point spin has frequency equal to Larmor frequency

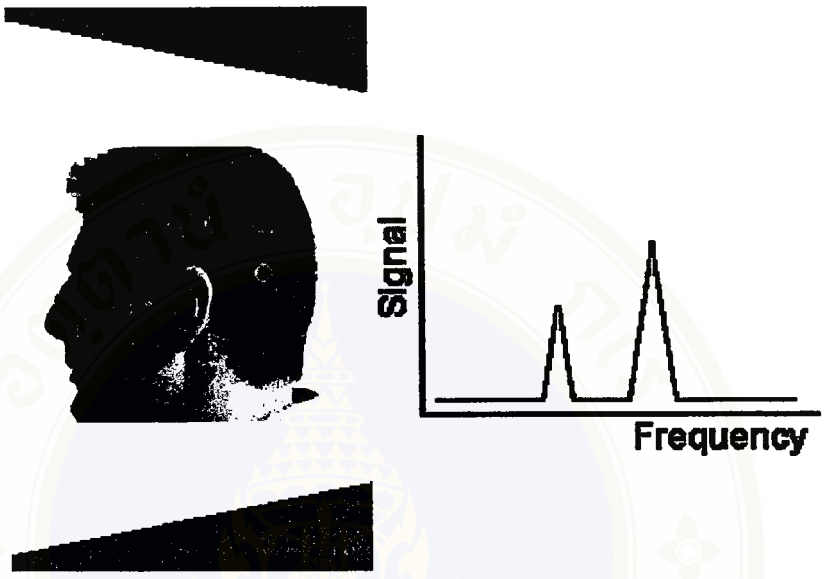

Figure 4-5 The frequency of MR signal when it is exposed by the linear magnetic field gradient (see more detail in text)(38).

4.4 Back Projection Imaging (1,2,6,33,38,39)

Backprojection imaging is a form of magnetic resonance imaging(figure4-6). It was one of the first forms of magnetic resonance imaging to be demonstrated. Backprojection is an extension of the frequency encoding procedure just described. In the backprojection technique, the object is first placed in a magnetic field. A one-dimensional field gradient is applied at several angles, and the NMR spectrum is recorded for each gradient (figure4-7)

For example, say we wished to produce an YZ plane image of an object. A magnetic field gradient in the +Y direction is applied to the object and an NMR spectrum is recorded. A second spectrum is recorded with the gradient now at a one

degree n 0° and 359°. Once this data has been recorded the data can be backprojected through space in computer memory (figure4-8).

Once the background intensity is suppressed an image can be seen (figure4-9). The actual backprojection scheme is called the inverse radon transform. In a conventional 90-FID imaging sequence this procedure might be applied with the aid of the following pulse sequence (figure4-10). Varying the angle of the gradient is accomplished by the application of linear combinations of two gradients. Here the Y and X gradients are applied in the following proportions to achieve the required frequency encoding gradient Gf.

$$G_y = G_f Sin\theta \qquad \text{(E.q.4.3)}$$

$$G_x = G_f Cos\theta \qquad \text{(E.q.4.4)}$$

For the backprojection technique to be a viable tomographic imaging technique we need to have the ability to image the spins in a thin slice. The Gz gradient in the last graphic accomplishes this. The following section will describe how slice selection is accomplished.

Figure4-6 The frequency of MR signal correlate to the position of three protons in human head (38).

Figure4-7 The backprojection method by rotate the linear magnetic field gradients around the human head (38).

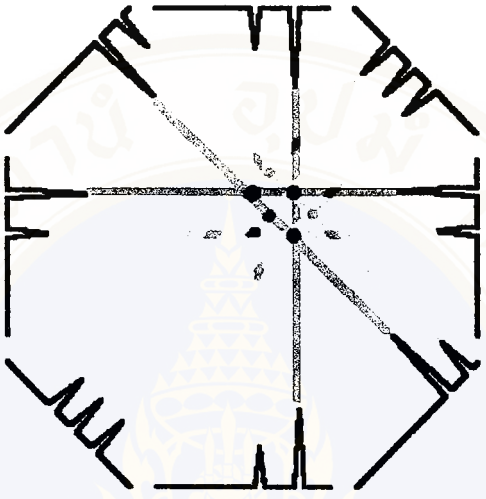

Figure4-8 The backprojection technique (see more detail in text)(23).

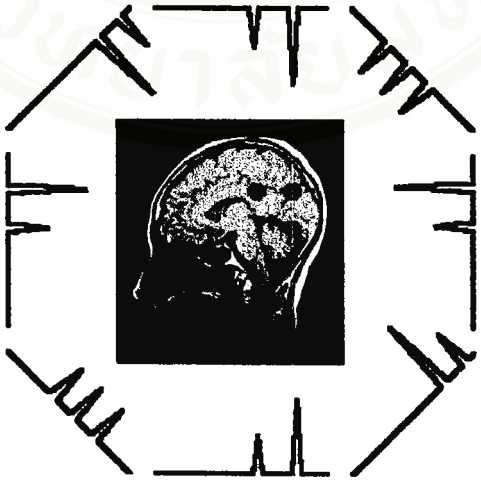

Figure4-9 The image which it come from by the backprojection techniques (23).

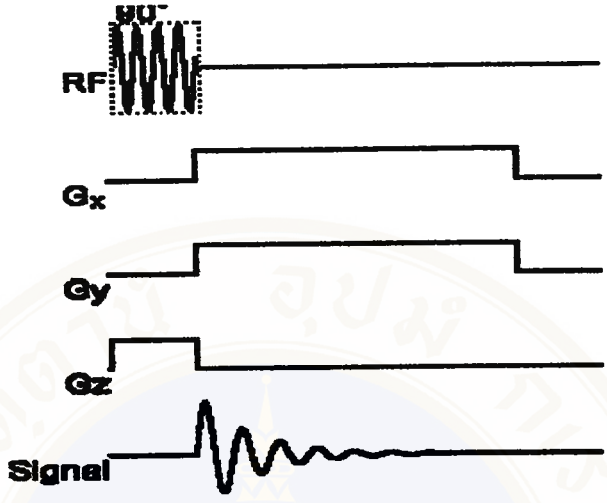

Figure4-10 The timing diagram of 90° RF pulse sequence (see more detail in text)

4.5 Slice Selection (1,2,6,33,38,39)

Slice selection in MRI is the selection of spins in a plane through the object. The principle behind slice selection is explained by the resonance equation. Slice selection is achieved by applying a one-dimensional, linear magnetic field gradient during the period that the RF pulse is applied. A 90° pulse applied in conjunction with a magnetic field gradient will rotate spins which are located in a slice or plane through the object. Picture what this would look like if we had a cube of small net magnetization vectors (figure4-11). To understand this we need to examine the frequency content of a 90° pulse. A 90° pulse contains a band of frequencies. This can be seen by employing the convolution theorem. The frequency content of a square 90° pulse is shaped as a sinc pulse. The figure4-12 displays the real components of this pulse. The amplitude of the sinc function is largest at the frequency of the RF which was turned on and off. This frequency will be rotated by 90° while other smaller and

greater frequencies will be rotated by lesser angles. The application of this 90° pulse with a magnetic field gradient in the x direction will rotate some of the spins in a plane perpendicular to the x axis by 90°. The word some was used because some of the frequencies have a B_1 less than that required for a 90° rotation. As a consequence the selected spins do not actually constitute a slice. A solution to the poor slice profile is to shape the 90° pulse in the shape of a sinc pulse. The figure 4-12 displays the real components of this function. A backprojection tomographic image can be achieved by the application of the following pulses. A apodized sinc pulse shaped 90° pulse is applied in conjunction with a slice selection gradient. A frequency encoding gradient is turned on once the slice selection pulse is turned off. The frequency encoding gradient is composed of a G_x and G_y gradient in this example. The FIDs are Fourier transformed to produce the frequency domain spectrum, which is then backprojected to produce the image. The backprojection imaging technique is highly educational but never used in state of the art imagers. Instead, Fourier transform

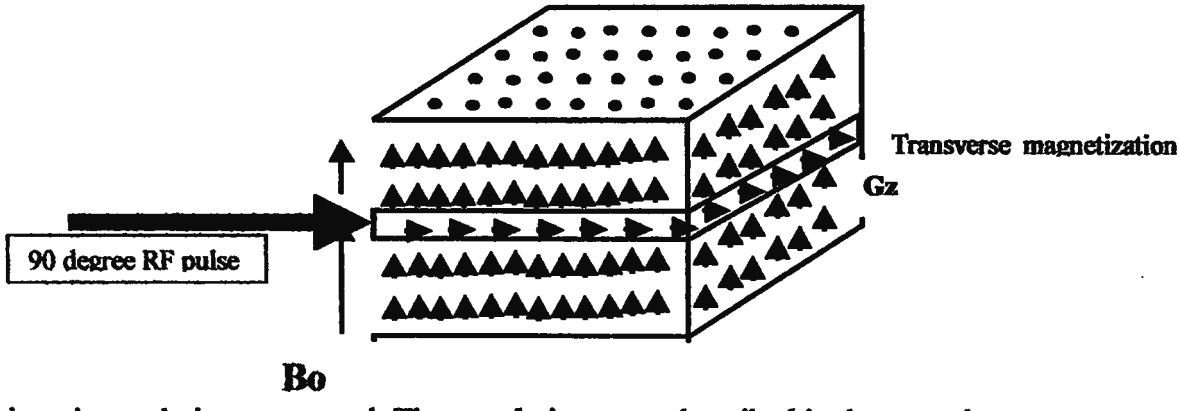

imaging techniques are used. These techniques are described in the next chapter.

Figure4-11 The grope of protons in the cube. This picture show net magnetization aligned along the direction of Bo. When we expose the net magnetization in the single plane the net magnetization which long the Bo will be tiped in the transverse plane(38).

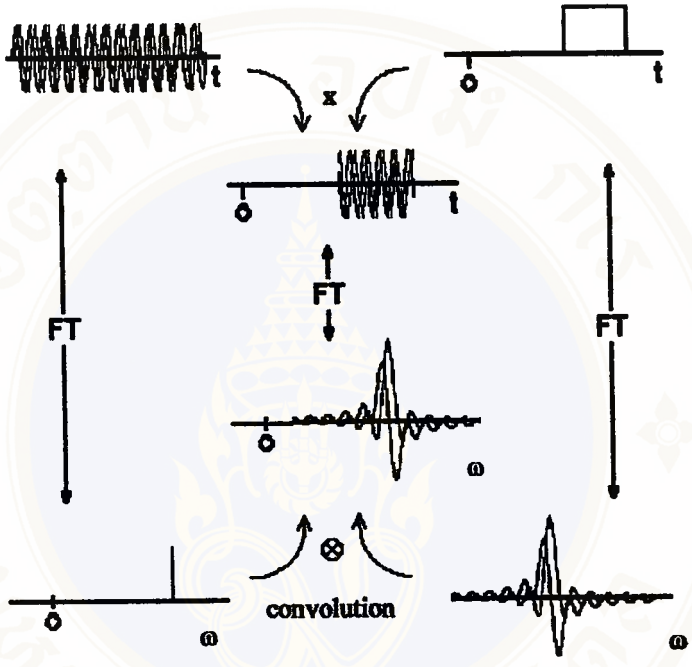

Figure4-12 The Fourier transform and convolution of the MR signal(38).

CHAPTER V

FT IMAGING PRINCIPLES

5.1 Introduction

In this chapter we will introduce the concept of a third category of magnetic field gradient called a phase encoding gradient and incorporate it plus the slice selection gradient and frequency encoding gradient, to see how present day tomographic, Fourier transform (see more detail in appendix B) MRI is performed.

5.2 Phase Encoding Gradient (1,2,6,33,38,39)

The phase encoding gradient is a gradient in the magnetic field Bo.The phase encoding gradient is used to impart a specific phase angle to a transverse magnetization vector. The specific phase angle depends on the location of the transverse magnetization vector. For example, lets imagine we have three regions with spin. The transverse magnetization vector from each spin has been rotated to a position along the X axis (figure5-1). The three vectors have the same chemical shift and hence in a uniform magnetic field they will possess the same Larmor frequency. If a gradient in the magnetic field is applied along the X direction the three vectors will precess about the direction of the applied magnetic field at a frequency given by the resonance equation.

$$\omega = \gamma(Bo + x\,Gx) = \omega o + \gamma x\,Gx \qquad \text{(E.q.5.1)}$$

While the phase encoding gradient is on, each transverse magnetization vector has its own unique Larmor frequency. Thus far, the description of phase encoding is the same as frequency encoding. Now for the difference. If the gradient in the X direction is turned off, the external magnetic field experienced by each spin vector is, for all practical purposes, identical (figure5-2). Therefore the Larmor frequency of each transverse magnetization vector is identical. The phase angle, θ, of each vector, on the other hand, is not identical. The phase angle being the angle between a reference axis, say the Y axis, and the magnetization vector at the time the phase encoding gradient has been turned off. There are three distinct phase angles in this example (figure5-3).

Just as in the examples of the frequency encoding gradient, if we had some way of measuring the frequency (in this case phase) of the spin vectors we could assign them a position along the X axis. We are now ready to explain the simple Fourier transform tomographic imaging sequence.

Figure5-1 The three net magnetization vectors when it precess in the same rate

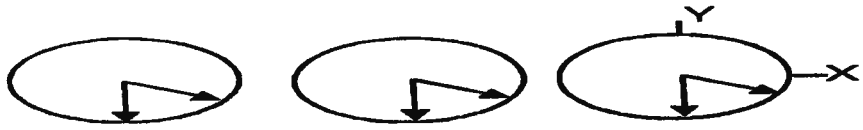

Figure5-2 The three net magnetization vector precess in the same frequency (see more detail in text).

Figure5-3 The three net magnetization precess in the different rate (see more detail in text).

5.3 FT Tomographic Imaging (1,2,6,33,38,39)

One of the best ways to understand a new imaging sequence is to examine a timing diagram for the sequence. The timing diagram for an imaging sequence has entries for the radio frequency, magnetic field gradients, and signal as a function of time. The simplest FT imaging sequence contains a 90° slice selective pulse, a slice selection gradient pulse, a phase encoding gradient pulse, a frequency encoding gradient pulse, and a signal (see figure4-10 in the chapter 4).The pulses for the three gradients represent the magnitude and duration of the magnetic field gradients. The actual timing diagram for this sequence is a bit more complicated, this one has been simplified for introductory purposes. The first event to occur in this imaging sequence is to turn on the slice selection gradient. The slice selection RF pulse is applied at the same time. The slice selective RF pulse is an apodized sinc function shaped burst of

RF energy. Once the RF pulse is complete the slice selection gradient is turned off and a phase encoding gradient is turned on. Once the phase encoding gradient has been turned off a frequency encoding gradient is turned on and a signal is recorded. The signal is in the form of a free induction decay.This sequence of pulses is usually repeated 128 or 256 times to collect all the data needed to produce an image.The time between the repetitions of the sequence is called the repetition time, TR. Each time the sequence is repeated the magnitude of the phase encoding gradient is changed. The magnitude is changed in equal steps between the maximum amplitude of the gradient and the minimum value. Here is a quick example of what eight phase encoding steps worth of the sequence would look like. The slice selection gradient is always applied perpendicular to the slice plane. The phase encoding gradient is applied along one of the sides of the image plane. The frequency encoding gradient is applied along the remaining edge of the image plane.The following table indicates the possible combination of the slice, phase, and frequency encoding gradient.

	Gradient		
Slice Plane	Slice	Phase	Frequency
XY	Z	X or Y	Y or X
XZ	Y	X or Z	Z or X
YZ	X	Y or Z	Z or Y

Table 5-1 is indicated the possible combination of the slice, phase and frequency encoding gradient.

Now we will examine the sequence from a macroscopic perspective of the spin vectors. Imagine a cube of spins placed in a magnetic field. The cube is composed of serveral volume elements each with its own net magnetization vector. Suppose we wish to image a slice in the XY plane. The Bo magnetic field is along the Z axis. The Slice selection gradient is applied along the Z axis. The RF pulse rotates only those spins packets within the cube which satisfy the resonance condition. These spin packets are located within an XY plane in this example.The location of the plane along the Z axis with respect to the isocenter is given by

$$\omega = \gamma G_s Z \qquad \text{(E.q.5.2)}$$

where ω is the Larmor frequency , Gs the magnitude of the slice selection gradient, and γ the gyromagnetic ratio. In the figure 4.11(the chapter4)if spins located above and below this plane are not affected by the RF pulse. They will therefore be neglected for purposes of this presentation. To simplify the remainder of the presentation, we shall concentrate on a 3x3 subset of the net magnetization vectors. The picture of these spins in this plane looks like grope of spin in the figure 4-11. Once rotated into the XY plane these vectors would precess at the Larmor frequency given by the magnetic field each was experiencing. If the magnetic field was uniform, each of the nine precessional rates would be equal (figure 5-4). In the imaging sequence a phase encoding gradient is applied after the slice selection gradient. Assuming this is applied along the X axis, the spins at different locations along the X

axis begin to precess at different Larmor frequencies (figure 5-5). When the phase encoding gradient is turned off the net magnetization vectors precess at the same rate, but possess different phases. (figure 5-6). The phase being determined by the duration and magnitude of the phase encoding gradient pulse.

Once the phase encoding gradient pulse is turned off a frequency encoding gradient pulse is turned on. In this example the frequency encoding gradient is in the -Y direction. The frequency encoding gradient causes spin packets to precess at rates dependent on their Y location. Please note that now each of the nine net magnetization vectors is characterized by a unique phase angle and precessional frequency. If we had a means of determining the phase and frequency of the signal from a net magnetization vector we could position it within one of the nine elements. A simple Fourier transform is capable of this task for a single net magnetization vector located somewhere within the 3x3 space. For example, if a single vector was located at (X,Y) = 2,2, its FID would contain a sine wave of frequency 2 and phase 2. A Fourier transform of this signal would yield one peak at frequency 2 and phase 2. Unfortunately a one dimensional Fourier transform is incapable of this task when more than one vector is located within the 3x3 matrix at a different phase encoding direction location. There needs to be one phase encoding gradient step for each location in the phase encoding gradient direction. The point is you need one equation for each unknown you are trying to solve for. Therefore if there are three phase encoding direction locations we will need three unique phase encoding gradient amplitudes and have three unique free induction decays. If we wish to resolve 256

locations in the phase encoding direction we will need 256 different magnitudes of the phase encoding gradient and will record 256 different free induction decays.

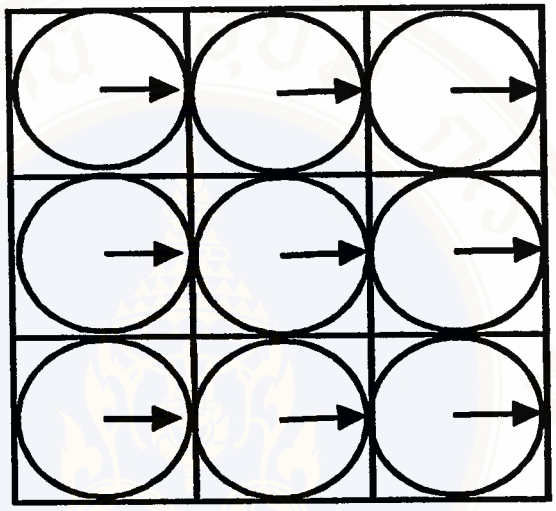

Figure5-4 .The nine magnetization vectors contain in three column and three row This picture is showed net magnetization vectors precess in the same rate.

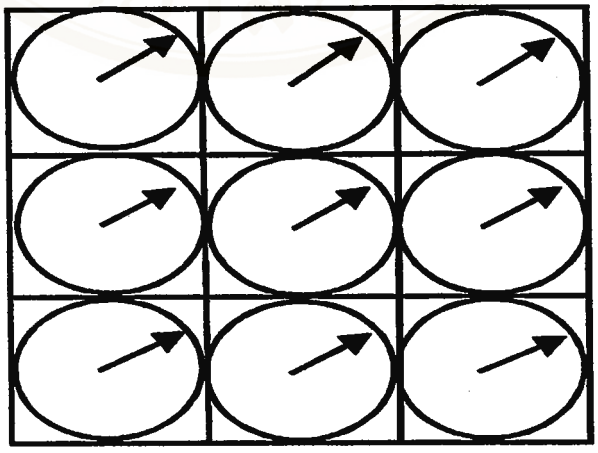

Figure 5-5. The number of nine magnetization vector precess in the same frequency rate (see more detail in text).

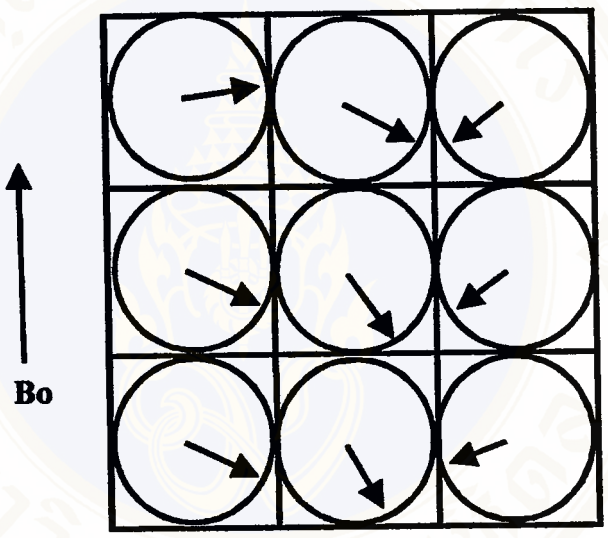

Figure 5-6.The number of nine magnetization vectors precess in the different rate ,in left column the net magnetization vector precess slower than the net magnetization in the right and middle column.

5.4 Signal Processing (1,2,6,33,38,39)

The free induction decays or signals described above must be Fourier transformed to obtain an image or picture of the location of spins. The signals are first Fourier transformed in the X direction to extract the frequency domain information and then in the phase encoding direction to extract information about the locations in the phase encoding gradient direction. To see two examples are presented.

For example :

There is a single voxel with net magnetization (figure5-7). The time and phase domain data, often referred to as the raw data, will look like this (figure 5-8). Notice there is one frequency of oscillation in the time domain. You may also be able to see one frequency of oscillation in the phase direction. Fourier transforming first in the frequency encoding direction yields a series of peaks at the frequency corresponding to the X location of the voxel with spin (figure 5-9).

$$\omega - \omega_0 = \gamma x G_f \qquad \text{(E.q.5.3)}$$

Notice how the amplitude of the peaks are oscillating as you look from top to bottom in the phase encoding direction. We can readjust our perspective of the data to make this more obvious (figure 5-10). Fourier transforming down in the phase encoding direction yields a single peak (figure 5-11). The frequency and phase of this peak correspond to the location of the voxel with spins (figure 5-7).

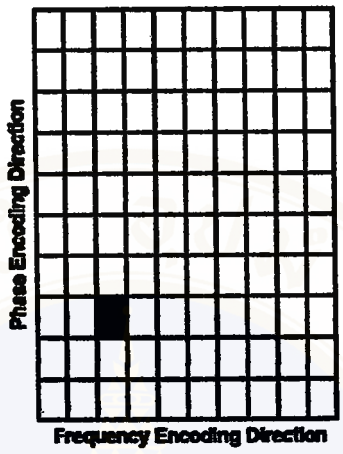

Figure 5-7.The net magnetization in the voxel that it is showed its position in the K-space.

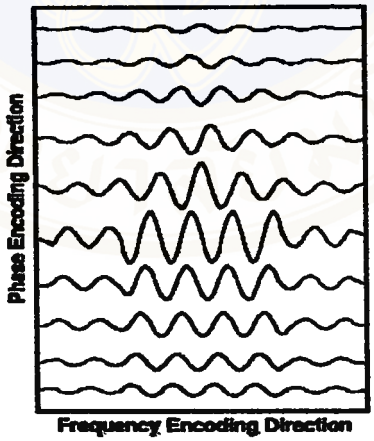

Figure 5.8 The MR signal in the time domain.

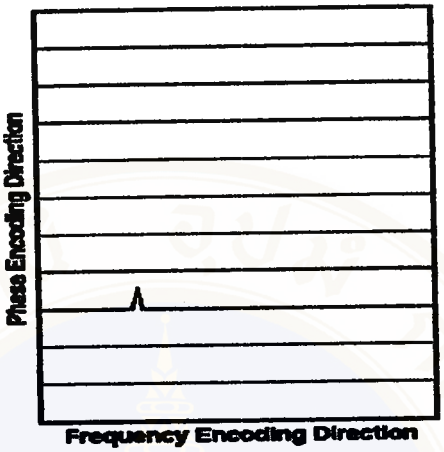

Figure 5-9 The MR signal from the figure 5-8 in the frequency domain when it is passed Fourier transform process.

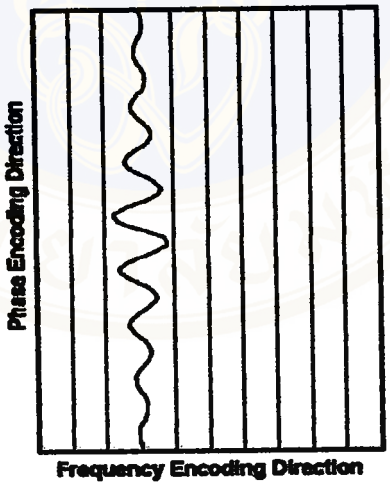

Figure 5-10 The MR signal in the time domain , it is converted to the frequency domain from the figure5-9 (see more detail in text)

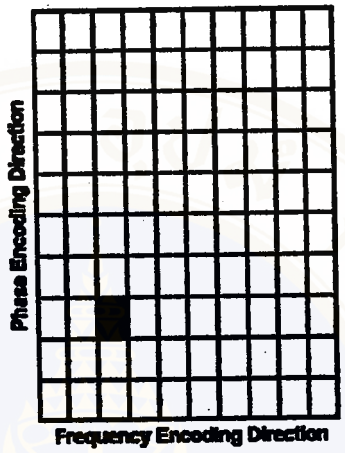

Figure 5-11.The MR signal in the frequency domain when it is passed Fourier transform process.

CHAPTER VI

BASIC IMAGING TECHNIQUES AND IMAGING PULSE SEQUENCE

6.1Introduction

In the previous chapter we mentioned the principles of Fourier transform magnetic resonance imaging. The examples presented were for a simplified 90-FID imaging sequence. Although the principles were correct, some aspects were simplified to make the presentation easier to understand. Some of these principles will be presented in a little more depth in this chapter. The 90-FID imaging sequence will be presented as a gradient recalled echo sequence in this chapter. The principles of multislice imaging and oblique imaging will be introduced. Two new imaging sequences called the spin-echo sequence and inversion recovery sequence will be introduced.

6.2 Multislice Imaging (1,2,6,33,38,39)

An imaging sequence based on a 90-FID was introduced in the section. Based on this presentation, the time to acquire an image is equal to the product of the TR value and the number of phase encoding steps. If TR were one second and there were 256 phase encoding gradient steps the total imaging time required to produce the

image would be 4 minutes and 16 seconds. If we wanted to take 20 images across a region of interest the imaging time would be approximately 1.5 hours. This will obviously not do if we are searching for pathology. Looking at the timing diagram for the imaging sequence with a one second TR it is clear that most of the sequence time is unused (figure 6-1). This unused time could be made use of by exciting other slices in the object. The only restriction is that the excitation used for one slice must not affect those from another slice. This may be accomplished by applying one magnitude slice selection gradient and changing the RF frequency of the 90° pulses (figure 6-2). Note that the three frequency bands from the pulses do not overlap. In this figure there are three RF pulses applied in the TR period. Each has a different center frequency ω_1, ω_2, and ω_3. As a consequence the pulses affect different slices in the imaged object (figure 6-3).

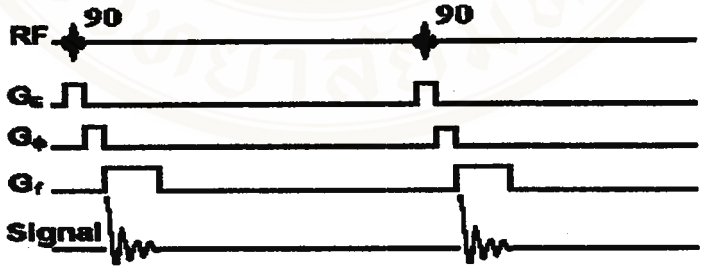

Figure 6-1. The 90--FID pulse sequence diagram.

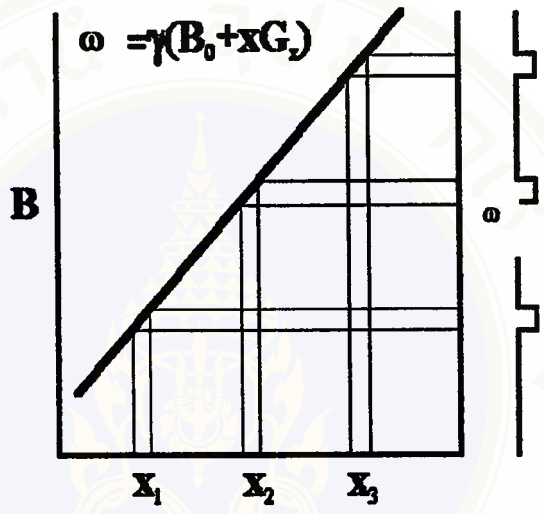

Figure 6-2 the slice selection by changing the RF frequency of the 90^0 pulse (38).

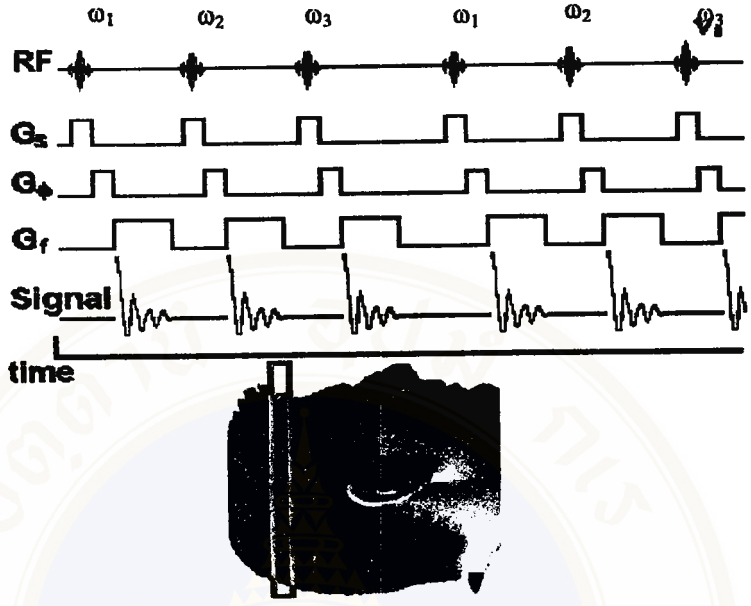

Figure 6-3 the slice selection by changing the center frequency ω_1, ω_2, and ω_3 (38).

6.3 Oblique imaging (38)

Orthogonal imaging planes along the X, Y, or Z axes are easily produced with the imaging sequence. However what if the anatomy of interest does not lie along one of the three orthogonal imaging planes? This is where the concept of oblique imaging comes in. Oblique imaging is the production of images, which lie between the conventional X, Y, and Z-axes. Oblique imaging is performed by applying linear combinations of the X, Y, and Z magnetic field gradients so as to produce a slice selection gradient which is perpendicular to the imaged plane, a phase encoding gradient which is along one edge of the imaged plane, and a frequency encoding gradient which is along the remaining edge of the image. For example, if we wanted to image a slice lying along the X axis but passing between the Z and Y axes such that

it made an angle of 30° with respect to the Y axis and 60° with the Z axis (figure 6-4), the following combination of gradients would be needed.

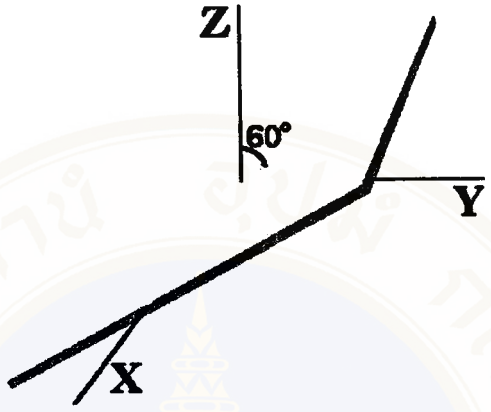

Figure 6-4 A slice lying along the X-axis but passing between the Z and Y axes such that it made an angle of 30° with respect to the Y-axis and 60° with the Z-axis.

Slice Selection Gradient (figure 6-5).

$$Gz = Gs \sin 60^\circ \qquad \text{(E.q.5.1)}$$

$$Gy = -Gs \cos 60^\circ \qquad \text{(E.q.5.2)}$$

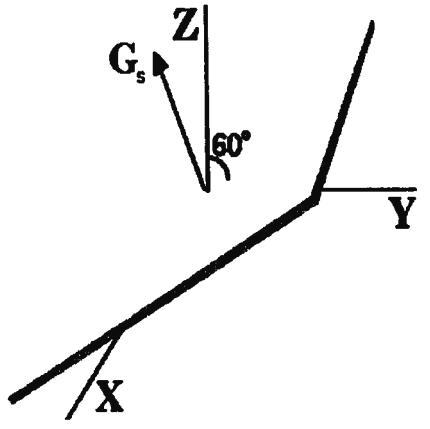

Figure 6-5 the slice selection gradient in the oblique imaging technique.

Phase Encoding Gradient (figure 6.6).

$$Gz = G\phi \text{Sin } 30^\circ \quad \text{(E.q.5.3)}$$

$$Gy = G\phi \text{Cos } 30^\circ \quad \text{(E.q.5.4)}$$

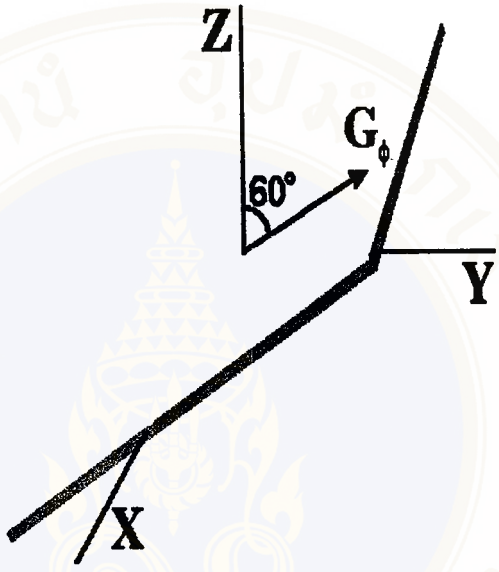

Figure6-6 the phase encoding gradient in the oblique images technique.

Frequency Encoding Gradient (figure 6-7).

$$Gx = Gf \qquad (5.5)$$

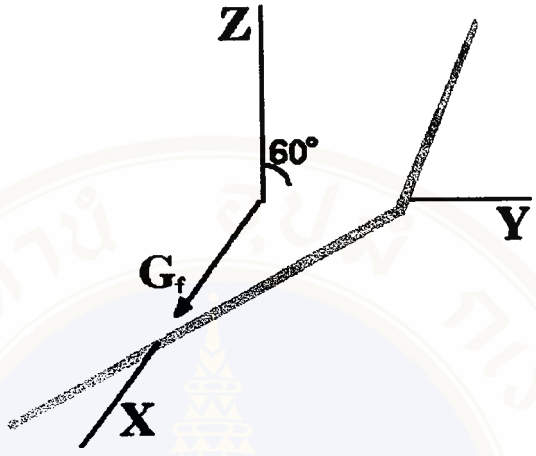

Figure 6-7 the frequency-encoding gradient in the oblique imaging technique.

The frequency and phase encoding gradients are interchangeable. The timing diagram for the sequence looks as follows (figure 6-8).

Figure 6-8 The imaging pulse sequence which it can interchangeable between frequency and phase encoding gradient (see more detail in text).

6.4 Spin-Echo Imaging (1,2,6,33,38,39)

An advantage of using a spin-echo sequence is that it introduces T_2 dependence to the signal. Since some tissues and pathologies have similar T_1 values but different T_2 values it is advantageous to have an imaging sequence which produces images with a T_2 dependence. The spin-echo imaging sequence will be presented in the form of a timing diagram only, since the evolution of the magnetization vectors from the application of slice selection, phase encoding, and frequency encoding gradients. The timing diagram for a spin-echo imaging sequence has entries for the RF pulses, the gradients in the magnetic field, and the signal (Figure 6-9). A slice selective 90° RF pulse is applied in conjunction with a slice selection gradient. A period of time equal to TE/2 elapses and a 180° slice selective 180° pulse is applied in conjunction with the slice selection gradient. A phase encoding gradient is applied between the 90° and 180° pulses. As in the previous imaging sequences, the phase encoding gradient is varied in 128 or 256 steps between $G_\phi m$ and $-G_\phi m$. The phase encoding gradient could be applied after the 180° pulse, however if we want to minimize the TE period the pulse is applied between the 90° and 180° RF pulses. The frequency-encoding gradient is applied after the 180° pulse during the time that echoes is collected. The recorded signal is the echo. The FID, which is found after every 90° pulse, is not used. One additional gradient is applied between the 90° and 180° pulses. This gradient is along the same direction as the frequency-encoding gradient. It dephases the spins so that they will rephase by the center of the echo. This gradient in effect prepares the signal to be at the edge of k-space (see more detail in appendix C) by the start of the acquisition of the echo. The

entire sequence is repeated every TR seconds until all the phase encoding steps have been recorded.

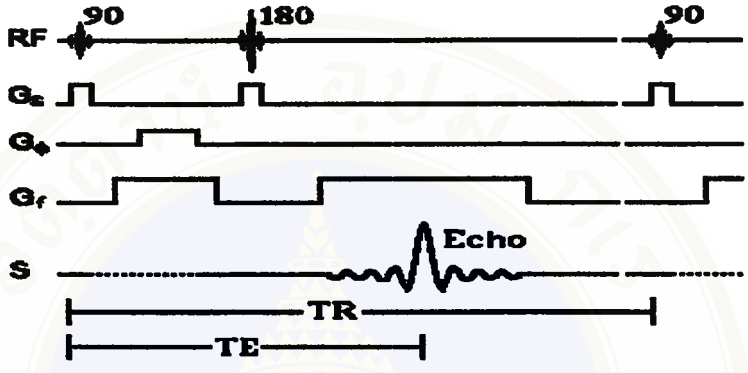

Figure 6-9 the timing diagram of spin-echo pulse sequence (see more detail in text)

6.5 Inversion Recovery Imaging (1,2,6,33,38,39)

An advantage of using an inversion recovery sequence is that it allows nulling of the signal from one component due to its T_1. The signal intensity is zero when $TI = T_1 \ln 2$. This sequence will be presented in the form of a timing diagram only, since the evolution of the magnetization vectors from the application of slice selection, phase encoding, and frequency encoding gradients .An inversion recovery sequence which uses a spin-echo sequence to detect the magnetization will be presented. The RF pulses are 180-90-180. An inversion recovery sequence that uses a 90-FID signal detection is similar, with the exception that a 90-FID is substituted for the spin-echo part of the sequence. The timing diagram for an inversion recovery

imaging sequence has entries for the RF pulses, the gradients in the magnetic field, and the signal (figure 6-10). A slice selective 180° RF pulse is applied in conjunction with a slice selection gradient. A period of time equal to TI elapses and a spin-echo sequence is applied. The remainder of the sequence is equivalent to a spin-echo sequence. This spin-echo part recorded the magnetization present at a time TI after the first 180° pulse. (A 90-FID sequence could be used instead of the spin-echo.) All the RF pulses in the spin-echo sequence are slice selective. The RF pulses are applied in conjunction with the slice selection gradients. Between the 90° and 180° pulses a phase encoding gradient is applied. The phase encoding gradient is varied in 128 or 256 steps between $G_\phi m$ and $-G_\phi m$. The phase encoding gradient could not be applied after the first 180° pulse because there is no transverse magnetization to phase encode at this point. The frequency-encoding gradient is applied after the second 180° pulse during the time that echoes is collected. The recorded signal is the echo. The FID after the 90° pulse is not used. The dephasing gradient between the 90° and 180° pulses to position the start of the signal acquisition at the edge of k-space, as was described in the section on spin-echo imaging. The entire sequence is repeated every TR seconds.

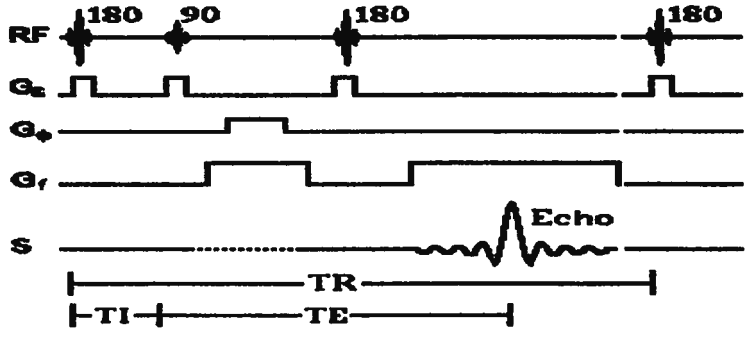

Figure 6-10.The timing diagram for inversion recovery pulse sequence imaging (see more detail in text)

6.6 Gradient Recalled Echo Imaging (1,2,6,33,38,39)

The imaging sequences mentioned thus far have one major disadvantage. For maximum signal, they all require the transverse magnetization to recover to its equilibrium position along the Z-axis before the sequence is repeated. When the T1 is long, this can significantly lengthen the imaging sequence. If the magnetization does not fully recover to equilibrium the signal is less than if full recovery occurs (figure 6-11).

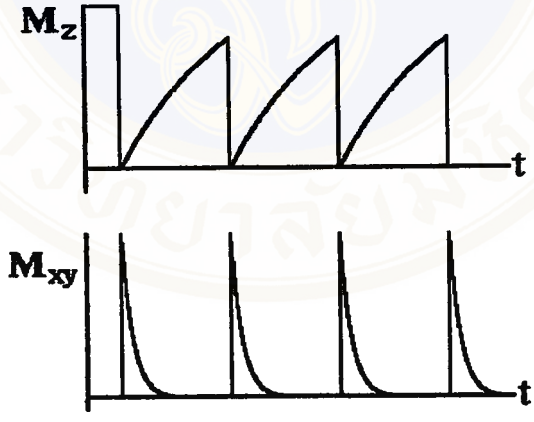

Figure 6-11.The transverse magnetization to recover to its equilibrium position along the Z-axis before the sequence is repeated

If the magnetization is rotated by an angle less than 90° its M_z component will recover to equilibrium much more rapidly, but there will be less signal since the

signal will be proportional to the Sinθ (figure 6-12). So we trade off signal for imaging time. In some instances, several images may be collected and averaged together and make up for the lost signal. The gradient recalled echo-imaging sequence is the application of these principles. Here is its timing diagram (figure 6-13). In the gradient recalled echo-imaging sequence a slice selective RF pulse is applied to the imaged object. This RF pulse typically produces a rotation angle of between 10° and 90°. A slice selection gradient is applied with the RF pulse. A phase encoding gradient is applied next. The phase encoding gradient is varied between $G_\phi m$ and $-G_\phi m$ in 128 or 256 equal steps as was done in all the other sequences. A dephasing frequency-encoding gradient is applied at the same time as the phase encoding gradient so as to cause the spins to be in phase at the center of the acquisition period. This gradient is negative in sign from that of the frequency-encoding gradient turned on during the acquisition of the signal. An echo is produced when the frequency-encoding gradient is turned on because this gradient refocuses the dephasing which occurred from the dephasing gradient . A period called the echo time (TE) is defined as the time between the start of the RF pulse and the maximum in the signal. The sequence is repeated every TR seconds. The TR period could be as short as tens of milliseconds.

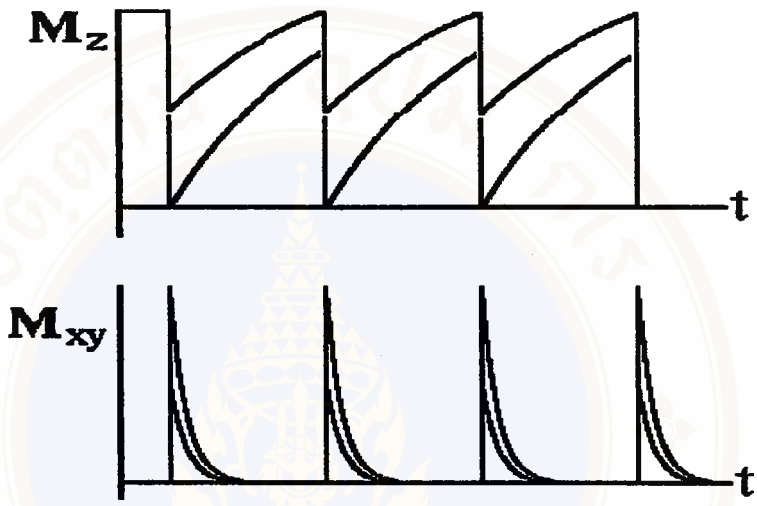

Figure 6-12. The magnetization is rotated by an angle less than 90° its M_z component will recover to equilibrium much more rapidly, but there will be less signal since the signal will be proportional to the Sinθ.

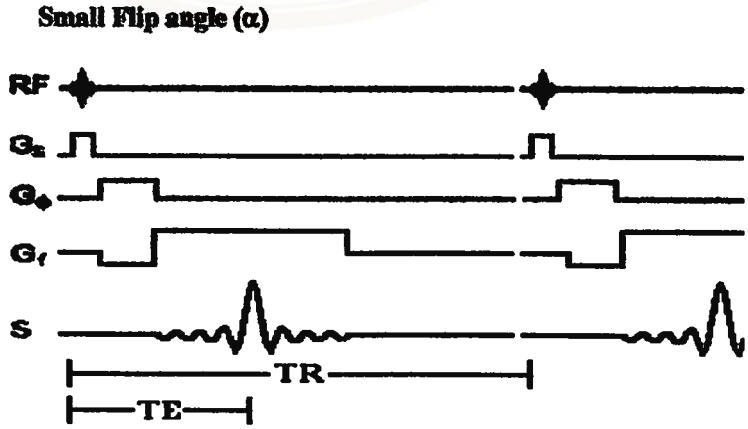

Figure 6-13. The timing diagram for gradient echo recalled (see more detail in text).

6.7 Image Contrast (1,2,6,33,38,39)

In order for pathology or any tissue for that matter to be visible in a magnetic resonance image there must be contrast or a difference in signal intensity between it and the adjacent tissue. The signal intensity, S, is determined by the signal equation for the specific pulse sequence used. Some of the intrinsic variables are the:

Spin-Lattice Relaxation Time, T1
Spin-Spin Relaxation Time, T2
Spin Density,P
T2*

Table 6-1.The intrinsic factors in MRI. These factors include of T1,T2, T2* and spin density(P).

The spin density is the concentration of signal bearing spins. The instrumental variables are the:

Repetition Time, TR
Echo Time, TE
Inversion Time, TI
Rotation Time, θ
T2*

Table 6-2.The extrinsic factor in MRI. These factors such as TR,TE, TI ,and T2*

T2* falls on both lists because it contains a component dependent on the homogeneity of the magnetic field and the molecular motions. The signal equations for the pulse sequences presented thus far are:

Spin-Echo

$$S = k\,P\,(1-\exp(-TR/T1))\,\exp.(-TE/T2)$$

Inversion Recovery (180-90)

$$S = k\,P\,(1-2\exp(-TI/T1) + \exp.(-TR/T1))$$

Inversion Recovery (180-90-180)

$$S = k\,P\,(1-2\exp(-TI/T1) + \exp.(-TR/T1))\,\exp.(-TE/T2)$$

Gradient Recalled Echo

$$S = k\,P\,(1-\exp(-TR/T1))\,\sin\theta\exp.(-TE/T2) / (1 - \cos\theta\,\exp.(-TR/T1))$$

In each of these equations, S represents the amplitude of the signal in the frequency domain spectrum. The quantity k is a proportionality constant that depends on the sensitivity of the signal detection circuitry on the imager. The values of T1, T2, and P are specific to a tissue or pathology. The following table lists the range of T1, T2, and P values at 1.5T for tissues found in a magnetic resonance image of the human head.

Tissue	T_1 (s)	T_2 (ms)	P*
CSF	0.8-20	110-2000	70-230
White matter	0.76-1.08	61-100	70-90
Gray matter	1.09-2.15	61-109	85-125
Meninges	0.5-2.2	50-165	5-44
Muscle	0.95-1.82	20-67	45-90
Adipose	0.2-0.75	53-94	50-100

*Based on P = 111 for 12 mM aqueous $NiCl_2$

Table 6-3. The intrinsic factors such as T1, T2, and P are in the human head.

The contrast, C, between two tissues A and B will be equal to the difference between the signal for tissue A, S_A, and that for tissue B, S_B.

$$C = S_A - S_B \qquad \text{(E.q.6.6)}$$

S_A and S_B are determined by the signal equations given above. For any two tissues there will be a set of instrumental parameters which yield a maximum contrast. For example in a spin-echo sequence the contrast between two tissues as a function of TR is graphically presented in the accompanying curve (figure6-14). A contrast curve for tissues A and B as a function of TE is presented in the accompanying curve (figure6-15). To assure that signals from all phase encoding steps possess the same signal properties a few equilibrating cycles through the sequence are added to the beginning of every image acquisition. Examining the MZ and MXY components as a function of

time in a 90-FID type sequence (figure6-16) may see the necessity of this. Note that the amount of transverse magnetization from a 90° pulse reaches an equilibrium value after a few TR cycles. This practice lengthens the imaging time by a few TR periods. The magnetic resonance community has adopted nomenclature to signify the predominant contrast mechanism in an image. An image whose contrast is predominantly caused by differences in T1 of the tissues is called a T1-weighted image. Similarly for T2 and P, the images are called T2-weighted and spin density weighted images. The following table contains the set of conditions necessary to produce weighted images.

Weighting	TR Value	TE Value
T1	<= T1	<< T2
T2	>> T1	>= T2
P	>> T1	<< T2

Table 6-4.The varied extrinsic factors would be acquire area to be image.

It is impressive to see how the choice of the instrumental parameters TR, TE, TI, and θ affect the contrast between the various tissues of the brain.

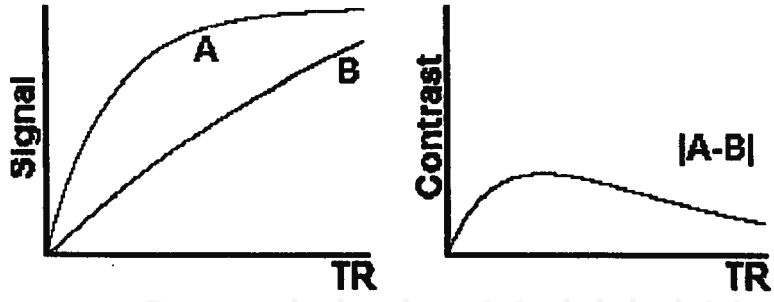

Figure 6-14.The relationship between signal, contrast and TR(see more detail in the text)

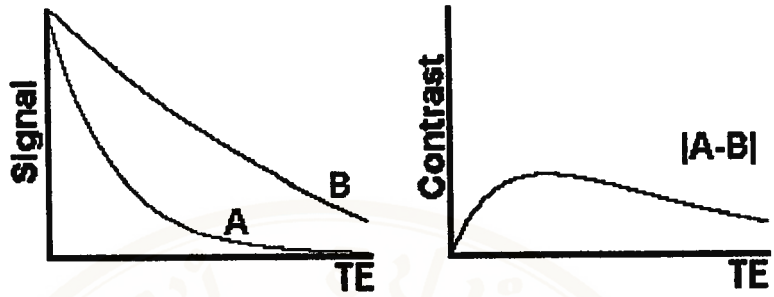

Figure 6-15.The relationship between signal, contrast and TE (see more detail in text)

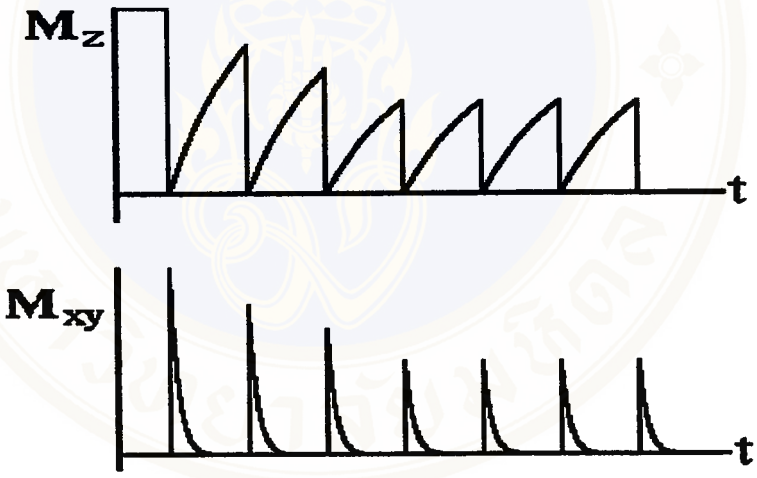

Figure 6-16 the amount of transverse magnetization from a 90° pulse reaches an equilibrium value after a few TR cycles

CHAPTER VII

IMAGING HARDWARE

7.1 Introduction

The diagram 7-1 is represented the major systems on a magnetic resonance imager and a few of the major interconnections. This overview briefly states the function of each component. Some will be described in detail later in this chapter.

At the top of the schematic representation you will find the components of the imager located in the scan room of a magnetic resonance imager. The magnet produces the Bo field for the imaging procedure. Within the magnet are the gradient coils for producing a gradient in Bo in the X, Y, and Z directions. Within the gradient a coil is the RF coil. The RF coil produces the B_1 magnetic field necessary to rotate the spins by 90° or 180°. The RF coil also detects the signal from the spins within the body. The patient is positioned within the magnet by a computer controlled patient table. The table has a positioning accuracy of 1 mm. An RF shield surrounds the scan room. The shield prevents the high power RF pulses from radiating out through the hospital. It also prevents the various RF signals from television and radio stations from being detected by the imager. Some scan rooms are also surrounded by a magnetic shield, which contains the magnetic field from extending too far into the hospital. In newer magnets, the magnet shield is an integral part of the magnet. The heart of the imager is the computer. It controls all components on the imager. The RF components under control of the computer are the RF frequency source and pulse

programmer. The source produces a sine wave of the desired frequency. The Pulse programmer shapes the RF pulses into apodized sinc pulses. The RF amplifier increases the pulse power from milli Watts to kilo Watts. The computer also controls the gradient pulse programmer who sets the shape and amplitude of each of the three gradient fields. The gradient amplifier increases the power of the gradient pulses to a level sufficient to drive the gradient coils. The array processor, located on some imagers, is a device, which is capable of performing a two-dimensional Fourier transform in fractions of a second. The computer off loads the Fourier transform to this faster device. The operator of the imager gives input to the computer is through a control console. An imaging sequence is selected and customized from the console. The operator can see the images on a video display located on the console or can make hard copies of the images on a film printer. The next three sections of this chapter go into more detail on the magnet, gradient coils, RF coils, and RF detector on magnetic resonance imagers.

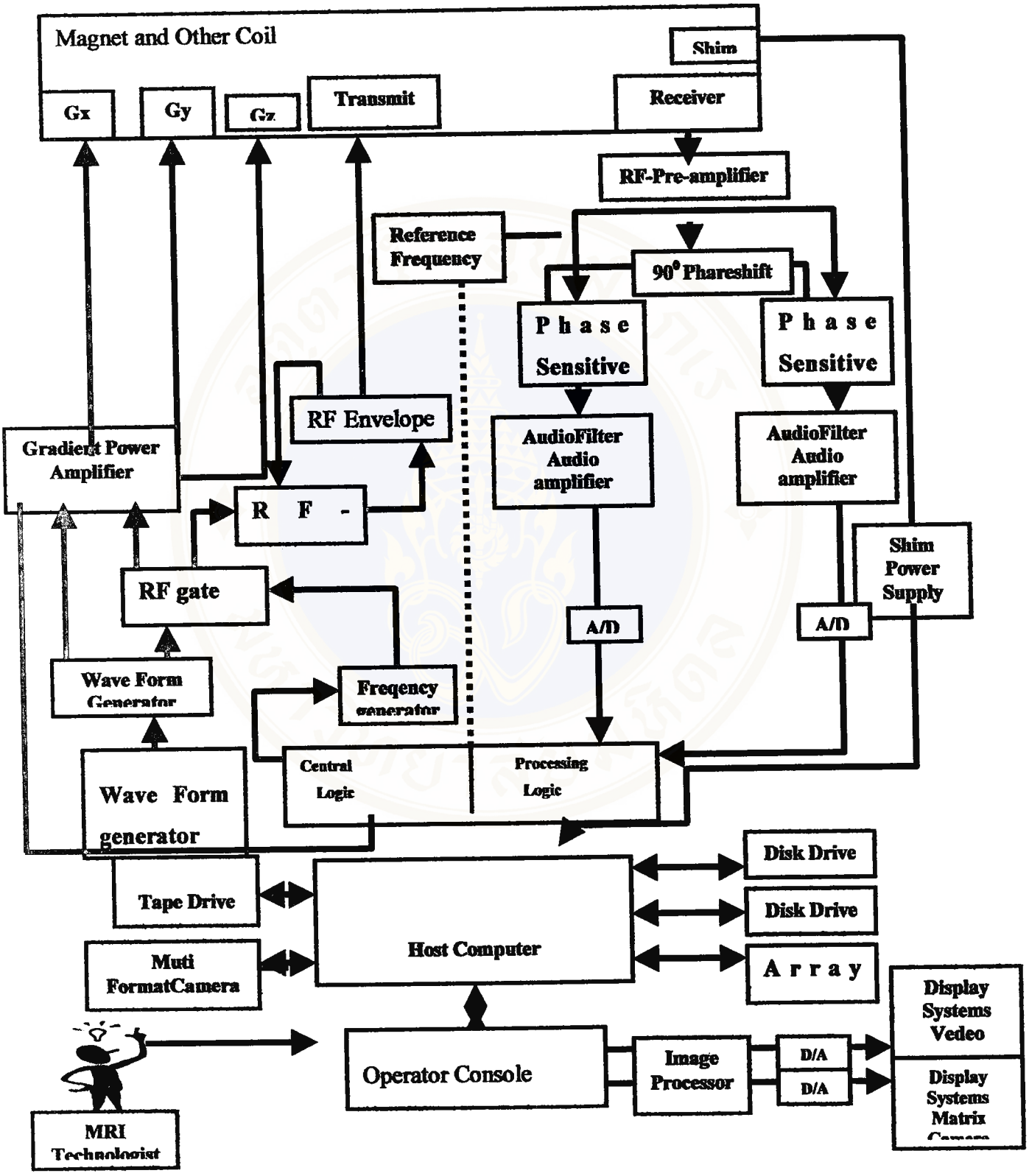

Figure 7-1.The major systems on a magnetic resonance imager and a few of the major interconnections.

7.2 Magnet (1,2,6,33,38,39)

The imaging magnet is the most expensive component of the magnetic resonance imaging system. Most magnets are of the superconducting type. A superconducting magnet is an electromagnet made of superconducting wire. Superconducting wire has a resistance approximately equal to zero when it is cooled to a temperature close to absolute zero (-273.15° C or 0 K) by emerging it in liquid helium. Once current is caused to flow in the coil it will continue to flow as long as the coil is kept at liquid helium temperatures. (Some losses do occur over time due to infinitely small resistance of the coil. These losses are on the order of a ppm of the main magnetic field per year.)

The figure 7-2 contains a cross sectional view of a superconducting imaging magnet. The length of superconducting wire in the magnet is typically several miles. The coil of wire is kept at a temperature of 4.2K by immersing it in liquid helium. The coil and liquid helium is kept in a large Dewar. This Dewar is typically surrounded by a liquid nitrogen (77.4K) Dewar that acts as a thermal buffer between the room temperature (293K) and the liquid helium.

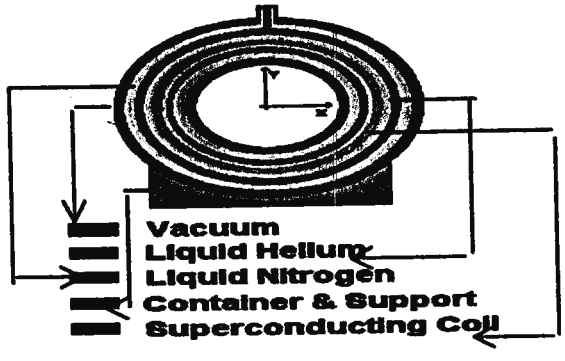

Figure7.2. The cross section superconductive magnets(38).

7.3 Gradient Coils (1,2,6,33,38,39)

The gradient coils produce the gradients in the Bo magnetic field. They are room temperature coils, which because of their configuration create the desired gradient. Since the horizontal bore superconducting magnet is most common, the gradient coil system will be described for this magnet.

Assuming the standard magnetic resonance coordinate system, a gradient in Bo in the Z direction is achieved with an antihelmholtz type of coil. Current in the two coils flow in opposite directions creating a magnetic field gradient between the two coils. The B field at one coil, called Maxwell's pair coil, adds to the Bo field while the B field at the center of the other coil subtracts from the Bo field (figure 7-3). The X and Y gradients in the Bo field are created by Golay's coils. The X axis figure-8 coils create a gradient in Bo in the X direction due to the direction of the current through the coils (figure 7-4). The Y axis figure-8 coils provides a similar gradient in Bo along the Y axis(figure7-5).

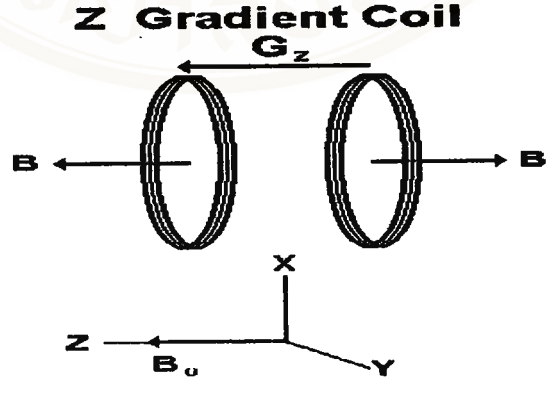

Figure 7.3 The Maxwell's pair coil (38).

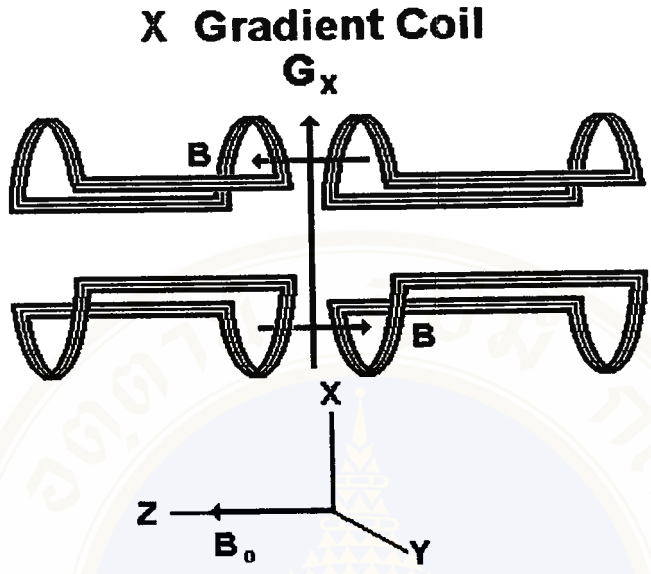

Figure 7-4.The Golay's coil (pair of figure-8 coil) creates a gradient in Bo in the X direction(38).

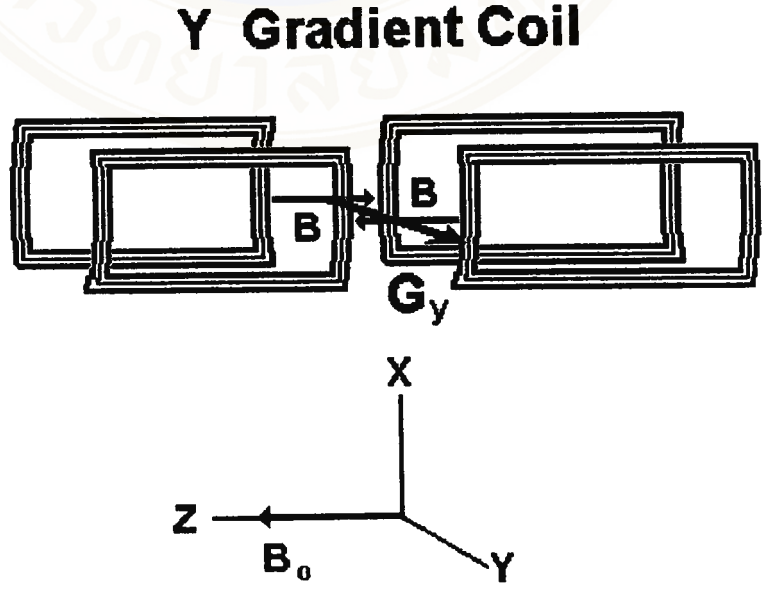

Figure 7-5.The Golay's coil (pair of figure-8 coil) creates a gradient in Bo in the Y direction(38).

7.4 RF Coils (1,2,6,33,38,39)

RF coils create the B_1 field, which rotates the net magnetization in a pulse sequence. They also detect the transverse magnetization as it processes in the XY plane. RF coils can be divided into three general categories; 1) transmits and receives coils, 2) receive only coils, and 3) transmit only coils. Transmit and receive coils serve as the transmitter of the B_1 fields and receiver of RF energy from the imaged object. A transmit only coil is used to create the B_1 field and a receive only coil is used in conjunction with it to detect or receive the signal from the spins in the imaged object. There are several varieties of each. The RF coil on an imager can be likened unto the lens on a camera. A photographer will use one lens for a close up shot and a different one for a wide angle long distance shot. Just as a good photographer has several lenses, a good imaging site will have several imaging coils to handle the variety of imaging situations, which might arise. An imaging coil must resonate, or efficiently store energy, at the Larmor frequency. All imaging coils are composed of an inductor, or inductive elements, and a set of capacitate elements. The resonant frequency,ω, of an RF coil is determined by the inductance (L) and capacitance (C) of the inductor capacitor circuit.

$$\omega = 1/2\pi\sqrt{LC}$$

Some types of imaging coils need to be tuned for each patient by physically varying a variable capacitor. The other requirement of an imaging coil is that the B_1 field must be perpendicular to the Bo magnetic field.

7.5 Solenoid coils(1,2,6,33,38,39)

Solenoid coil is one of the whole volume coils. Its advantages are the uniformity of field strength and the good sensitivity. However, its disadvantage is the limited direction of field strength in horizontal plane, then it is not appropriate for magnet design in MR imaging. Solenoid coils can be classified by purpose and design into 4 categories as followings:

7.5.1 Multi-turn Solenoid coil(1,2,6,33,38,39)

The multi-turn turn solenoid (figure 7-6) is useful for imaging large volume, such as the body and the abdomen.

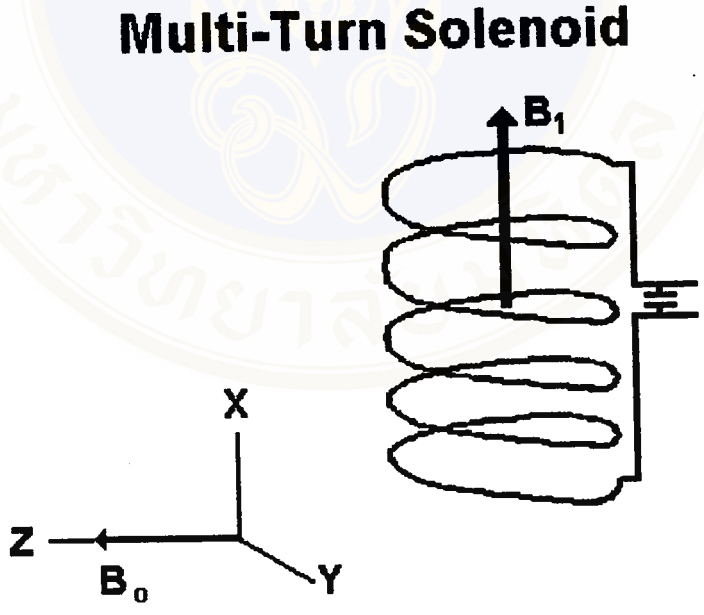

Figure7-6 The Multi-turn Solenoid (38).

7.5.2 Single Turn Solenoid (1,2,6,33,38,39)

The single turn solenoid (figure 7-7) is useful for imaging extremities, such as the breasts and the wrist.

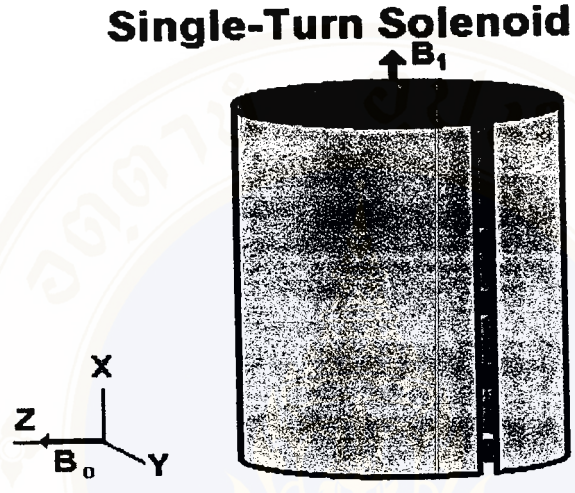

Figure 7-7 the single –turn Solenoid(38)

7.5.3 Surface Coil (1,2,6,33,38,39)

Surface coils (figure 7-8) are very popular because they are a receive only coil and have a good signal-to-noise ratio for tissues adjacent to the coil.

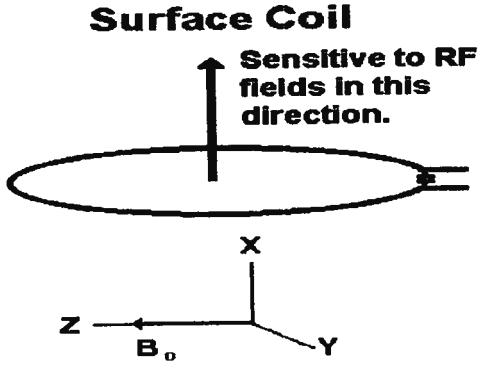

Figure 7-8 the surface coil (38).

7.5.4 Bird Cage Coil (1,2,6,33,38,39)

The bird cage coil (figure 7.9) is the coil of choice for imaging the head and brain.

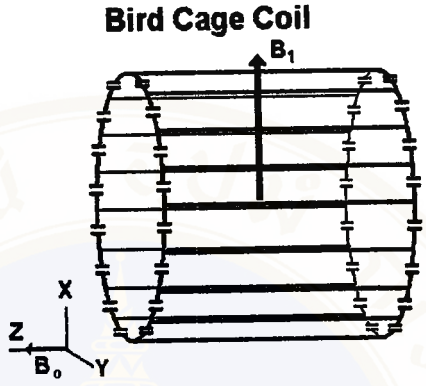

Figure 7.9. The bird cage coil(38).

7.6 Saddle Coil(1,2,6,33,38,39)

The multiturn solenoid, bird cage coil, single turn solenoid, and saddle coil (figure7-10) are typically operated as the transmitter and receiver of RF energy. The surface coil is typically operated as a receive only coil. When a surface coil is used, a larger coil on the imager is used as the transmitter of RF energy to producing the 90° and 180° pulses.

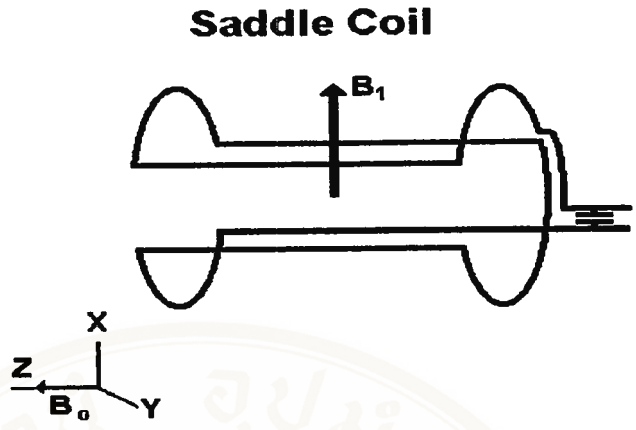

Figure 7-10 represented the saddle coil(38).

7.7 Quadrature detector (1,2,6,33,38,39)

The quadrature detector is a device which separates out the Mx' and My' signals from the signal from the RF coil. For this reason it can be thought of as a laboratory to rotating frame of reference converter. The heart of a quadrature detector is a device called a doubly balanced mixer (figure 7-11). The doubly balanced mixer has two inputs and one output. If the input signals are Cos(A) and Cos(B), the output will be 1/2 Cos(A+B) and ½ Cos(A-B). For this reason the device is often called a product detector since the product of Cos(A) and Cos(B) is the output. The quadrature detector typically contains two doubly balanced mixers, two filters, two amplifiers, and a 90° phase shifter (figure7-12). There are two inputs and two outputs on the device. Frequency ω and ωo are put in and the MX and MY components of the transverse magnetization come out. There are some potential problems, which can occur with this device, which will cause artifacts in the image. These will be addressed in Chapter 10.

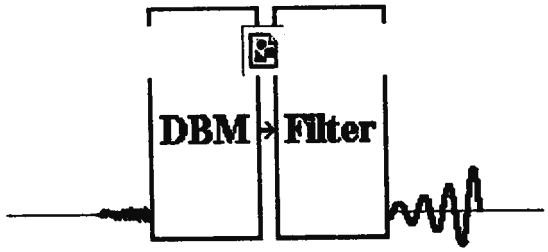

Figure 7-11. The function of doubly balanced mixer.

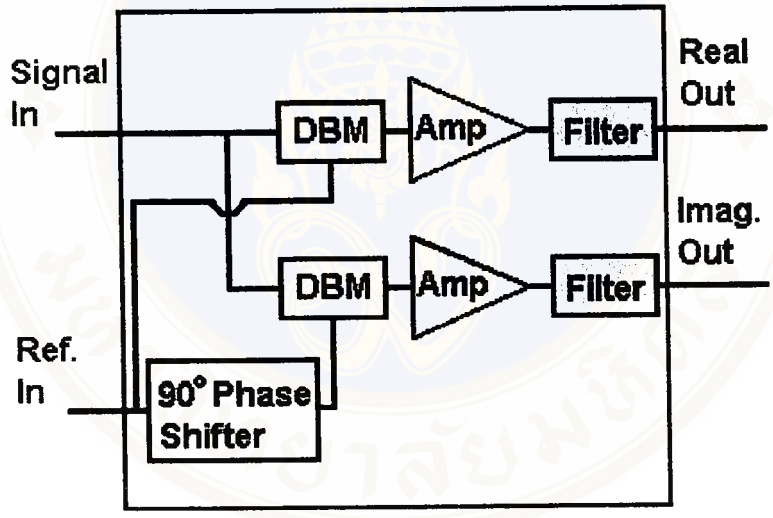

Figure 7.12 The schematics of quadrature detector typically contains two doubly balanced mixers, two filters.

CHAPTER VIII

ADVANCE IMAGING TECHNIQUES

8.1 Introduction

A new application of MRI or a new pulse sequence which opens up new imaging opportunities with MRI seem to be developed each year. This chapter will be mentioned some of these techniques. Each of the entries is not covered in depth due to space limitations. The reader is directed to the cited literature references for more detailed information.

8.2 Volume Imaging (3-D Imaging) (1,2,6,33,38,39,40)

Volume imaging is the acquisition of magnetic resonance data from a volume rather than a tomographic slice. It can be thought of as collecting several contiguous slices through a region of imaged object (figure8-1).

Figure 8-1 The single slice and the contiguous slice(38).

The number of contiguous slices will always be a multiple of 2. The actual timing diagram for a volume imaging pulse sequence looks like in the figure 8-2. There is a volume selection RF pulse and gradient which rotates only those spins in the imaged volume of the object. This combination of pulses is equivalent to a slice selection combination except the slice thickness may be 10 or 20 cm. The volume selection pulses are followed by a phase encoding gradient in dimension and another one in dimension 2. Each is varied between a maximum and minimum value, just as all the phase encoding gradients have been. The two gradient pulses are applied at the same time and are cycled through all possible combinations. The frequency encoding gradient has its dephasing negative lobe to cause the spins to be in phase at the center of the acquisition window. The frequency encoding gradient is applied and a signal recorded, just as it has been in all the previous sequences. The imaging time is equal to the product of the TR value times the number of phase encoding steps in dimension 1 times the number of steps in dimension 2. Because of this large value, a gradient recalled echo sequence is typically used for volume imaging.

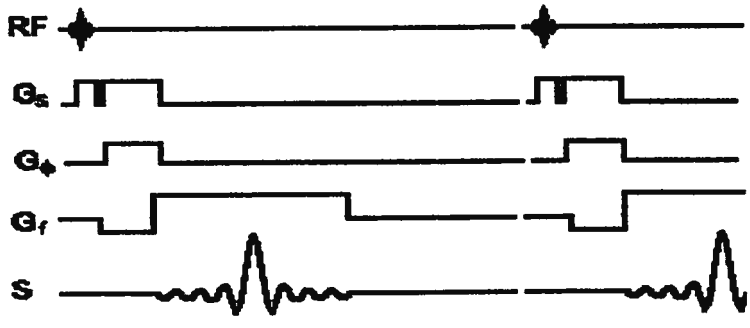

Figure 8-2.The timing diagram of volume imaging.

8.3 Flow Imaging (MRI Angiography) (1,2,6,33,38,39,40)

Angiography is the imaging of flowing blood in the arteries and veins of the body. In the past, angiography was only performed by introducing a x-ray opaque dye into the human body and making an X-ray image of the dye. This procedure produced a picture of the blood vessels in the body. It however did not produce an image which distinguished between static and flowing blood. It was therefore a less than adequate technique for imaging circulatory problems. Magnetic resonance angiography (MRA) on the other hand produces images of flowing blood. The intensity in these images is proportional to the velocity of the flow. There are two general types of MRA, time-of-flight and phase contrast angiography. They are described next.

8.3.1 Time-of-Flight Angiography (1,2,6,33,38,39,40)

Time-of-flight angiography can be performed in several ways. One method uses a spin-echo sequence where the slice selective 90° and 180° pulses have different frequencies. The 90° pulse excites spins in one plane. The 180° pulse excites spins in another plane. In the absence of flow, no signal is seen because no spins experience both the 90° and 180° pulses. In the presence of flow and the correct TE time, blood from the 90° plane flows into the 180° plane and produces an echo.

Recall the following flow artifact description from Chapter 10. When the blood experiencing the 90° pulse does not experience the 180° pulse, no echo is observed (figure 8-3). If the spice location of the 180° pulse is now changed to match the

location of the blood which experienced the 90° pulse only that blood will contribute to the echo signal (figure 8-4).

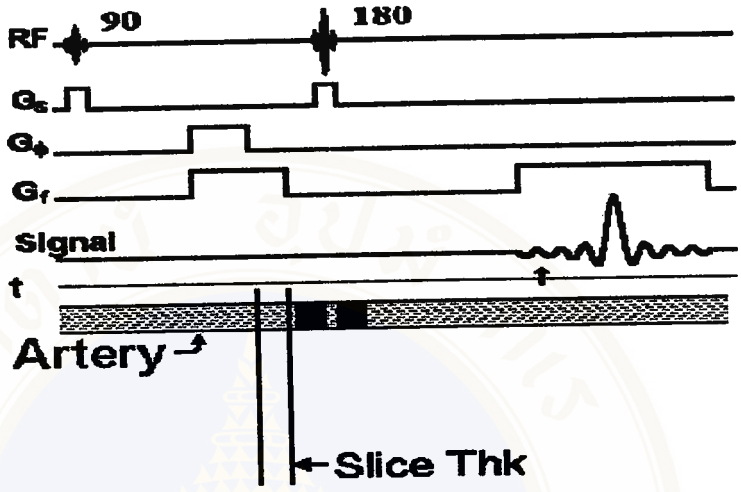

Figure 8-3.Blood experiencing the 90° pulse does not experience the 180° pulse, no echo is observed (38).

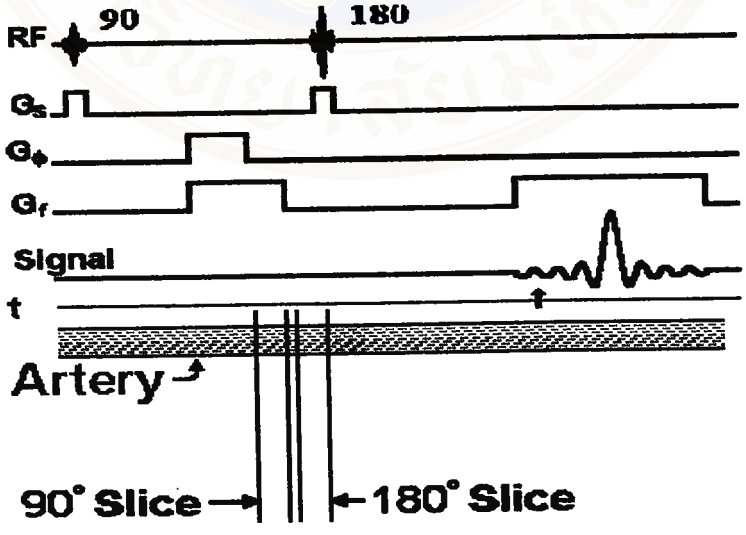

Figure 8-4. The spice location of the 180° pulse is now changed to match the location of the blood which experienced the 90° pulse only that blood will contribute to the echo signal(38).

8.3.2 Phase Contrast Angiography(1,2,6,33,38,39,40)

Phase contrast angiography is a little more complicated. The first new concept which you need to understand is that of a bipolar magnetic field gradient (GBP) pulse. A bipolar gradient pulse is one in which the gradient is turned on in one direction for a period of time then turned on in the opposite direction for an equivalent amount of time. A positive bipolar gradient pulse has the positive lobe first and a negative bipolar gradient pulse has the negative lobe first. The area under the first lobe of the gradient pulse must equal that of the second (figure8-5). A bipolar gradient pulse has no net effect on stationary spins. Spins which have a velocity component in the direction of the gradient will be effected by the bipolar gradient pulse. For example, a stationary spin exposed to the first lobe of the bipolar gradient pulse will acquire a phase in radians given by

$$\phi_A = 2\pi\gamma \int x\, G_{BP}\, dt$$

and

$$\phi_B = -2\pi\gamma \int x\, G_{BP}\, dt$$

from the second lobe. If G_{BP} of the two lobes are equal and the positions are equal during the two pulses the phase acquired from the A lobe equals that from the B lobe.

If this bipolar gradient pulse is placed in any one of the imaging sequences, in addition to the other gradients, it will not effect the image since all we have done is imparted a phase shift to the moving spins. Since an image is a magnitude

representation of the transverse magnetization there is no effect. However if two imaging sequences are performed in which the first has a positive bipolar gradient pulse and the second a negative bipolar gradient pulse, and the raw data from the two is subtracted, the signals from the stationary spins will cancel and the flowing blood add. Look at the animation to convince yourself of this. A positive bipolar gradient pulse will have this effect on stationary and flowing spins, compared to a reference spin experiencing no gradient (figure8-6). A negative bipolar gradient pulse will have this effect on the same stationary and flowing spins (figure8-7).

If the vectors (and hence signals) from the positive and negative bipolar gradient pulses are subtracted, the vectors from the stationary spins cancel and the moving spins have a net magnitude (figure 8-8). The net effect is an image of the flowing spins. From this animation it is easy to see that for optimum signal, you would like the vectors from the fastest flowing blood to acquire 90° of phase from each bipolar gradient pulse. Spins with lesser flow rates will acquire lesser phase shifts. The direction of the bipolar gradient yields signal from only those spins with a component in that direction.

A pulse sequence for one phase encoding gradient step of a phase contrast angiography sequence looks like in the figure 8-9. Signals from the two parts are subtracted and used to produce that phase encoding line of the raw data.

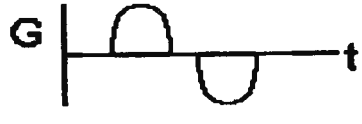

Figure8-5 The bipolar gradient(38).

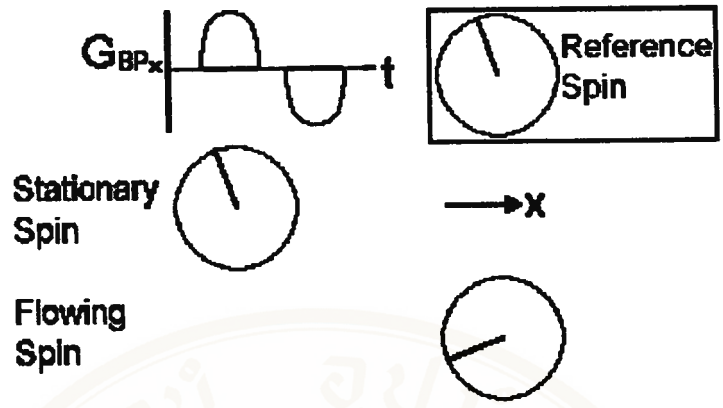

Figure8-6. The relationship between station spin, flowing blood and using bipolar gradient(38).

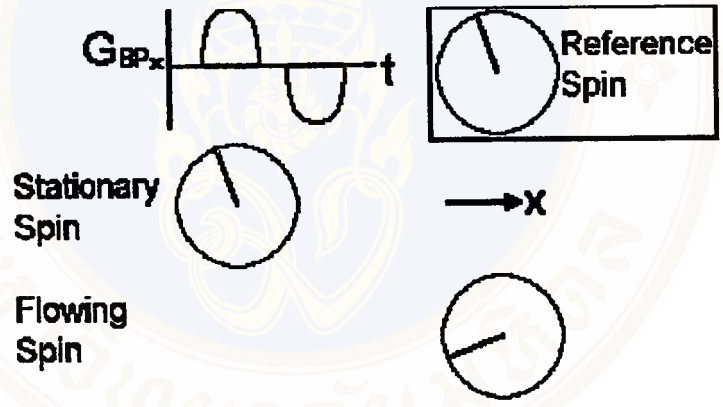

Figure8-7.The relationship between stationary spin, flowing blood and bipolar gradient when we alternative negative bipolar gradient and positive bipolar result it change phase shift between stationary spin and flowing blood(38).

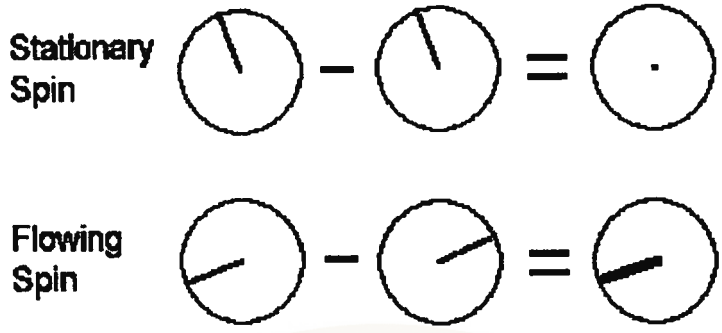

Figure8-.8. The vectors from the positive and negative bipolar gradient pulses are subtracted, the vectors from the stationary spins cancel and the moving spins have a net magnitude(38).

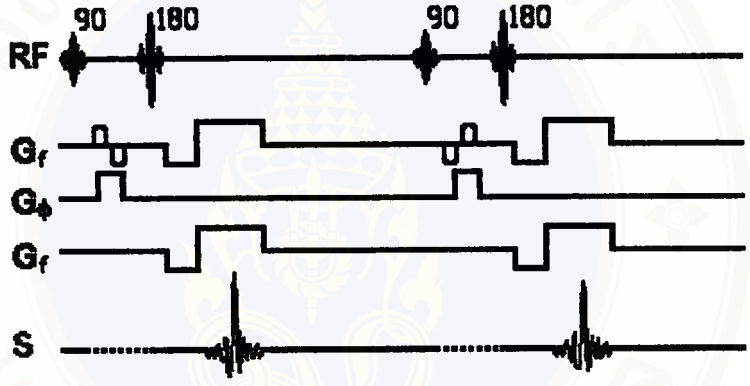

Figure8-9. A pulse sequence for one phase encoding gradient step of a phase contrast angiography sequence(38).

8.4 Diffusion Imaging(38,41)

Diffusion imaging can be performed in a manner identical to the phase contrast angiography sequence. The major difference is that the gradients must be increased in amplitude so as to image the much slower motions of molecular diffusion in the body.

8.5 Fast Spin-Echo Imaging (1,2,6,33,38,39,40)

A fast spin echo imaging sequence is a multi-echo spin-echo sequence where different parts of k-space are recorded by different spin-echoes. For example we might have a four echo spin-echo sequence with a TE of 15 ms (figure8-10). The k-space will be divided into four sections. The first echo is used to fill the central part, lines 96-160, of k-space. The second echo is used for lines 64-96 and 160-192. The third echo fills lines 32-64 and 192-224. The last echo fills lines 1-32 and 224-256 of k-space. There are some problems with the steps between the parts of k-space, but since there is little data in these regions the steps can be corrected for. The benefit of the technique is that a complete image may now, as was shown in this example, be recorded in one fourth of the time.

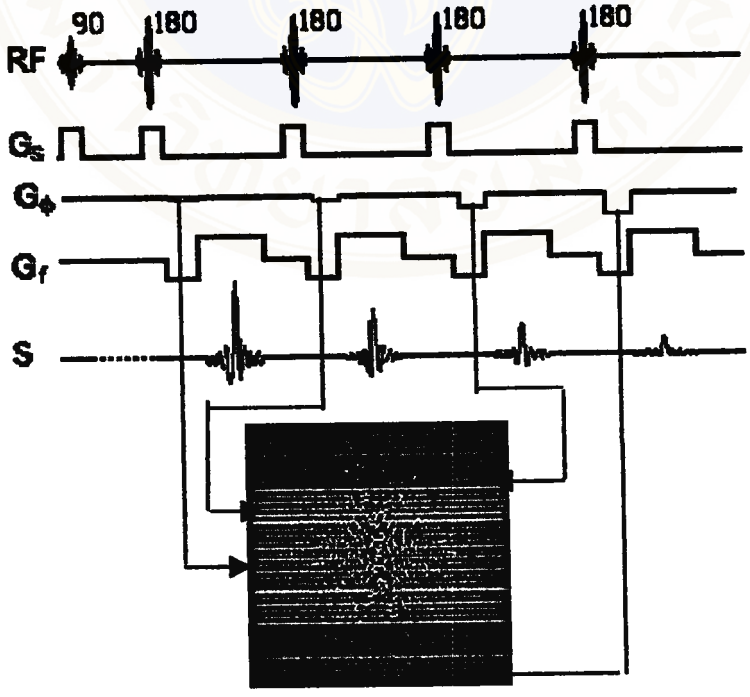

Figure 8-10. The timing diagram for fast spin-echo imaging(38).

8.6 Chemical Shift Imaging (Fat Suppression) (1,2,6,33,38,39,40)

Chemical shift imaging is the production of an image from just one chemical shift component in a sample. For example if the object being imaged is composed of water and fat hydrogens, each with a different chemical shift, a chemical shift image would be an image of either the fat or water in the object. Since most routine chemical shift imaging is done to suppress the fat signal it is often times referred to as fat suppression imaging. There are several methods of performing chemical shift imaging, the two which are covered here the inversion recovery method and the saturation method.

In the inversion recovery method an inversion recovery imaging sequence is used and the TI time is set to T1 ln2 where T1 is the spin-lattice relaxation time of the component one wishes to suppress. For fat suppression that component is fat, for water suppression it is water. This technique only works when the T1 values for the two components are different (figure8-11).

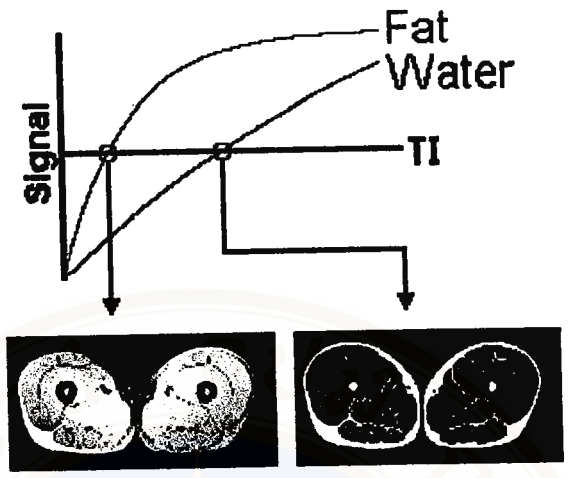

Figure 8-11.The signals between water and fat when we using the inversion recovery pulse sequence (38)

In the saturation method a frequency selective saturation pulse is applied before the standard imaging pulses of a sequence, for example a spin-echo sequence. The saturation pulse sets to zero the magnetization from the component we wish to suppress. When the standard imaging sequence follows it detects no signal from the suppressed component. The accompanying animation shows an RF timing diagram for the sequence (figure8-12). The saturation pulse consists of the frequency selective pulse which causes the Z magnetization for a specific chemical shift to be zero. In the case of a fat saturation sequence, this chemical shift compound is fat. This pulse is followed by a dephasing gradient to force the transverse magnetization from this chemical shift component to zero. The saturation pulse is followed by, in this example, a spin-echo sequence. This technique works best when the T1 for the suppressed sequence is long compared to the time between the saturation pulse and the spin echo sequence.

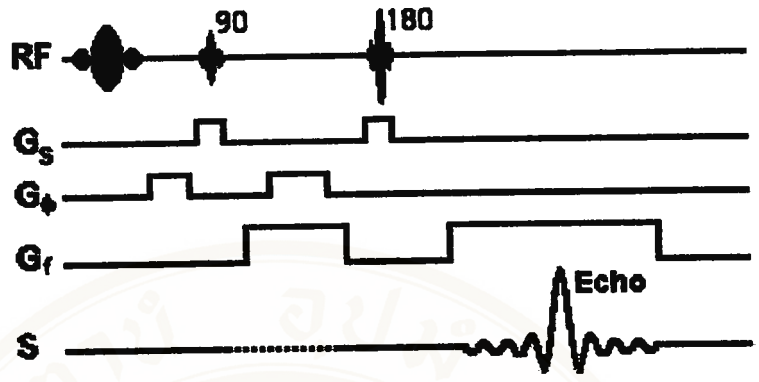

Figure 8-12 The timing diagram for suppression techniques

8.6 Echo Planar Imaging (Functional MRI)(36,38)

Echo planar imaging is a rapid magnetic resonance imaging technique which is capable of producing tomographic images at video rates. The technique records an entire image in a TR period. To understand echo planar imaging it is helpful to understand the concept of k-space. A magnetic resonance image is referred to as image space. Its Fourier transform is referred to as being k-space. In magnetic resonance imaging, k-space is equivalent to the space defined by the frequency and phase encoding directions. Conventional imaging sequences record one line of k-space each phase encoding step. Since one phase encoding step occurs each TR seconds the time required to produce an image is determined by the product of TR and the number of phase encoding steps. Echo planar imaging measures all lines of k-space in a single TR period. A timing diagram for an echo planar imaging sequence is represented in the figure 8.13. There is a 90° slice selective RF pulse which is applied in conjunction with a slice selection gradient. There is an initial phase encoding gradient pulse and an initial frequency encoding gradient pulse to position

the spins at the corner of k-space. Next there is a 180° pulse. Since the echo planar sequence is typically a single slice sequence, the 180° pulse need not be a slice selective pulse. The phase and frequency encoding directions are next cycled so as to transverse k-space. This is equivalent to putting 128 or 256 phase and frequency encoding gradients in the usual period when the echo is recorded. If we zoom into this region of the timing diagram it will be clearer(figure8-14). You can see that there is a phase encoding gradient, followed by a frequency encoding gradient, during which time a signal is recorded. Next there is another phase encoding gradient followed by the reverse polarity frequency encoding gradient during which time a signal is recorded. Looking at the k-space trajectory map at the same time as we are zoomed into the phase and frequency encoding gradient area we can see how the gradients trace out k-space(figure8-15). The rate at which k-space is traversed is so rapid that it is possible, depending on the image matrix, to obtain 15 to 30 images a second. This is video rate acquisition.

When echo planar imaging was first developed, it was thought that echo planar imaging would have its greatest impact in providing real time magnetic resonance images. Its greatest application appears to be in the area of functional MRI of the brain. Functional imaging is imaging which relates body function or thought to specific locations in the brain. During brain activity there is a rapid momentary increase in the blood flow to the specific thought center in the brain. For example when you move your right index finger there is a rapid momentary increase in the circulation of the specific part of the brain controlling that movement of the finger. The increase in circulation means an increase in oxygen which is paramagnetic which

affects the T1 and T2 of the local brain tissues. The difference in T1 and T2 relative to surrounding tissues causes a contrast between the tissues.

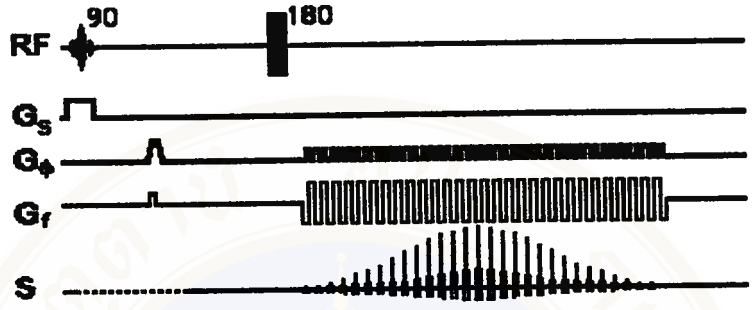

Figure8.13. The timing diagram for echo planar imaging pulse sequence(38).

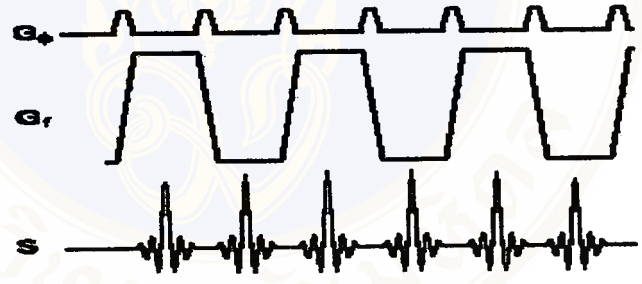

Figure8.14 The timing diagram of gradient (see more detail in the text)(38).

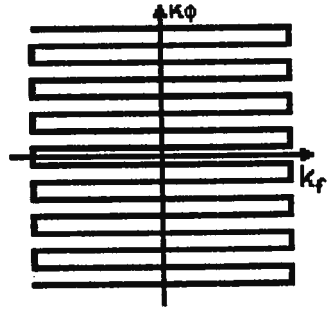

Figure 8.15 The trajectory in k-space of EPI(38).

8.7 Spatially Localized Spectroscopy (38)

Spatially localized spectroscopy is the application of RF pulses and gradients to produce a spectrum from a specific voxel in an object. The easiest demonstration of this is the following multi-echo sequence (figure8-16). A slice selective RF pulse is applied in conjunction with a X magnetic field gradient. This excites spins in an YZ plane. A 180° slice selective RF pulse is applied in conjunction with a Y magnetic field gradient. This rotates spins located in an XZ plane. A third 180° slice selective RF pulse is applied in conjunction with a Z magnetic field gradient. The second 180° pulse excites spins in a XY plane. The second echo is recorded as the signal. This echo represents the signal from those spins in the intersection of the three planes. Fourier transforming the echo produces an choice of the X, Y, and Z gradients the signal voxel can be positioned anywhere in the imaged object.

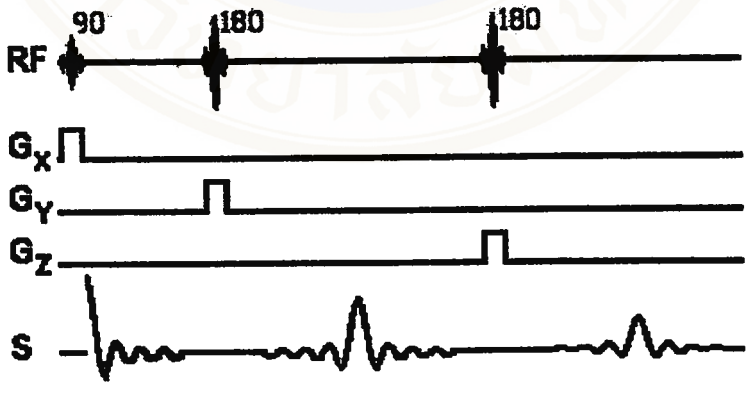

Figure 8.16 The timing diagram of multi-echo imaging.

8.8 Chemical Contrast Agents(42)

A chemical contrast medium is a substance which is introduced into the body to change the contrast between the tissues. The contrast is changed by varying the T1 and T2 of the tissues. The T1 and T2 values are changed by changing the number of fluctuating magnetic fields near a nucleus at the Larmor frequency. A typical chemical contrast media is a complex of a paramagnetic metal ion such as gadolinium (Gd). The paramagnetic field creates many oscillating fields as it tumbles through a water environment. Unfortunately gadolinium is toxic. To lessen its toxic effects the gadolinium is complexed to various organic complexing agents. Some of the complexes can be shown in the figure 8.17, 8.18 and 8.19 respectively.

Gd-EDTA

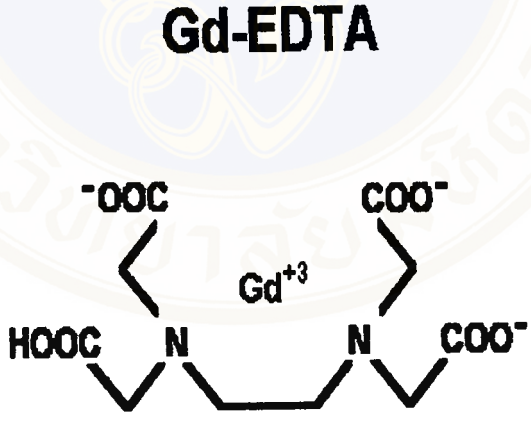

Figure 8.17 . The molecule of Gd-EDTA

Gd-DTPA

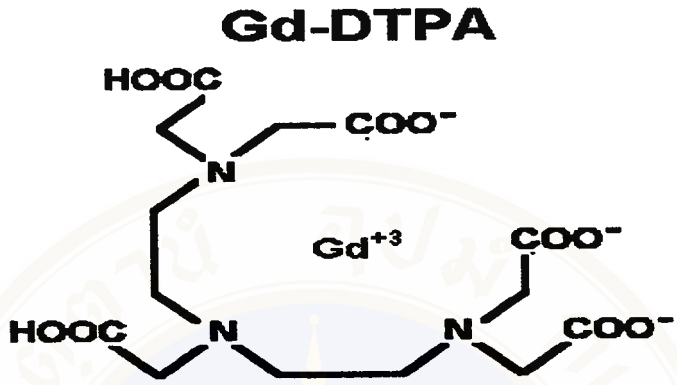

Figure 8-8 The molecule of Gd-DTPA.

Gd-DOTA

Figure 8.19.The Gd-DOTA

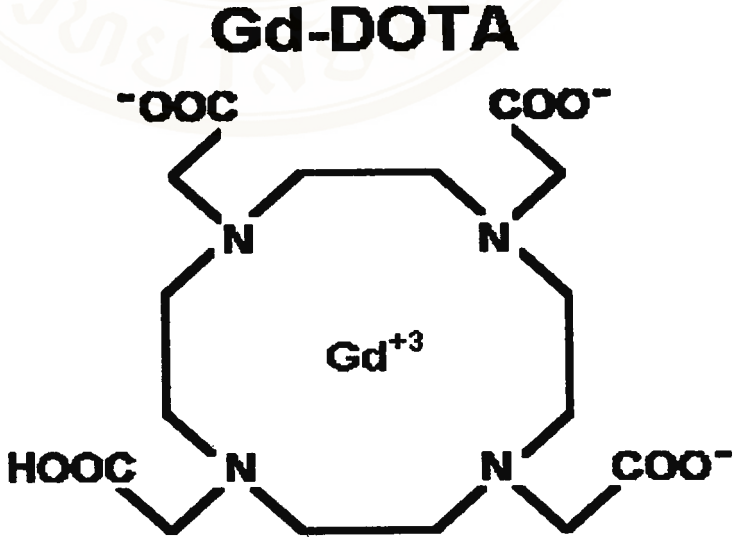

After the injection of Gd into a tissue, the concentration of Gd increases then starts to decrease as it is eliminated from the tissues. A contrast enhancement is obtained by one tissue having a higher affinity or vascularity than another. Most tumors for example have a greater Gd uptake than the surrounding tissues, causing a shorter T1 and a larger signal.

8.9 Magnetization Transfer Contrast(38)

Magnetization transfer contrast is a new method of increasing the contrast between tissues by physical rather than chemical means. For this technique to be effective, there must be at least two spin systems in the imaged anatomy which are capable of exchanging energy between themselves and one of the systems must have a much shorter T2 than the other system. The pulse sequence looks very similar to the fat saturation imaging sequence described earlier in this chapter. A saturation pulse is applied with a frequency approximately 1 kHz from the center frequency. The saturation pulse is followed by a gradient-echo or spin-echo sequence (figure8.20).

The two spin systems could be protein and water. The protein has a very short T2 relative to the water T2. Because of the inverse relationship between T2 and the spectral linewidth, the NMR spectra of these two spin systems would have a very broad peak from the protein and a very narrow peak from the water(figure8-21). The signal from the protein will therefore not be visible in the image due to its broad linewidth which causes its signal to be spread out over the entire image. Applying the saturation pulse (figure8.22) 1 kHz away from the center of these peaks could directly saturate the protein spin system and not the water. Any water molecules in contact with the protein may be capable of exchanging magnetization with the protein.

Therefore saturating the protein will affect the signal of the water and the contrast between water in contact with the protein and not.

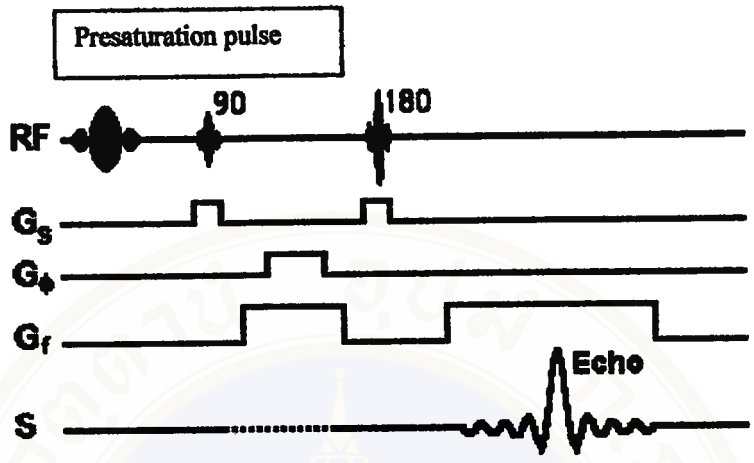

Figure 8.20. The timing diagram of the presaturation pulse

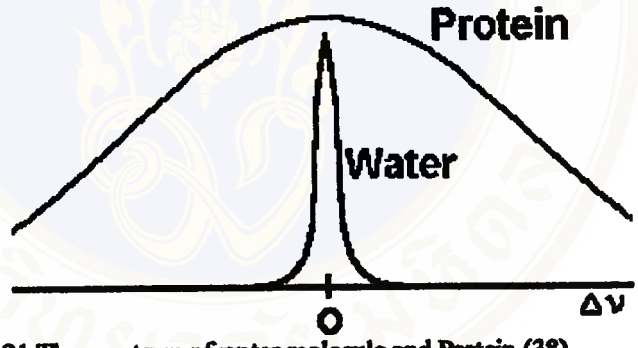

Figure8.21 The spectrum of water molecule and Protein (38).

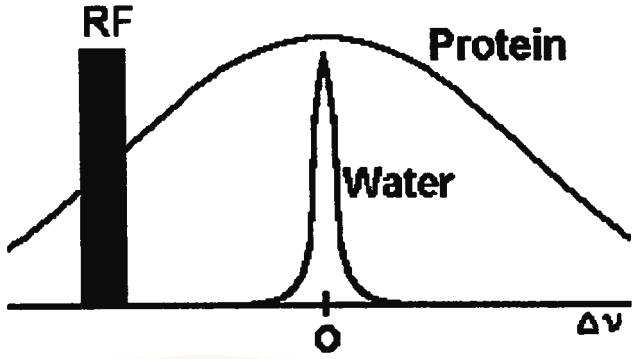

Figure8-22 The RF presaturation of Magnetization transfer contrast.

8.11 Variable Bandwidth Imaging(38)

The amount of noise in an image is related to the sampling frequency of the FID or echo. The higher the sampling rate the more noise in the image. Similarly, lowering the sampling frequency allows less noise in the image. In the interest of improving the signal-to-noise ratio in an image, it is advantageous to use the smallest possible sampling rate. Since the sampling rate, fs, is related to the field of view (FOV) the frequency encoding gradient, Gf, must be lowered proportionately to the sampling frequency in order to keep the FOV constant.

$$FOV = fs / \gamma Gf$$

Here is what the timing diagram would look like for a spin-echo sequence using a fast sampling frequency, and a slow sampling frequency. There are three disadvantages associated with the use of a slower sampling frequency.

1. An increase in the chemical shift artifact. (See Chapter 10.)
2. A loss of contrast.
3. A restricted range of echo times, TE.

CHAPTER IX

PRACTICAL CONSIDERATION IN MR IMAGING

9.1 Introduction

MR image quality is judged by clinical efficacy, not by visual appearance. Magnetic resonance images are the result of a complex interaction of extrinsic (i.e. selectable) and intrinsic (i.e. patient characteristic) factor which produce an image with sufficient spatial resolution and object contrast to permit a physician to complete a diagnostic evaluation. This confluence permits manipulation of the image acquisition parameters to maximize clinical efficacy in a specific area of an image at expense of overall image appearance.

The intrinsic factors include proton density (PD), T1 relaxation time, T2 relaxation time, magnetic susceptibility and flow phenomena. The proton density, T1, and T2 can be seen more detail in the chapter 3, the magnetic susceptibility in the chapter 10 and the flow phenomena in the chapter 8 respectively.

The extrinsic factors include repetition time (TR), echo time (TE), field of view (FOV), matrix size, number of signal average(NEX or NSA), magnetic field strength ,properties of the detection coils and magnetic field inhomogeneities.

This chapter is mentioned some extrinsic factors and provided a basis for the understanding the relationships between them.

9.2 Image quality(43,44,45)

A magnetic resonance image is composed of small elements (pixels) which its gray-scale intensity (brightness) is related to the amplitude of the MR signal arising from corresponding volume elements (voxels) in the tissue slice. The more the signal intensity emitted by the voxel, the more the corresponding pixel-brightness in the image.

For an image to be diagnostically useful, anatomic features within the image must be distinguishable from the others. For optimizing the image quality (include contrast, spatial resolution, signal-to-noise ratio, and reduced artifacts) and the imaging speed in order to find the most appropriate balance, the MR user can select many parameters, such as geometric characteristic of slices, pulse sequence, scan mode, artifact reduction techniques, etc.

Ideally, an image would have high signal, low noise, high spatial resolution, excellent contrast and no artifacts. However, to achieve optimum conditions the trade-off including consideration of imaging time is required. The required steps to improve spatial resolution and signal-to noise ratio generally result in longer imaging time.

9.3 Voxel size and spatial resolution(43,44,45)

The image matrix defines the number of pixels used to construct an image, determined by steepness of the read-out gradient (x-axis) and number phase-encoding steps used (y-axis) for given field of view (FOV). The actual volume of each voxel is determined by field of view, the maxtrix size and the selected slice thickness. The equation below demonstrates the relationship between FOV, maxtrix size and slice thickness.

$$W = FOV(mm)/\ matrix\ size(64,128,256,etc.)$$

Where W is the spatial resolution

Spatial resolution defines the ability to resolve the closely spaced anatomic details. Since the radio frequency signals from nuclei in a voxel are averaged, the detail within a voxel are lost during image acquisition and reconstruction. The larger the voxel dimensions, the greater the amount of unresolved fine detail. However, resolution alone does not determine a distinguishable detail, an image-contrast and signal-to-noise ratio are also the determined factors.

Field homogeneity and the steepness of the gradients which is employed to control the spatial resolution can be increase until the voxel become so small, but the too small voxel is the limiting factor of the signal-to-noise ratio. Resolution equals to the field of view (FOV) divided by the image matrix.

9.4 Signal-to-noise ratio(43,44,45)

The brightness of each pixel in an MR image is determined by the signal intensity of its corresponding voxel in the tissue slice. However, the detection coil in an MR imaging system also detects RF emission from tissue surrounding the voxel. This RF noise results from small, random electrical current within the detection volume, reducing the ability to distinguish between contrast anatomical features. In magnetic resonance imaging, the presence of background noise is the limiting factor in the detection of very weak signal.

In addition to the noise generated from within the patient, the RF coils also generate frequency-dependent noise through the resistance of the coil. This effect decreases as the strength of the applied static magnetic field increases.

The signal-to noise ratio (SNR) is a function of both operation and data processing parameters. While data processing procedure (data filtering, sampling rate, zero filling, truncation,etc.) affect the signal-to-noise ratio, they are never as effective as reducing noise collection or increasing the relative signal to begin with.

The following operational parameter exert considerable influence on the SNR: voxel size, signal averaging, pulse sequence timing (TE, TR, flip angle), Magnetic field strength, RF coils halfscan reduced scan ,and water-fat shift.

9.5 Signal Averaging (43,44,45)

Signal averaging means that signal are measured more than once and the signal from successive measurements are summed, producing a total intensity which increases linearly with the number of measurements. Noise, however, is a random process, whose intensity increases only as the square root of the number of averages. Therefore, by increasing the number of signal averages (NSA) from 1 to n the SNR improves by square root n

9.6 Pulse sequence parameters(43,44,45)

The magnitude of the transverse magnetization in an imaging voxel is a function of proton density and inherent relaxation phenomena. The dependence on the proton density is obvious. The more nuclei present, the greater the signal.

The signal magnitude is also a function of T1 and T2 relaxation process which control the magnitude and rate of decay of transverse magnetization. By adjust RF pulse timing you can optimize SNR in a certain scan time. In spin echo measurement,

two pulse timing parameters affect the magnitude of the MR signal: the repetition time(TR), and the echo time(TE.)

The rate of recovery of the longitudinal magnetization is characterized by the T1 relaxation time, and the degree of recovery at the end of TR determined by the relationship of the repetition time toT1 relaxation time.A short TR, one which is approximately the same as the shortest T1 of interest, reduces the signal intensity, and since noise remains fixed, the SNR decreases For example, at TR approximately T1 , the net magnetization has recovered to only about 63% of its maximum value. Of course, a short TR reduces the total imaging time, hence its use may be advantageous in specific studies.

The intensity of the MR signal is also dependent on the degree of spin-spin relaxation which has occurred, characterized by the T2 relaxation time. The longer T2 dispersion evolves, the weaker the net magnetization in the transverse plane. A long TE, one which is approximate equivalent to the T2 relaxation time, produces an image whose relative contrast is primarily dependent on differences in T2 relaxation rate(i.e. T2-weightd), and which has greatly reduced signal intensity. At TE approximately T2, the relative signal intensity is only a bout 37% of its maximum value.

9.7 Magnetic field strength (43,44,45)

Although this parameter is fixed in a given MR system, it is important to understand that signal strength varies as the square of the applied field. Noise id also a

function of field strength, increasing linearly with field strength. Form this, it follows that the SNR improves linearly with applied field strength.

9.8 Effect of the coils(43,44,45)

As discussed, the detection coils are sensitive to noise from surrounding tissue, with the magnitude of the noise related to the detection volume. While only the imaging slice is actively excited during an MR measurement, a much larger volume of the body is actually present in the detection volume of a coil. Thus, the physical configuration-size and shape of the RF coil affects the relative magnitude of the noise.

Surface coils, with their smaller sensitive volume provide a higher ratio of signal relative to background noise when compared to a volume coil such as the body coil. The size of the body coil and its distance from the patient permits a much greater contribution of noise from out side the selected slice.

In summary in this chapter, many factors are influenced image quality. Some factors can be control and eliminate. Many factors can not be eliminate such as MR artifacts but we can reduce them for improve image quality. The next chapter in this thesis will mention the more detail and suggestion the reduction techniques of MRI artifacts.

CHAPTER X

IMAGE ARTIFACTS AND REDUCTION TECHNIQUES

10.1 Introduction

An image artifact is any feature, which appears only in an image but not really presents, in the original imaged object. An image artifact is sometime resulted from improper operation of the imager, and other times from a cause of natural processes or properties of the human body. Artifacts are typically be classified by their sources. They can interfere with the correct interpretation of MR images. So it is critical for operator to be able to minimize or eliminate them whenever possible, and for radiologist to be able to distinguish false from true detail and to identify the nature and cause of a particular artifact.

This chapter is consolidated about the available MRI artifacts which can be classified according to their sources into 7 categories as followings: static magnetic field artifacts, radio-frequency field artifacts, data acquisition and gradient artifacts, motion and flow artifacts, pulse sequence related-artifacts, and artifacts in fast imaging techniques and their MRI reduction techniques.

10.2 Static magnetic field inhomogeneity

10.2.1 B_0 inhomogeneity or nonuniformity (1, 2, 6, 46, 47)

When the magnetic field inhomogeneity is mentioned, we consider its components into 2 parts including the main magnetic field and static or

radiofrequency (RF) field. In the part of static or radiofrequency, artifacts will be mentioned on the next section.

Let us first deal with main magnetic field inhomogeneity. Magnetic field inhomogeneity or nonuniformity is important to avoid the nonuniform RF excitation due to the off-resonance effects and to avoid the rapid spin dephasing across a voxel before accomplishing the frequency encoding. Thus field-strength homogeneity is expressed with range of Larmor frequencies (in part per million) for a variety of sizes of imaging regions. Good uniformity is a result of quality of the design of the main field coils and also of how many correction coils, called shim coils, which have been included in the design.

All magnetic resonance imaging assumes a homogeneous Bo magnetic field. An inhomogeneous Bo magnetic field will cause the distorted images. The distortions can be either spatial, intensity, or both. Intensity distortions result from the field homogeneity in a location being greater or lesser than that in the rest of the imaged object. The T2* in this region is different, and therefore the signal will tend to be different. For example, if the homogeneity is less, the T_2* will be smaller and the signal will be less. Spatial distortion results from long-range field gradients in B_0 that are constant. They cause spins to resonate at Larmor frequencies other than that prescribed by an imaging sequence. The figure 10-1 illustrates the artifacts that occurred from main magnetic field inhomogeneity.

Figure 10-1 Effect of static magnetic field gradient caused by poor x shim, causing image-shading (36).

10.2.2 Susceptibility Artifacts (1, 2, 6, 35, 48)

Magnetic susceptibility is defined as the ratio of intensity of magnetization produced in a substance to the intensity of the applied the external field. Difference in magnetic susceptibility result in local field inhomogeneities. Ferromagnetic artifact is common extreme example of susceptibility artifact. Less pronounced effects can be seen at interfaces between paramagnetic and diamagnetic substances with different susceptibilities such as air, bone, tissue and blood product.

Variable magnetic susceptibility can cause both geometric and signal intensity distortions. Local field inhomogeneities cause spatial misregistration by altering the linear frequency-position relationship generated by the readout gradient. This produces image distortion that is most pronounced along the frequency-encoding axis. Geometric distortion caused by local gradient nonlinearity is associated with both signal attenuation and compression.

Local field inhomogeneities from magnetic susceptibility differences promote spin dephasing and signal loss. This phenomenon is accentuated with along TE, which allows for greater dephasing before signal readout. Because a gradient echo sequence lacks a 180^0 refocusing pulse, it is more sensitive to signal loss from dephasing. Susceptibility artifacts depend on field strength and they are more apparent on high field system.

Susceptibility artifacts occur as the result of microscopic gradients or variations in the magnetic field strength that occurs near the interfaces of substance of different magnetic susceptibility. Large susceptibility artifacts are commonly seen surrounding ferromagnetic objects inside of diamagnetic materials (such as the human body). These gradients cause dephasing of spins and frequency shifts of the surrounding tissues. The net results are bright and dark areas with spatial distortion of surrounding anatomy. These artifacts are worst with long echo times and with gradient echo sequences.

Susceptibility artifacts can be reduced by many ways as followings

1. Using a lower field strength
2. Choosing a spin-echo instead of a gradient echo pulse sequence
3. Selecting the frequency-encoding axis.
4. Increasing in readout gradient strength at given field of view.
5. Signal loss from spin dephasing can be reduced with a short TE.
6. Using thin section or three- can minimize dephasing across the slice Dimensional volume imaging.

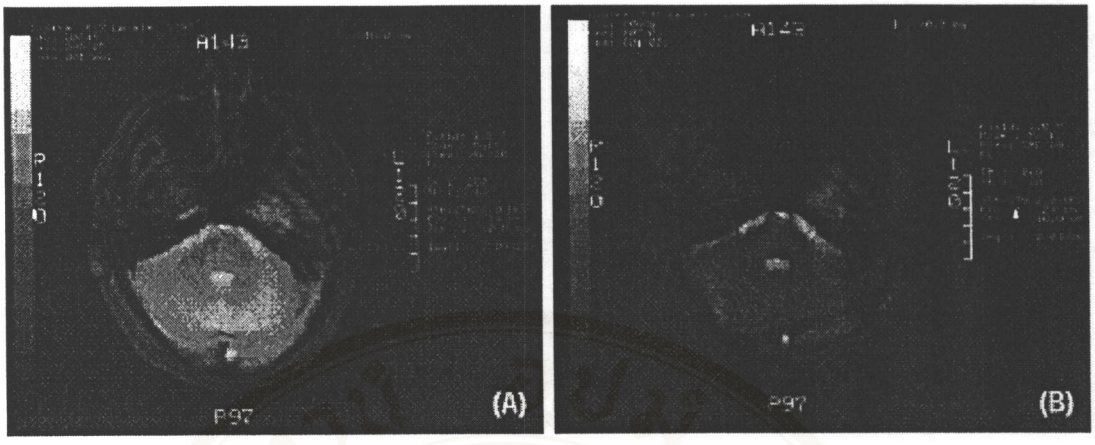

Figure 10-2, The susceptibility induced signal losses are more prominent at longer echo delay (B). Note signal drop-out near frontal and mastoid sinuses in (B), not present in (A)(36).

10.3 Radio-frequency field artifacts

10.3.1 Radio-frequency noise or external noise (1, 2, 6, 35)

Since the MR Signal received from the patient is very weak; it is easily degraded by extraneous RF near the operational frequencies of the MR scanner. To prevent RF interference, site planning requires a scanning room that is RF shielded. RF shielded walls, doors and windows, are commercial available and effective in eliminating RF contamination. Radio-frequency noise from outside the scanner enclosure can still cause image degradation if there is a breech in the RF shielding. This can occur, for example, if the RF-shielded door is not closed properly or if door jam electrical connectors and damaged. Radio-frequency noise can also originai in the scanner room from improperly installed lighting fixtures or other electric devices. In this case, extraneous RF noise is emanated from the cryogen meter within the scanning room that had been inadvertently left on by the service representative.

Radio-frequency noise will be present in a clinical image if its frequency is near that of the operational frequency of the MR scanner. Broadband noise can degrade the entire image. In this case, however, narrow BW noise results in linear columns of RF interference displayed perpendicular to the frequency-encoding axis. The exact position of the band of noise is determined by the difference between center frequency of the extraneous RF. The width of the artifactual band is determined by the frequency BW of RF noise in comparison to the BW of signal comprising the visible FOV in the image. The figure 10-3 illustrates artifact that occurred from radio-frequency noise.

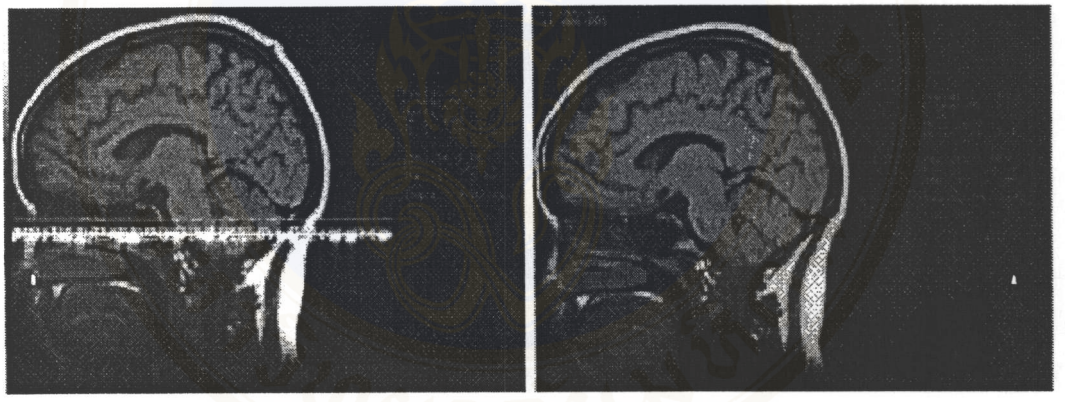

Figure10-3 the effect of RF interference causing streak artifacts. Artifacts of this kind can be caused by leaking RF screen, causing pick-up of external RF signal (36).

10.3.2 Surface coil sensitivity (1, 2, 6, 23, 35, 49, 50)

Surface coil imaging improves the SNR when compared with equivalent imaging using standard head and body coil. Improvement of amount of SNR results from placing the surface coil close to the imaged anatomical structure. The closer proximity of the coil to the ROI enhances signal by increasing the magnetic flux coupling between spin and coil.

While Signal is increased only from the selected slice, noise is received from the entire sensitive volume of the coil. Noise is decreased by reducing the volume of tissue to which the receiver coil is sensitive. The increased SNR allows for a decrease in voxel size, thus permitting an increase in spatial resolution.

The sensitivity of the surface coil is nonuniform and decreases sharply beyond a distance of one radius. This is suitable for clinical imaging, because surface coils are usually employed for small FOV, high-resolution imaging. However, the use of surface coils is restricted to superficial structures. Although the increases of SNR can make artifacts from nearby structures more conspicuously, the signal intensity fall-off reduces ghosting and aliasing from regions beyond the FOV of the surface coil.

10.3.3 Improper radiofrequency attenuation (1, 2, 6, 35)

Radiofrequency transmitter attenuation determines the amount of RF power transmitted into patient and the resultant magnetization tip angle. Whenever the patient move or change a new position in the scanner, RF attenuation must be adjusted every time because the amount of RF power required to produce a given tip angle varies with patient size, anatomy, and coil tuning. Radiofrequency tip angle inhomogeneity associated with an improper RF transmitter attenuation setting can cause disproportionate signal intensity or signal loss in an image. This problem is easy corrected by proper selection of the RF transmitter attenuation setting.

10.3.4 RF quadrature artifact

RF quadrate artifacts are caused by problems with the RF detection circuitry. More specifically, these problems are typically associated with the hardware section as the quadrature detector that is previously referred in the hardware-imaging chapter. These problems arise from improper operation of the two channels of the detector. For example if one of the amplifiers has a DC offset in its output, the Fourier transformed data may display a bright spot in the center of the image. If one channel of the detector has a higher gain than the other one, it will result in a ghosting of objects diagonally in the image. This artifact is the result of a hardware failure and must be addressed by a service representative. The figure 10-4 is represented artifacts occurred from misadjustment of two channels in quadrature receiver.

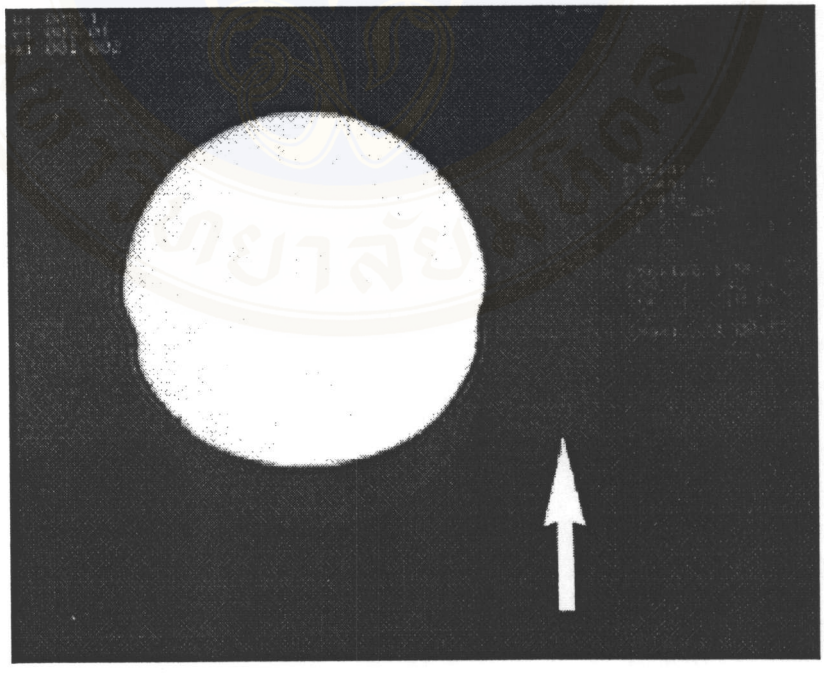

Figure 10-4 Phase mismatch in quadrature receiver causing ghost (36).

10.3.5 RF inhomogeneity artifacts (1, 2, 6, 25, 35, 36)

This section will be mentioned only RF uniformity for extending the understanding artifacts occurred from RF nonuniformity.

RF coils are transmitting antennae for the RF excitation field (the B1 field) and the reception of the MR signal. It is usually important to have very uniform RF excitation field strength and, similarly, a uniform sensitivity for signal reception.

For imaging, RF transmission is never necessary to occur during receiving; therefor, an antenna can perform the dual duty of transmission and reception. Such coils are called transmit-receive coils. It is also possible to use separate coils for transmission and reception. RF coils can be divided into broad classes consisting of volume coils and surface coils. A volume coil is optimized to give good RF-field strength homogeneity over a reasonably large imaging region, whereas a surface coil is designed to give improved signal-to-noise performance compared with a volume coils, at cost of increased RF inhomogeneity. There are many forms of the surface coils. One of these is a circular coil that will have useful sensitivity to depth that is only about equal to its radius. Imaging of deep structures is best preformed with the smallest volume coil that will fit the region. Since most imaging systems have the body size RF coil and usually creates the most uniform RF field strength, a common arrangement is to use the body coil for all RF transmission so that all other coils are only for signal reception. Some system, however, still will have local transmit-receive coils for head or extremities. Surface coils always use the bodies coil for excitation except in very rare situation in which the uniform RF excitation pattern is used for addition localization.

Uniform-volume coils are usually constructed on the principle of the birdcage design for superconducting systems for which Bo along the bore and patient axis. This is because of the need to create a B1 field that is perpendicular to the Bo direction. Low field strength magnets that have vertical Bo can use solinoidal winding, which are theoretically able to achieve better sensitivity than birdcage design. In addition, low field strength systems can usually achieve high RF field strength homogeneity due to the better RF penetration into tissue at lower RF frequencies.

Addition uniformity of excitation is achieved with volume coils by exciting the coil with two or more RF signals that is 90^0 out of phase. The phase difference is supplied most easily with passive RF splitter or combiner. The result is that instead of the RF field strength oscillating in amplitude in the so-called linear mode, a rotating or polarized RF field strength of constant amplitude is created. This technique is often called quadrature excitation. (Artifacts which are occurred in quadrature coil it is mentioned in the previous section)

RF inhomogeneity problem is variation in intensity across an image. The cause is either a nonuniform B1 field or a nonuniform sensitivity in only a receive coil. Some RF coils, such as surface coils, naturally have variations in sensitivity and will always display this artifact. The presence of this artifact in other coils represents the failure of an element in the RF coil or the presence of nonferromagnetic material in the imaged object.

RF inhomogeneity correlates to the amplitude of the excitation field arising across the field-of-view; the spins are not equally excited. For example, there will be under flipping (e.g. $70^0/140^0$) at some locations and over flipping (e.g., $110^0/220^0$) at other locations instead of all spins experiencing a 90^0 and 180^0 pulse. Both under and

Over flipping cause a reduction in the magnitude of the transverse magnetization and in signal intensity. In other words, image shading occurs with a highest image intensity where excitation and refocusing pulses are closest to a 90^0 and 180^0 f lip angle, respectively. It is somewhat less evident that inhomogeneity of the static magnetic field has a similar effect. This is because the effective field experienced by the spins is the vector sum of B_1 and B_0 (RF and static field amplitudes) in the rotating frame, as shown schematically in the figure 10-5. The effect field of the spins experience (B_{eff}) is given as the vector sum of the RF field (B_1) and local field inhomogeneity (ΔB)

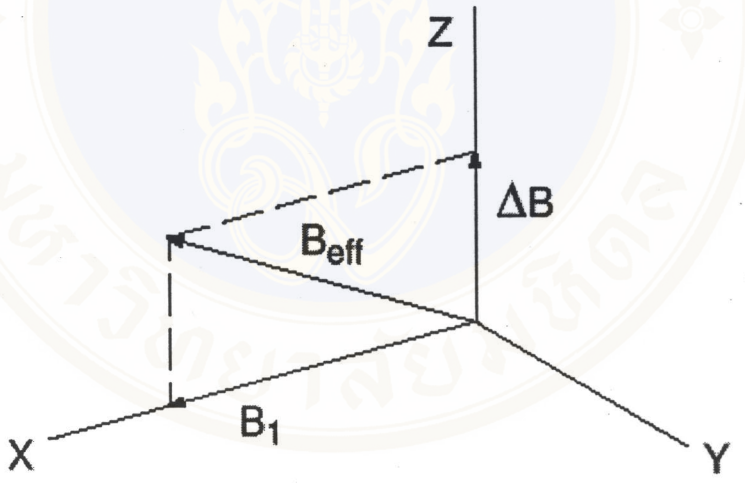

Figure 10-5. The cause and mechanism of RF uniformity artifacts. The image example in this effect similar to the main magnetic field artifact (36).

10.3.6 RF defective preamplifier failure (1, 2, 6, 36)

The primary magnetic resonance signal received by the head or body coil is extremely weak. To recover the signal from the noise, amplification occurs at several stages. Immediately following detection, the signal enters a preamplifier. Preamplification needs to occur with a minimum of additional noise generated. The quality of a preamplifier therefore is measured in terms of its "noise figure." Good preamplifiers have a noise figure of less than 1db. Typically, a faulty preamplifier results in deterioration in the signal-to-noise (figure 10-6).

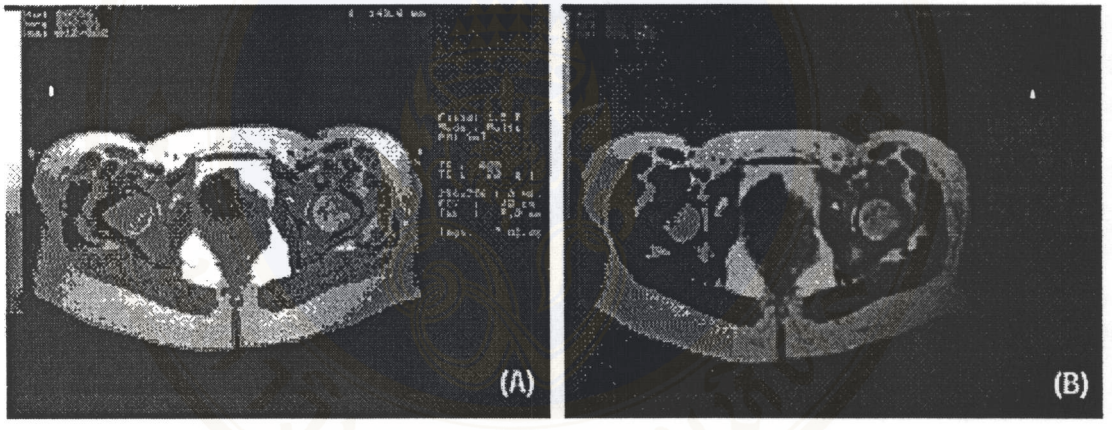

Figure 10-6 Effect of defective preamplifier on image SNR: (A) good preamplifier; (B) defective preamplifier (36).

10.3.7 Array processor failure (36)

The array processor (AP) is part of the computational system. It is a very fast parallel processor for execution of simultaneous tasks. The AP is involved in the signal averaging process during data acquisition and reconstruction. Artifacts produced by a defective AP and have different manifestations. The figure 10-7 illustrates some typical artifacts caused by a faulty AP.

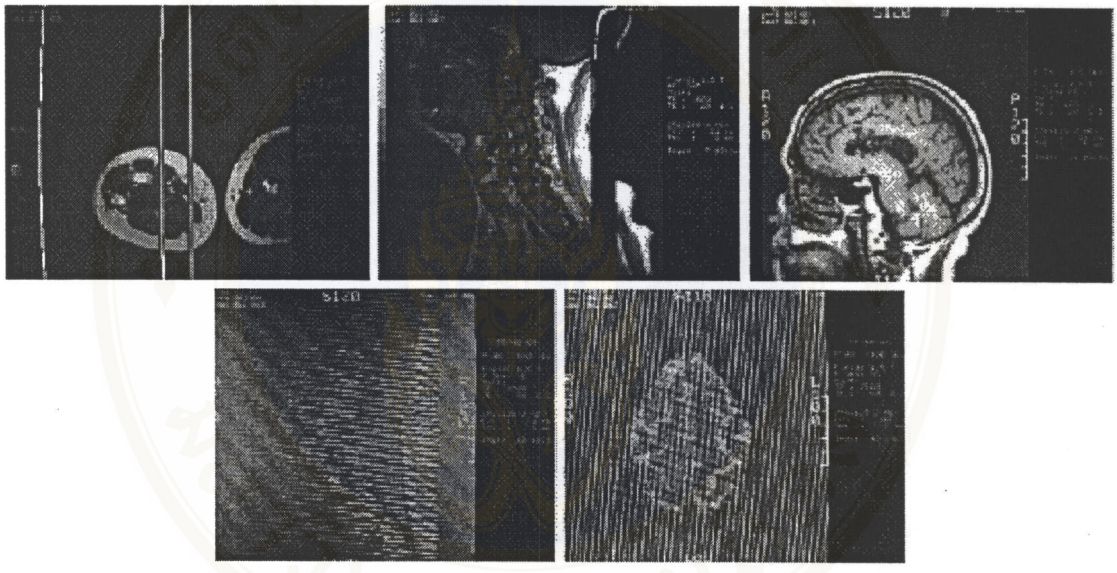

Figure 10-7 Grid-like artifact superimpose on the image are characteristic of faulty array processor (36).

10.4 Gradient and data acquisition artifacts

10.4.1 Gradient amplifier failures (1, 2, 6, 36)

Gradient amplifier failures can cause artifacts of varied appearance, depending on the temporal characteristics of the failure. An example of a bad gradient master amplifier and its effect on a sagittal image is illustrated in the figure 10-8.

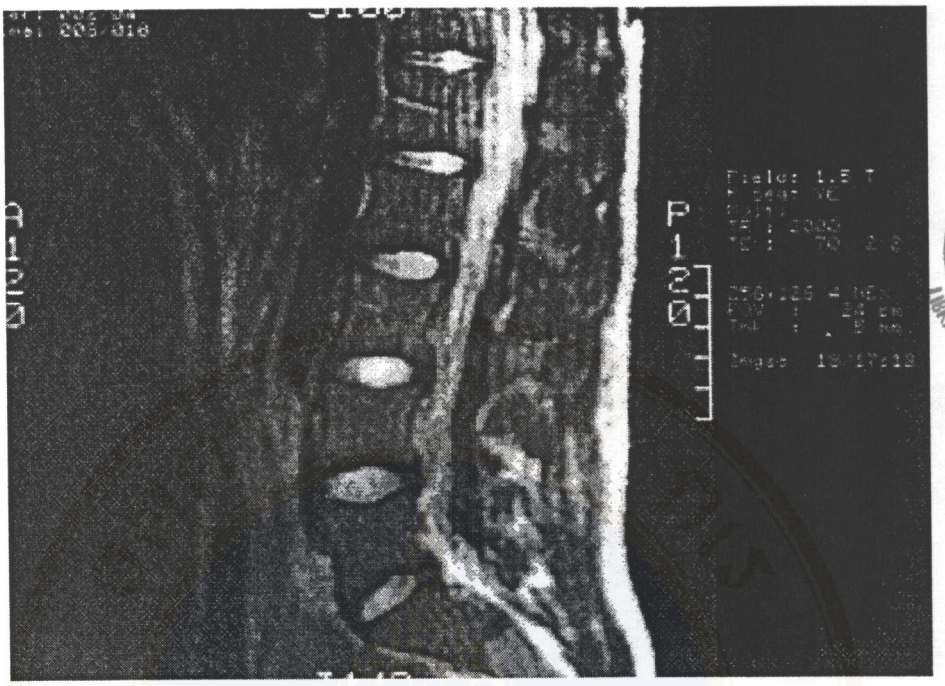

Figure 10-8. Structured noise caused by gradient amplifier failure (y gradient of master amplifier) (36).

10.4.2 Receiver gain adjustment (Clipping artifact) (1, 2, 6, 35)

On occasion one may encounter an image with a peculiar ghostlike quality, a snowstorm background, and loss contrast between soft tissues. This is a data-clipping artifact, resulting from having signal intensity outside the digitization range of the analog-to-digital converter (ADC). The artifact may be encountered on some section and not on the others in multi-section acquisition. The problem is most severe on surface coil images in obese patient that subcutaneous fat contributes high signal and in techniques using large numbers of slices or thick sections. Normally, the receiver adjustment is performed using the zero phase line (i.e., no phase encoding gradient), since the data line produces the highest signal. As result, maximal signal will occur a few lines away from zero, rather than at zero line.

If the automatic receiver adjustment results in clipping, the receiver gain can be manually reduced, typically by a few decibels. However, excessive reductions in receiver gain may worsen image contrast.

10.4.3 Loss of data (1, 2, 6, 35, 36)

Loss of one or more line of data causes a variable degree of artifacts in the image. For example, loss of the central data lines (weakest phase-encoding step) results in the largest artifacts. Loss of data can result from communication problems, gradient in stability, or excessive receiver noise and ADC error. ADC errors are unavoidable on any MRI system because more than 10 million analog-to-digital conversions take place in a study of the single patient. An error in the digitization of a single data point can result in uniform background of vertical, horizontal, or obliquely oriented stripes. The intensity of stripes can be severe or barely noticeable, depending on where the bad data point digitization falls in the raw data. Spontaneous occurrence of single data point digitization errors cannot be prevented but can eliminated by post acquisition processing of the raw image data. It has been suggested that spontaneous discharge of static electricity from patient's blankets can result in these single data point errors. From the observation of many studies, this artifact results from corroded scan room light bulbs, noisy cryogen scavenger system, and defectively arcing RF body coil induction drive bars.

10.4.4 Eddy current artifact (1, 2, 6, 35, 36)

Magnetic field gradients are rapidly switched on and off during the imaging process. Such time-varying magnetic fields induce eddy currents in conductive structures of the magnet. These time-varying currents have magnetic fields associated with them. The eddy current induced by magnetic fields and superimposed on the main magnetic field decay with time constants of several hundred milliseconds. When a gradient is switched on, instead of instantly, the gradient field will grows exponentially toward its final amplitude (figure 10-9).

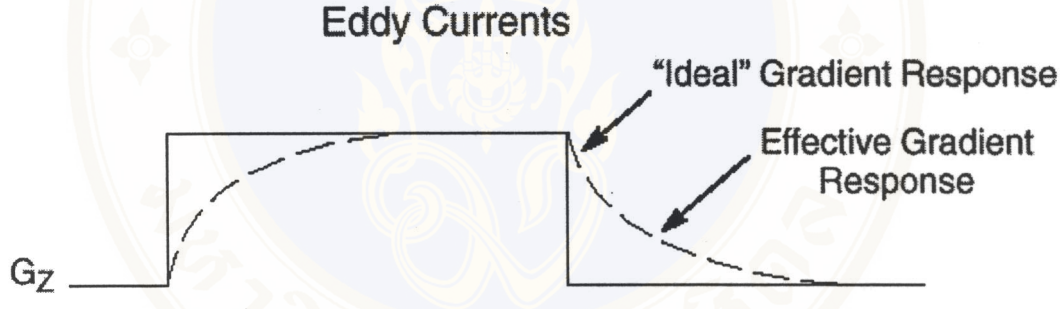

Figure 10-9. Effect of eddy current on effective gradient amplitude. Instead of a rectangular gradient, profile the gradient amplitude rises and decay exponential (36).

Likewise, when it is turned off, the gradient field will decay exponentially to zero. Therefore, even if no gradient is present, a residual magnetic field gradient may persist. Residual eddy currents are particularly detrimental in multi-echo imaging or cine. A first more powerful remedy is the shielded gradient. The flux outside the coil (which is the cause of the eddy current but has no function for generating imaging gradients) is compensated by a counter-flux of equal magnitude in the opposite

direction. The figure 10-10 illustrates the significant improvement in image quality with shielded gradients.

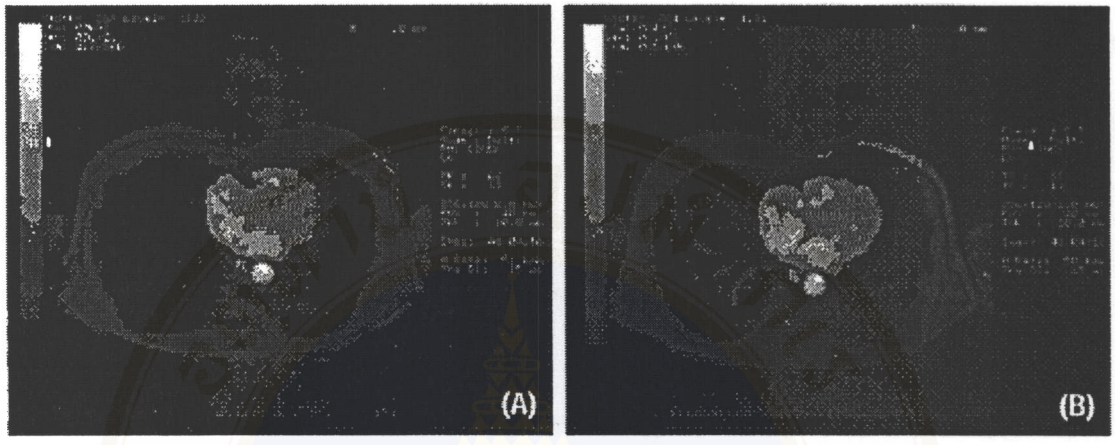

Figure 10-10. Cine images obtained in a system equipped with conventional (A) and shield gradient (B). Note absence of phase encoding streak artifacts in the image of (B)(36).

10.4.5 Gradient artifacts (1, 2, 6, 23, 35, 36)

Every MR imaging system has three gradient coils, which provide the linear change in Bo with position (the gradient in Bo) in the X, Y or Z direction. Whereas the gradient direction may be in a direction perpendicular to Bo, the actual field direction is still in the original direction in the Bo since the gradient is a result of the field strength becoming stronger (or weaker) as the distance along the gradient direction is changed. The strength of the gradient is expressed in Tesla per meter or Gauss per centimeter (1 G/cm = 0.01 T/m = 10mT/m). The maximum gradient strength of MR imaging system is a very important parameter that defines the limiting resolution of the system. Use of stronger gradient allows higher resolution and / or faster imaging if there is sufficiently high SNR to make a usable image at the desired resolution or speed.

Artifacts arising from problems with the gradient system are sometimes very similar to those described as Bo inhomogeneities. A gradient not constant with respect to the gradient direction will distort an image. It is typically or possibly occurred only when a gradient coil has been damaged. Other gradient related artifacts are due to abnormal currents passing through the gradient coils. In this image the frequency encoding (left/right encoding) gradient is operating at half of its expected value.

Gradient nonlinearity causes anatomic distortion in MR images. It is caused by loss of gradient strength and linearity that more severe at the increased distance from magnet isocenter. Drop-off in gradient strength is most pronounced along the Z-axis, the direction of the main static magnetic field. This is due to differences in gradient coil design for respective axes.

The computer reconstruction algorithm assumed a linear relationship between phase or frequency and distance along the respective axes. Along the phase encoding and read-out axes, a decrease in gradient strength at the periphery of anatomic ROI results in respective phase changes and processional frequencies that under represent true distance from isocenter. This causes spatial mismapping or telescoping of peripheral anatomy in the resultant image. Anatomic distortion from gradient nonlinearity is most apparent on large FOV images.

10.4.6 Ringing or Truncation artifact (1, 2, 6, 25, 35, 36)

Truncation artifact is caused by the failure of 2DFT reconstruction methods which reproduces a high contrast interface accurately. The most common clinical manifestation of truncation artifact is a fluctuating intensity pattern presenting as alternating bands of high and low signal parallel to and extending away from a high

contrast boundary. Truncation artifacts become less apparent with increased distance from the interface, which help to differentiate them from ghost artifacts due to motion. Motion ghost artifacts are propagated across the entire image along the phase-encoding axis.

Truncation artifacts are also known as ringing or edge ringing artifacts. The term Gibb's artifacts and Gibb's phenomenon are also used to describe this truncation error. However, it is more accurate to use the term Gibb's phenomenon to describe signal intensity undershoot and overshoot on either side of a high contrast boundary.

Although edge ringing is the most commonly recognized and discussed manifestation of truncation artifact, there are other features of truncation artifact error causing image degradation. Edge enhancement will occur because of the primary undershoot and primary overshoot at the high intensity boundary (figure 10-11) Artifactual widening and blurring of edges is occurred because reconstructed signal intensity has a sloping profile compared with the actual vertical anatomic interface. In combination with photographic technique, this sloping line of intensity cons result in the underestimation of true object size (figure 10-12). Methods for decrement of the conspicuity of truncation artifact include:

1. An increase in matrix size (e.g. increased number of phase-encoding steps)
2. A decrease in FOV to decrease pixel size
3. Switching the Phase- and frequency-encoding axes
4. Filtering the raw data

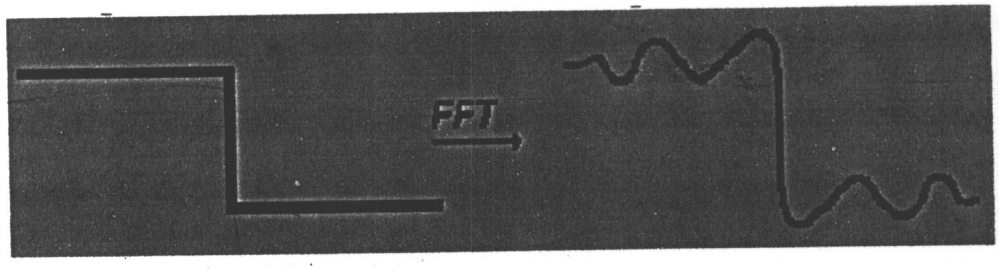

Figure 10-11. The diagram above shows the Gibbs effect resulting from a Fourier transformation of a sharp change in image intensity (36).

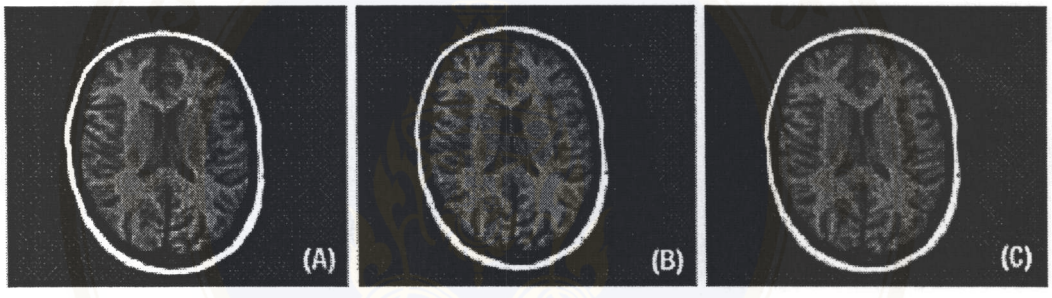

Figure 10-12. Effect of matrix on truncation artifacts. Notice the reduction in truncation artifacts as we increase the matrix size from 128x128(A) to 160x160(B) to 256x256(C)(36).

10.4.7 Chemical shift artifacts (CMSA) (1, 2, 6, 23, 35, 36, 51)

In conventional 2DFT (spin-wrap) MRI, an image is created systematically by selection of slice, then spatial encoding of signals from the slice in the phase- and frequency-encoding directions, and Fourier transform of the raw data. The behavior of the fat and water magnetization will vary in each of these steps as a result of their chemical shift (figure10-13).

The chemical shift is the difference in Larmor frequency of hydrogen nuclei bounded into different chemical compounds. The chemical shift between water and

body fat is 3.5 ppm, regardless the field strength. The chemical shift frequency difference is 225 and 52 Hertz at 1.5 T and 0.35 T, respectively.

The frequency shift between water and fat resonance typically results in spatial mismapping of one of the two components in MR image. Since the MR system is typically tuned to the frequency of water, fat will mismapped in the image relative to its true position. These spatial misregistration are most readily visualized in the frequency-encoding direction, but also can occur in the slice select direction.

The CSMA measured in pixel ($N_{\text{pixle shifted}}$) can be expressed as

$$N_{\text{pixle shifted}} = [\Delta v/BW]N_x$$

Where Δv is chemical shift in Hertz, BW is bandwidth of data acquisition in Hertz, and N_x is the number of pixels comprising the image in the frequency direction.

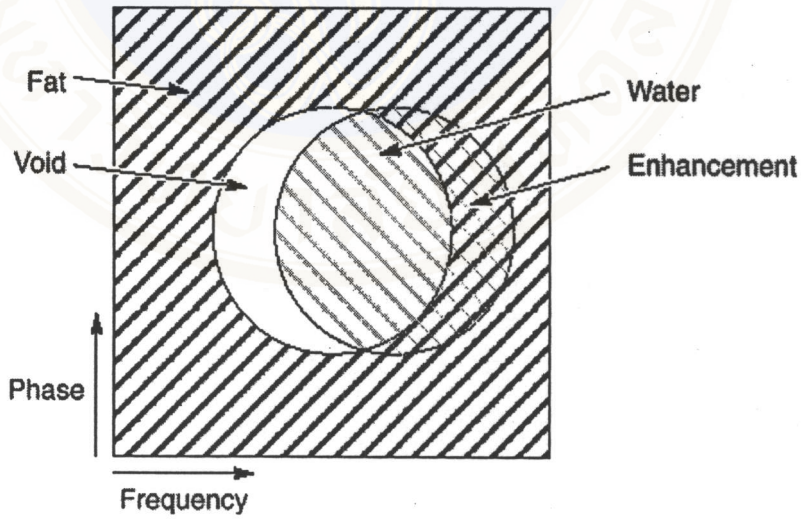

Figure 10-13. Schematic illustration of displacement artifacts caused by spins in water and fat containing tissues having slightly different resonance frequency. The effect is an artifactual void on one side where the two structures meet and an artifactual signal enhancement where the signal intensities from the two structures add (36).

Practical methods for decrement of the effect of CMSA in MR imaging include reversing the phase and frequency direction, using fat or water suppression techniques, and maintaining a relatively high data sampling bandwidth.

10.4.7.1 Chemical shift and variable bandwidth (1, 2, 6, 36)

Chemical shift is a phenomenon appearing in the direction of the read-out or frequency gradient. It means that pixels of information have literally been shifted in the image. That is because a particular proton's precise resonant frequency depends in part on its chemical environment and the magnetic field. For example, hydrogen attached to oxygen (as in water) experiences a slightly different magnetic field than hydrogen bonded to carbon (as in fat). At 0.5T, water and fat differ in their resonance frequency by about 74 Hz; in other words, they do not resonate at the same frequency.

The frequency split, as determined through NMR spectroscopy, is about 3.5 ppm. So at 0.5T the frequency difference is calculated by:

$3.5 \times 10^{-6} \times 21\text{mHz} = \Delta f$, or approximately 74 Hz. (hydrogen resonate frequency at 0.5T)

Thus, the chemical shift will be about millimeters in each image. The reason: $Bw_{pix} = 1/(T\ read)$ In this equation, BW_{pix} = pixel bandwidth; T read = the duration of the signal readout window. Chemical shift is therefore inversely proportional to pixel bandwidth: The larger the bandwidth, the less chemical shift there will be. Note, however, that SNR suffers as bandwidth increases. The bandwidth and read-out time are then adjusted so not to exceed the requested amount of chemical shift. The figure 10-19 illustrates both the standard default bandwidth and the three variable bandwidth options. Notice the SNR changes in the images. The chemical shift

phenomenon may make it difficult to interpret images of such areas as the orbit, pelvis, and kidney, as well as axial spine images. Using the variable bandwidth option in these areas may prove its benefit. Remember, in addition, that the chemical shift phenomenon appears in the frequency-encoding direction; at times, swapping phase and frequency (see more detail in next section of motion artifacts) may also be helpful.

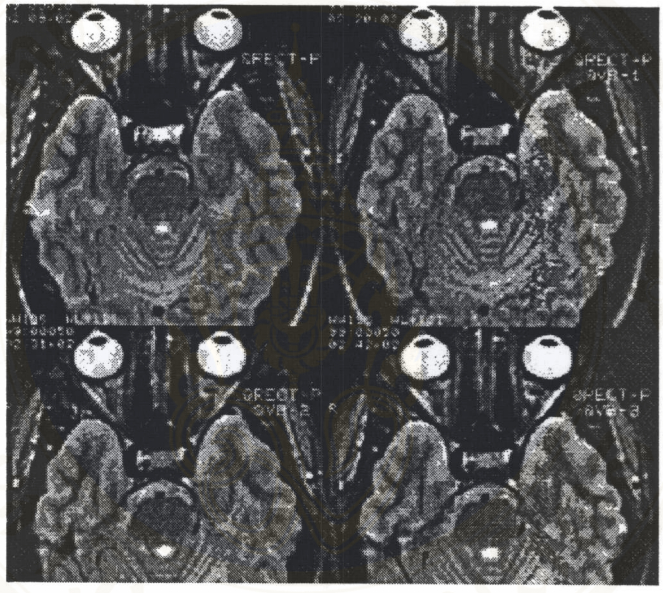

Figure 10-14. Chemical shift and SNR both increase as the bandwidth is narrowed. Figure (A), default bandwidth, demonstrates the highest SNR as well as the most chemical shift. Figure (B), gives the lowest SNR and the least chemical shift. Chemical shift can be noted as the white line anterior to the temporal horns (36).

10.4.8 Aliasing or Wraparound artifact (1, 2, 6, 23, 35, 39)

Wraparound artifact is manifestation of aliasing in clinical MRI. Aliasing results from undersampling of the MR signal. The Nyquist theorem states that unambiguous sampling of periodic function, for example, digitization of analog MR signal, requires sampling frequency twice that of the highest frequency component contained in the

signal. If the signal is undersampled, high frequency is artifactually superimposed on low frequency bands and assigned as the revered phase polarity (figure 10-15). These linear errors result in spatial mismapping to low frequency location of opposite phase polarity. This results in nondistorted anatomic structures being transposed to the opposite side of image, often overlapping accurately mapped anatomy.

Wraparound artifact from aliasing is most commonly encountered when the FOV is smaller than a cross-section dimension of the body part being imaged. Reduced FOV imaging contributes to wraparound artifact when signal-producing tissue is outside the selected FOV because of the insufficient data sampling for encoding correctly the location of tissue outside the FOV. If the phase-and frequency-encoding apply only to tissue within the selected FOV, then a redundancy will exist in the encoding of location inside and outside the FOV. Undersampling will result without a corresponding increase in the number in frequency-or phase-encoding steps.

There are several ways to avoid aliasing. The simplest way is to make the FOV greater than the dimensions of the anatomy within the imaging plane. This aliasing is seldom occurred because the chosen dimension of the anatomic imaging plane is seldom greater than both directions of the FOV. If a small FOV is required, the area of interest should be positioned in the center of the FOV for allowing the acceptable imaging of the structure, since wraparound artifact overlaps primarily at the image margins.

Aliasing along the frequency-encoding axis is easier to control without a time penalty compared to wraparound along the phase-encoding axis. Orienting the longest dimension of the anatomic structure along the frequency axis is therefor and important strategy. In fact, some commercially available scanner default this orientation is the

orthogonal planes. Aliasing in the frequency direction is also reduced by oversampling and using bandpass filter. A commercially available approach that involves oversampling in the frequency –encoding direction is to double the sampled FOV by doubling the acquisition matrix or number of pixels along the frequency axis. This doubling correctly encodes tissue lying out side the selected FOV up to a distance of half the selected FOV on either side. However, when the image is presented for viewing, only the central half of the frequency-encoded and reconstructed image is presented. A bandpass filter can be used to reduce the receiver sensitivity (to resonant frequencies that correspond to tissue located outside the selected FOV). A combination of oversampling and bandpass filtering can usually eliminate aliening in the frequency-encoding direction without a time penalty.

Aliasing in the phase-encoding direction is more difficult to eliminate. It can be reduced by decreasing the signal intensity form outside the FOV. This can be achieved by imaging with surface coil to restrict tissue-produced signal inside the FOV or by presaturation pulses applied to tissue outside the selected FOV. Phase-encoding wraparound can be reduced by increasing the FOV at the expense of spatial resolution or by increasing the number phase-encoding steps at the expense of time. A commercially available approach is to double the sampled FOV in the phase-encoding steps but presenting only the central half of the reconstructed image. This maintains pixel size and spatial resolution. However, some systems automatically have the specified number of excitation or assume phase-conjugate symmetry to avoid an increase in total imaging time. During image display, data collected outside the specified FOV are discarded.

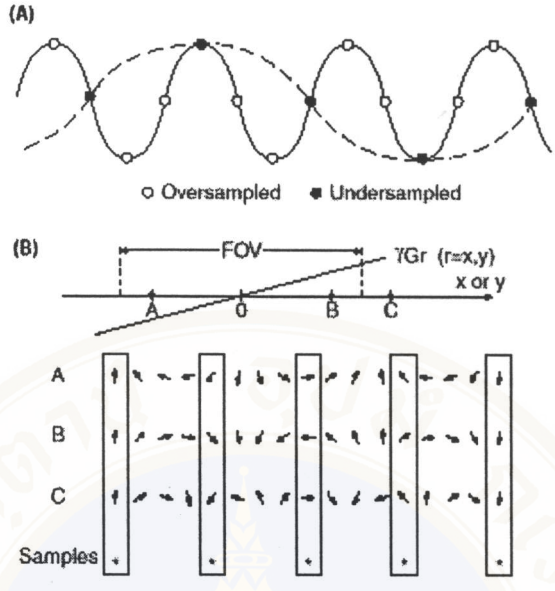

Figure 10-15. Aliasing: (A) Low frequency (dashed line) results from under-sampling, causing aliening: (B) Protons residing in position C outside the FOV will be aliased back and appear at location A (36).

10.4.8.1 Aliasing: wraparound artifact / No Phase Wrap (1, 2, 6, 35, 36)

Aliasing is also called "wraparound," because it literally wraps anatomy back into the image figure 10-16.

Figure 10-16 the sagittal images of the nose appears to be wrapped around to the posterior position because of phase-encoding aliasing (36).

This relatively common artifact has complex causes. If the prescribed FOV is smaller than the actual anatomy, there will obviously be nuclei outside its boundaries nuclei that will be affected by the RF and gradient pulses, and will return a readable signal to the system. The system will, in turn, digitize these signals and include them in the resulting image, thereby creating an artifact. The figure 10-16 shows a sine wave being sampled four times per oscillation. If we were to remove three of those sampling points, however, the signal would be under-sampled, and the system would not be able to digitize it correctly. The remaining sampling points (full circles) would therefore define a sine wave of a much lower frequency; and that is precisely how the system will interpret their signals, translating them into wraparound artifacts. If these signals are detected in the frequency-encoding process, the direction corresponding to spatial position they will translate into an incorrect spatial location. The same principle applies to the phase-encoding process.

Aliasing in either direction con be disturbing, particularly in coronal body studies, where both frequency- and phase-wraparound often occur. These artifacts can usually be avoided, however, One way is to avoid situations in which they are likely to occur. Consider what happens when prescribe a field-of-view (FOV): The system executes the command via frequency- and phase-encoding gradient amplitudes, frequency-sampling bandwidth, and the number of frequency- and phase-encoding steps. Phase wraparound problems can sometimes be avoided by using a scan plane that the phase-encoding steps put in a direction keeping wraparound away from the anatomy of interest. On the other hand, you can instruct the system to swap the phase and frequency directions to achieve this goal (see swapping phase and frequency in the next section on the motion artifacts).

Action	Result
FOV is doubled in the phase –encoding direction	SNR is increased Resolution due to larger voxel dimension is decreased FOV encompasses lager anatomical area
Double number of phase encoding steps	Resolution to original selection is decreased Doubled scan time
Halve the NEX	Scan time and SNR Black to original Choice

Table 10-1 the factors effect to using No phase wrap.

Remember that SNR is dependent on the number of phase and frequency samples, which are equal in both examples. Thus, there is no change in SNR. The figure 10-17 shows graphically what event happens when No phase Wrap is enabled. The figure 10-18 illustrates what event can happen when No phase Wrap is either used or not.

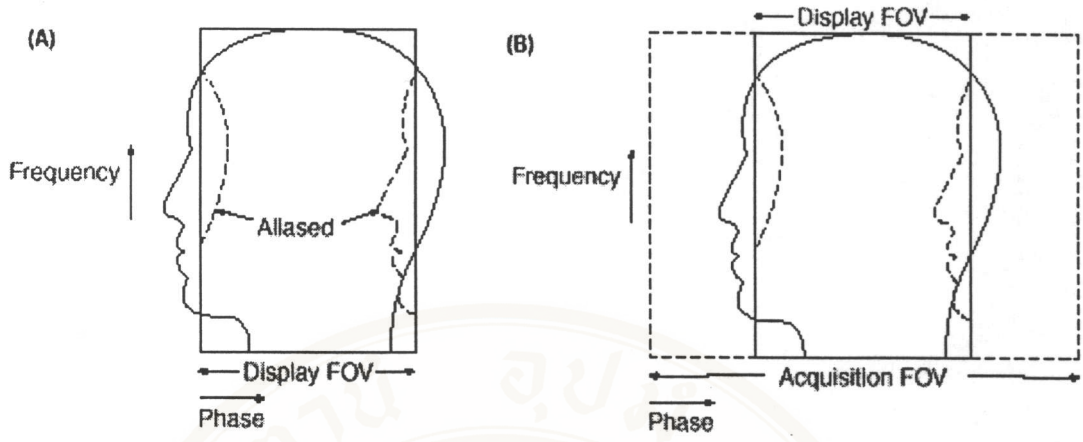

Figure 10-17. Aliasing: An object extending beyond the FOV chosen will have those portions of the object that are outside the FOV wrapped around to appear at artifactual locations (A). By extending the FOV in the direction where aliening occurs (phase or frequency), the undesired effect can be prevented (B). Note that the data outside the display field of view are discarded after reconstruction (36).

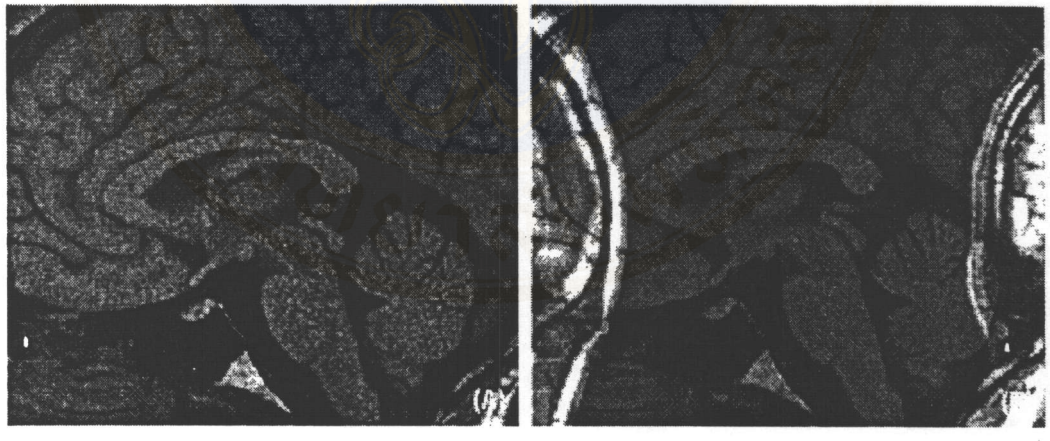

Figure 10-18. Image (A) demonstrates a 15 cm FOV pituitary with No Phase Wrap enabled and (B) demonstrates the same anatomy without the No Phase Wrap option (36).

10.4.9 Partial volume averaging (1, 2, 6, 23, 35)

Partial volume averaging occurs when anatomic interface or two structures with different signal intensities are included within the same voxel. Because voxel thickness is usually the greatest voxel dimension, partial volume averaging tend to pronounce mostly in the slice-select direction. Partial volume averaging is more likely increased when section thickness and larger inter slice gap increase.

Partial volume results in an averaging of signal intensities within in the voxel. Artificial increased or decreased in signal intensity can mimic or obscure pathology. Partial volume can cause apparent pseudomasses or decrease the conspicuity of low contrast objects.

Partial volume averaging can be reducing in the voxel size. This can be achieved by decreasing either the slice thickness or the FOV. Because the voxel dimension is usually greatest in the slice-select direction, a decrease in partial volume averaging is easily accomplished by using a thinner slice. Partial volume in often most problematic at contrast boundaries. It can be avoid by choosing a plane of section orientated perpendicular to these interfaces. The figure below illustrates the image artifact occurred from partial volume averaging.

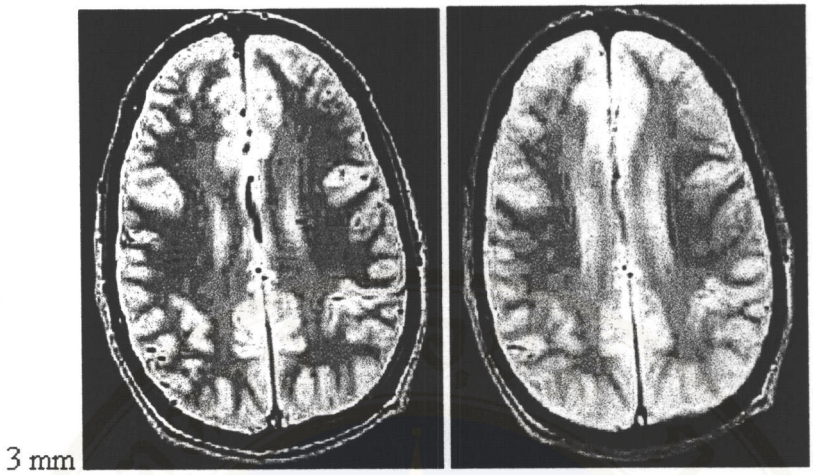

Figure 10-19. Here is a comparison of two axial slices through the same location of the head. One is taken with a 3 mm slice thickness and the other with a 10 mm thickness. Notice the loss of resolution in the 10 mm thickness image. The solution to a partial volume artifact is a smaller voxel, however this may result in poorer signal-to-noise ratio in the image (23).

10.5 Motion artifacts (1, 2, 6, 14, 15, 16, 17, 18, 20, 23, 35, 36, 37, 38)

Motion can be divided into 2 types consisting of random (aperiodic) and periodic physiological motion. Random motion is resulted from the voluntary patient's motion. Periodic physiological motion includes respiration, heartbeat, blood and CSF flow. Each motion produces individual artifacts. Random motion causes image blurring (one type of artifact) with decreased definition of anatomic structures. The signal from an object is displayed over its range of motion. Periodic motion or intensity variation causes image harmonics or ghost artifact. These periodic changes affect the outcome of 2DFT reconstruction in such a way that the ghost artifact is propagated along the phase-encoding direction. If the periodicity has constant frequency, discrete ghost image is display. If the periodicity has a variable frequency,

then mismapped signal will be ill defined and appear as streaks. In clinical MR imaging, ghost artifact is most commonly caused by pulsatile flow and breathing.

As long as it has significant amplitude, virtually any motion will cause one or more types of image artifacts:

1. Edge blurring cause by positional uncertainty from random motion
2. Ghosting from periodic motion
3. Decreased SNR in the moving area from both random and periodic motion

It is interesting to note that ghosting occurs in the phase-encoding direction not in Frequency-encoding. This is because the entire phase sampling process is much slower; time between phase samplings takes seconds (NEX*TR) vs. the fraction-of-a-millisecond required for frequency-encoding.

Motion artifact from breathing can be reduced by using several techniques such as followings

1. The increased number of signal averages or excitations increases the parent signal to ghost signal ratio as the square roots the number of excitations.
2. Presaturation slabs applied to anterior abdominal wall reduce the intensity and amplitude variation from abdominal fat contributing to ghosting.
3. Inversion recovery or chemical shift pulse sequences decreases signal intensity from fat.
4. Respiratory gating or phase-reordering methods reduces view-to-view phase shift due to unsynchronization of the phase-encoding steps with the respiratory cycle.

10.5.1 Respiratory (Breathing) Motion

10.5.1.1 Respiratory Compensation (1, 2, 6, 35, 36)

This section is mentioned about an appropriate reduction technique from many techniques for the respiratory motion.

Completely random motion merely results in a large number of low-intensity ghosts and a slight increase in background noise. Nevertheless, periodic motion like the respiratory and circulatory systems produces the discrete ghosts caused by the amplitude modulation or the effect of chest and abdominal wall movement on the signal. These artifacts appear most prominently in axial images of the chest and abdomen (figure 10-20 AB) becoming even more severe in T2-weighted image (figure 10-20 C) but they are less prominent in the coronal plane (figure 10-20 D). A number of remedies of varying effectiveness are available.

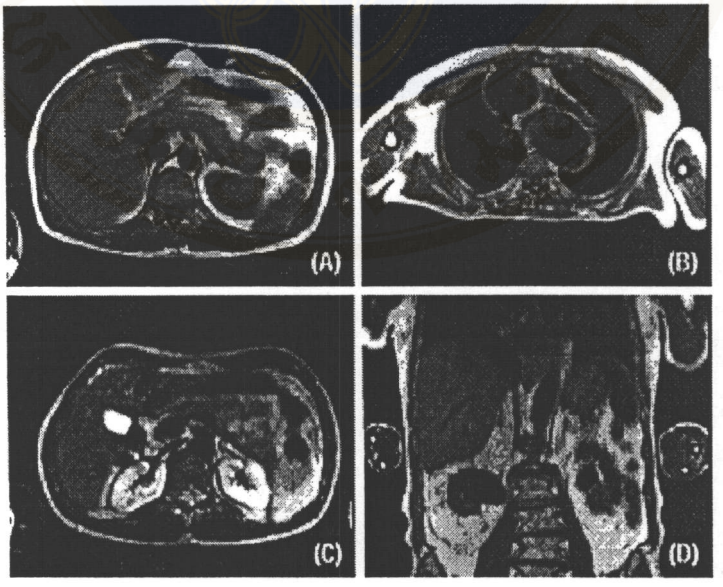

Figure 10-20. A and B illustrates periodic motion ghosting is evident here in T1-weighted axial abdomen and C and D illustrates T2-weighted imaged of abdomen and chest. The coronal plane exhibits the least (36).

10.5.1.2 Respiratory gating (1, 2, 6, 35, 36)

Respiratory gating is one approach similar to cardiac gating (see Cardiac Motion / Cardiac Gating), it synchronizes the scan to the respiratory cycle. Although this technique will indeed eliminate these artifacts in principle, it has not proven practical; because the long, 2-4 second respiratory cycle mandates long scan times.

10.5.1.3 Number of excitation or Signal averaging (1, 2, 6, 36)

Multiple signal averaging (increasing the number of NEX) can be used as an effective way to "smear out" ghosts (figure 10-21). Multiple averaging can be practical for short-TR acquisitions, although it, too, extends scan time. Yet, another apparent solution is acquiring T2-weighted SE images. Some users report that the second echo of two equally spaced echoes exhibits some artifact suppression, presumably because of spin (even-echo) rephasing (figure 10-22).

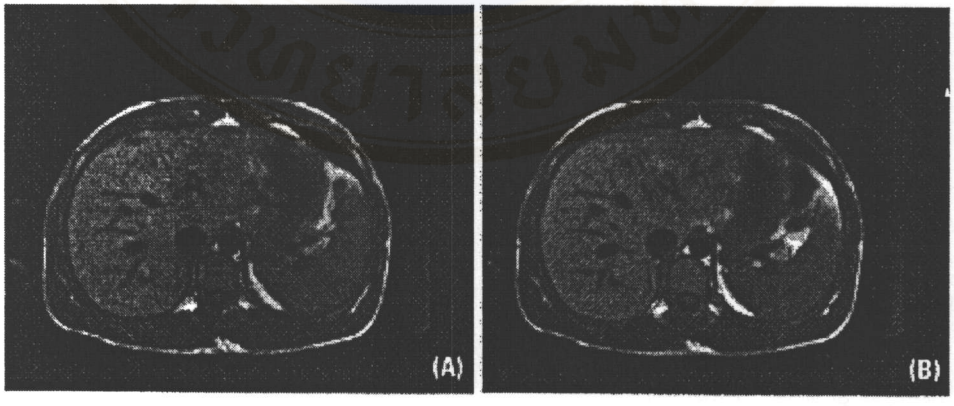

Figure 10-21. Increasing NEX is one variable that can be used to decrease motion artifacts. Increasing from two to eight NEX eliminates most of the respiratory motion as well as flow artifact from the aorta at the expense of a four-fold increase in scan time (36).

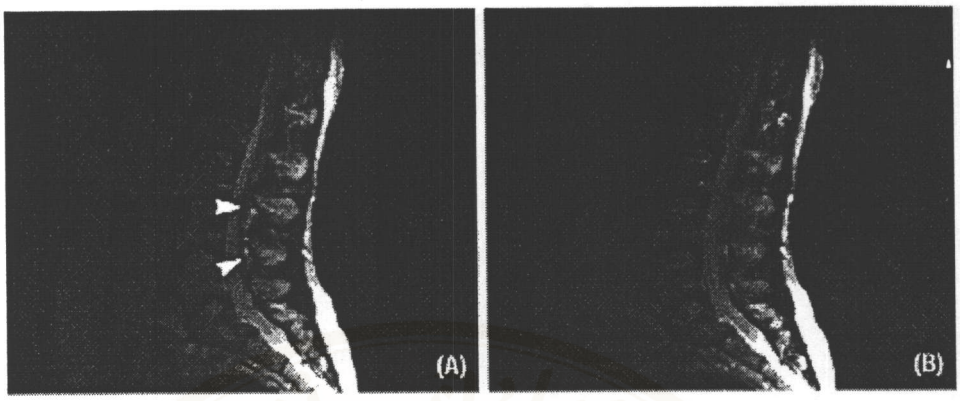

Figure 10-22. TE times chosen such that the second echo is a multiple of the first (i.e. 45 ms/90 ms) may help to reduce motion artifacts through spin rephasing also known as even echo rephasing. Compare the clarity within the thecal sac of (A), utilizing even echo rephasing, with (B) obtained without the benefit of even echo rephasing (36).

10.5.1.4 Respiratory-ordered phase artifact (ROPE) Or Respiratory compensation. (1, 2, 6, 36)

Respiratory compensation (Resp Comp) which is a phase-encoding sorting technique is the most effective approach to eliminate ghosting. Unlike respiratory gating, respiratory compensation does not limit the user's choice of TR, and allows data acquisition throughout the entire respiratory cycle resulting in slightly increase of the scan time (based on 16 overscans times the selected TR). With Resp Comp is activated, the system collects the phase encoding in a manner that controls view-to-view brightness variations (figure 10-23A), and (figure 10-23B).

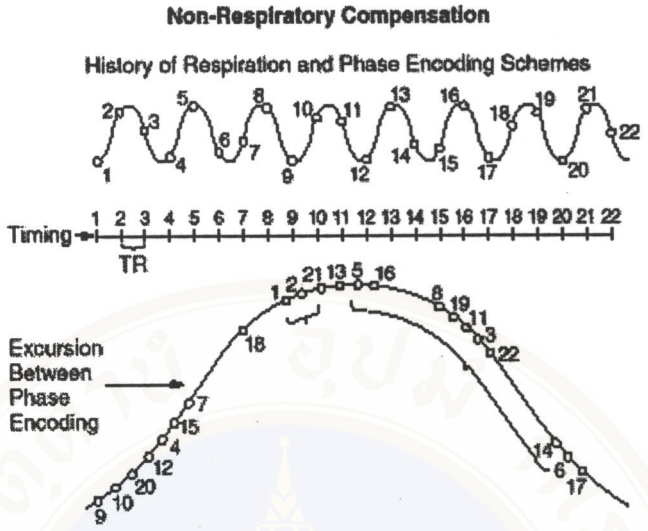

Figure 10-23A – Without Respiratory Compensation (A), the excursion between phases 1 and 2 through 5 and 6 creates ghosts in the FOV(36).

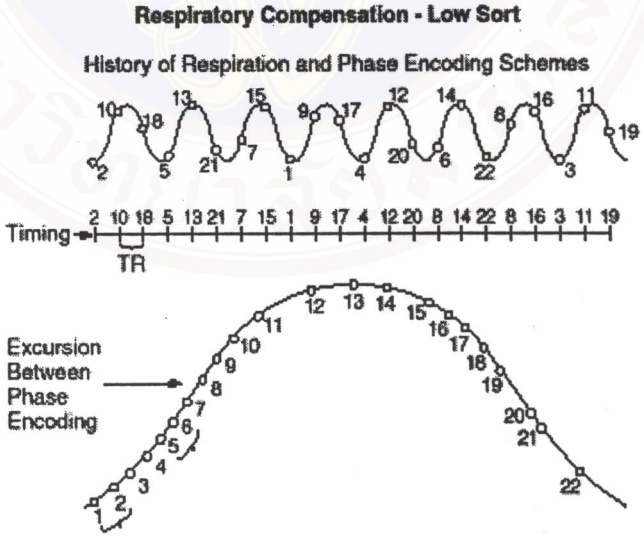

Figure 10-23B. Similarly, using Respiratory Compensation with low sort (B) creates ghosts in the FOV. In this case, however, the ghosts are very closely spaced to one another (or, on top of each other). Note that the excursions remain constant (36).

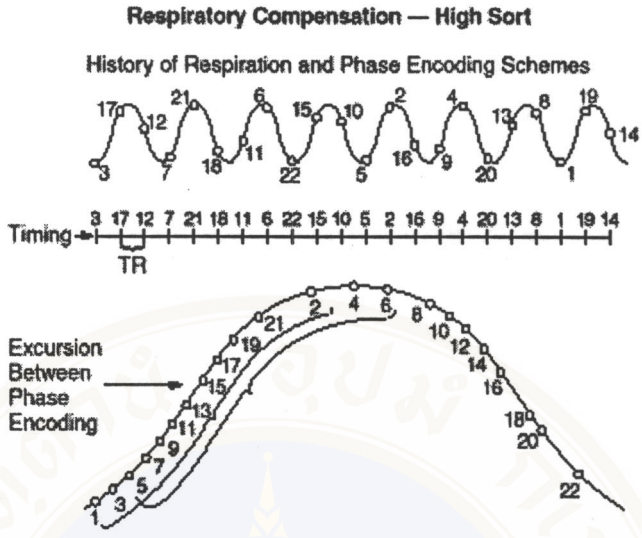

Figure 10-23C. If Respiratory Compensation high sort (C) is used, the excursions between phase-encoding create ghosts that are widely spaced. These ghosts are separated as far as possible, placed at the edge of the FOV, then thrown out. Note how the phase encoding between excursions remains constant (36).

The first method is low-frequency sort, which minimizes these variations (for minimal chest wall motion view-to-view). The second method is high-frequency sort, which maximizes the variations (for maximum chest wall motion view-to-view). The high-sort technique usually provides better results. While low-sort Resp Comp can be used with 1 NEX, high-sort Resp Comp requires that NEX be a power of 2 (2, 4, 8, 16, etc.). It doubles the FOV both in the phase-encoding direction, as in (figure 10.24), and the frequency-encoding steps as No Phase Wrap was done (see Aliening: Wraparound Artifacts / No Phase Wrap), and then reorders the phase-encoding steps, on the fly, matching to the respiratory cycle. Since the number of excitations (NEX) in high sort is cut in half, some multi-signal averaging loses.

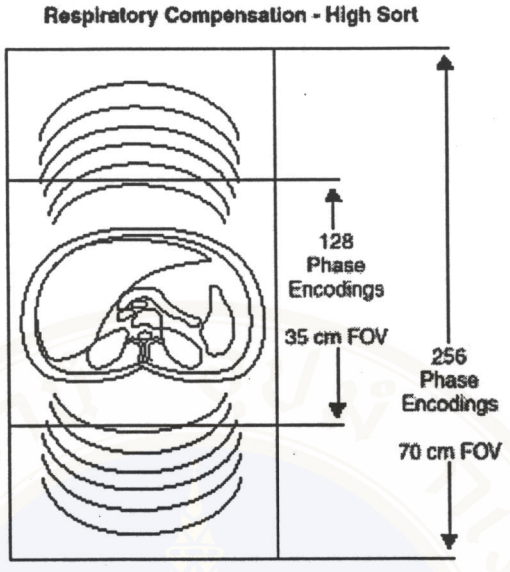

Figure 10-24. Respiratory Compensation High Sort doubles the FOV in the phase encoding direction to allow artifacts which are placed near the edge of the FOV to be discarded during the reconstruction process (36).

10.5.2 Cardiac Motion

10.5.2.1 Cardiac Gating (1, 2, 6, 36)

During the cardiac cycle, the heart's chambers contract and dilate cyclically. To obtain clinically useful images, each view must be sampled precisely at the same phase of this cycle by synchronizing data acquisition to a signal reflecting the cardiac phase typically, the R-wave of the ECG. Images can then be obtained at different phases by varying the delay time between trigger signal and excitation pulses (figure 10-25A) and (figure 10-25BC).

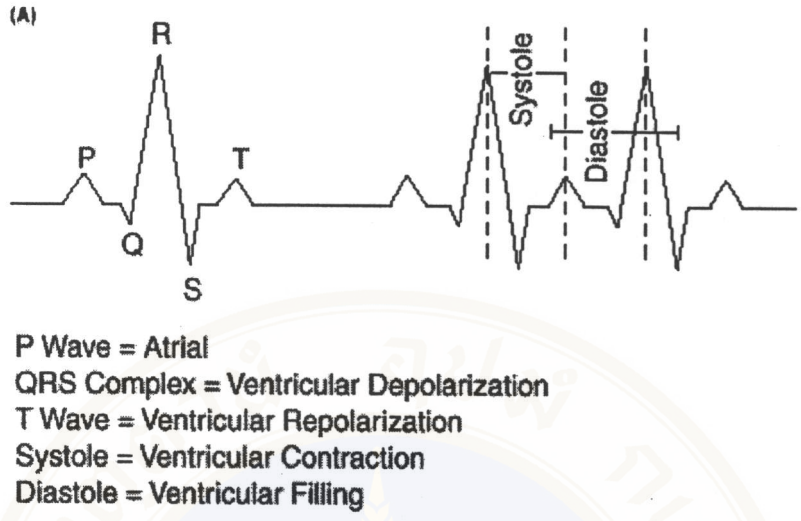

Figure 10-25. (A) illustrates the ECG trace and corresponding labeling. Varying the trigger delay allows images to be acquired demonstrating different times of the cardiac cycle. Short delay times will provide images demonstrating systolic phases. Diastolic images are obtained by increasing the delay time (36).

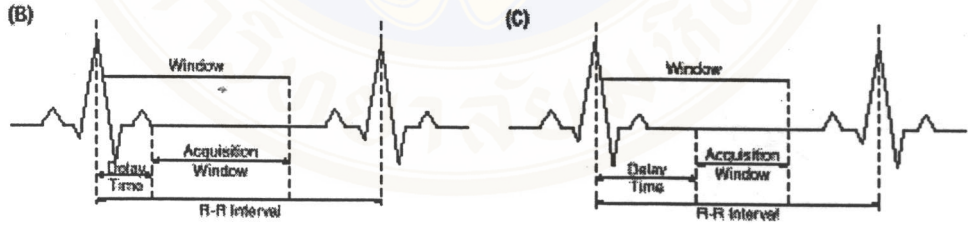

Figure 10-25 BC. Diastolic images are obtained by increasing the delay time. Increasing delay time will shorten the acquisition window and thereby decrease the number of slices available (B) and (c) (36).

Four ECG gating acquisition modes are:

1) Multi-slice, single phase, in which each slice represents a different phase of the cardiac cycle, in other words, a specific time in the patient's R-R interval (figure 10-26).

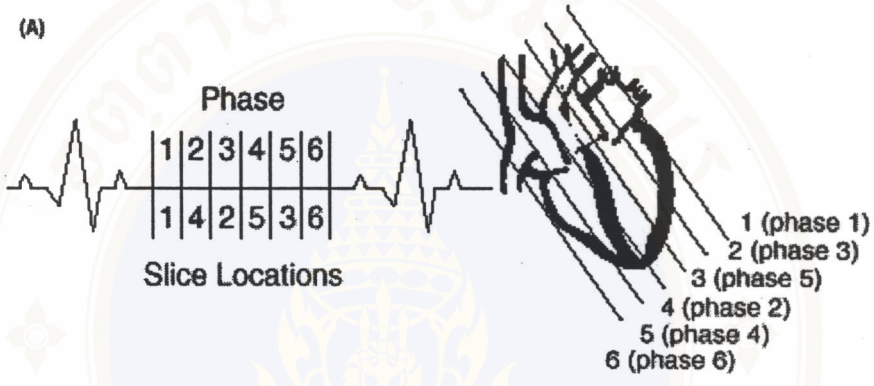

Figure 10-26A. Multi-slice, single phase: Each slice location represents a different phase of the cardiac cycle (e.g.slice location one represents phase 1, slice location two represents phase 3, slice location three represents phase 5, etc.) (36).

2) Multi-slice, multi-phase balanced matrix, in which the number of slices and phases is equal, in other words, the number of acquisitions is equal to the number of slices prescribed (figure 10-26B). An example: four anatomic slices and four cardiac phases will result in 16 images.

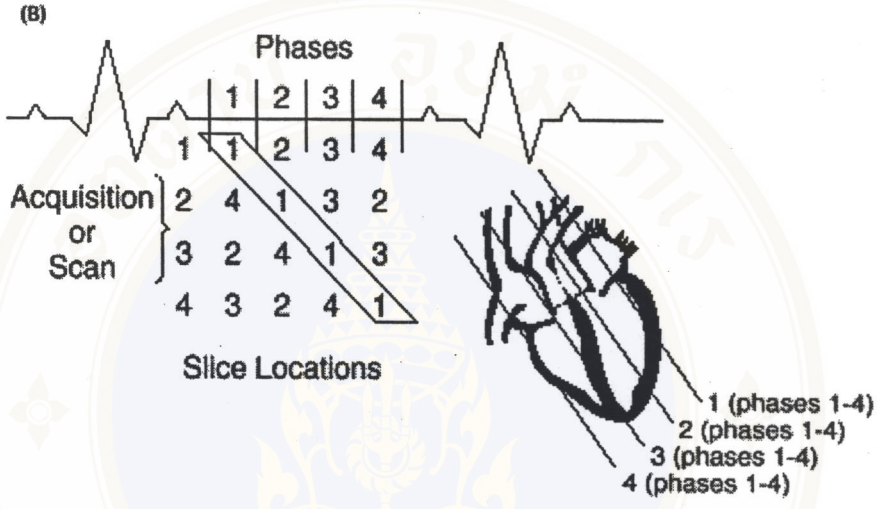

Figure 10-26B. In multi-slice, multi-phase acquisitions, multiple phases can be acquired at each slice location by prescribing either the same number of phases and slice locations (a balanced matrix), or an unequal number or phases and slice locations (an unbalanced matrix)(36).

3) Multi-slice, multi-phase unbalanced matrix, in which the number of slices dose not equal the number of phase, instead, multiple phase each slice location is produced from a few acquisition (figure 10-26C). For example, three anatomic slices six cardiac phases will yield 18 images.

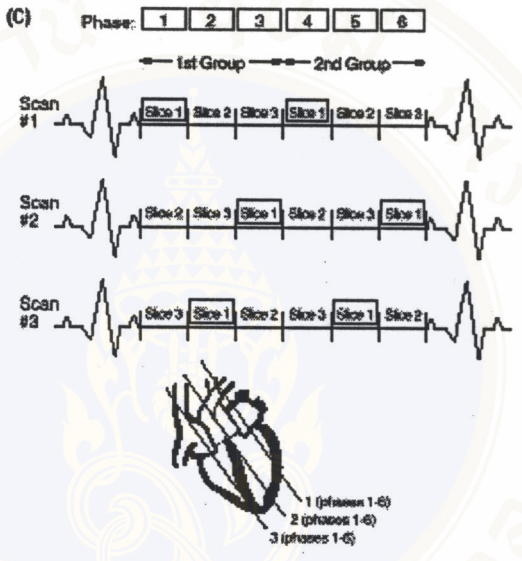

Figure 10-26C. Multi-slice, multi-phase unbalanced matrix: Note that in a multi-slice, multi-phase unbalanced matrix, six cardiac phase images can be acquired at three unique locations representing one of the six phases of the cardiac cycle. This differs significantly from a single-slice, multi-phase acquisition (36).

4) Single-slice, multi-phase, in which multiple phases are collected at a single slice location in a single acquisition (10-26D). In interpreting gated studies, it helps to understand the order and position of each slice within the TR and anatomical location.

Figure 10-26D. Single-slice, multi-phase acquisition: Each slice location represents a different phase of the cardiac cycle (e.g., slice one represents phase 1, slice two represents phase 3, slice three represents phase 5, etc.)(36).

Method 1, for instance, yields images through an area of interest with a reduction in cardiac-induced motion artifacts. The temporal order of slices is not sequential within the TR/cardiac cycle. Instead, slices appear in a different order for each number of slices requested. For example, for slice number = 5, the order are 1, 4, 2, 5, 3. For slice = 9, the order is 1, 6, 2, 7, 3, 8, 4, 9, 5. (10-27) illustrated this point. Methods 2, 3 and 4 yield images with dynamic functional information about a specific location; these studies are therefore often displayed dynamically, using the paging function.

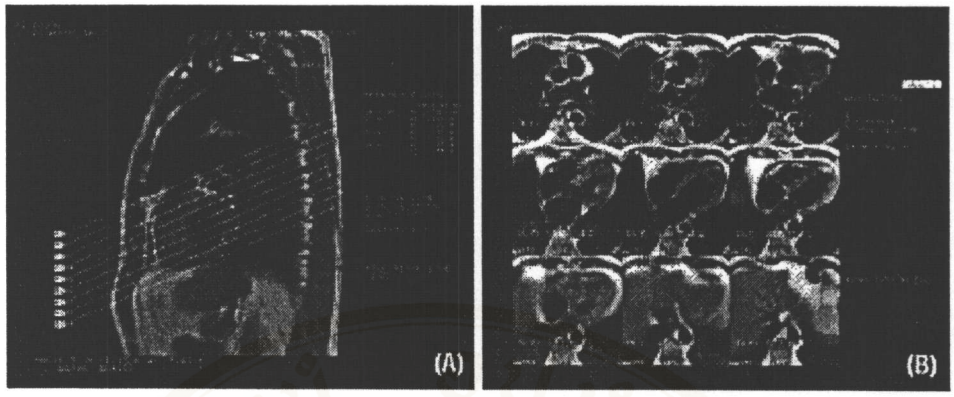

Figure 10-27. Image (A) illustrates slice positions for a nine slice cardiac gated acquisition. Image (B) demonstrates images one through nine acquired with delay times of 150, 272, 394, 516, 638, 211, 333, 455 and 577 ms respectively. With respect to ascending delay times, this highlights the slice collection order as being 1, 6, 2, 7, 3, 8, 4, 9, 5 (36).

The phases are displayed in order for each slice location (figure 10-28). It should be noted that arrhythmias alterations in the rhythm of a patient's heart beat in terms of time or force can cause significant artifacts in any gated study, particularly when they occur during the middle of the scan. This artifact is patient-dependent; it does not indicate a system malfunction. Note, too, that whichever gating technique is used, TR and resulting image contrast is primarily determined by the patient's cardiac cycle. Variations in SNR are inevitable, since heart rates may vary considerably. Image contrast is altered by the number of cardiac cycles used to acquire the data (skip number). A larger ship number will give images demonstrating increased T2 contrast.

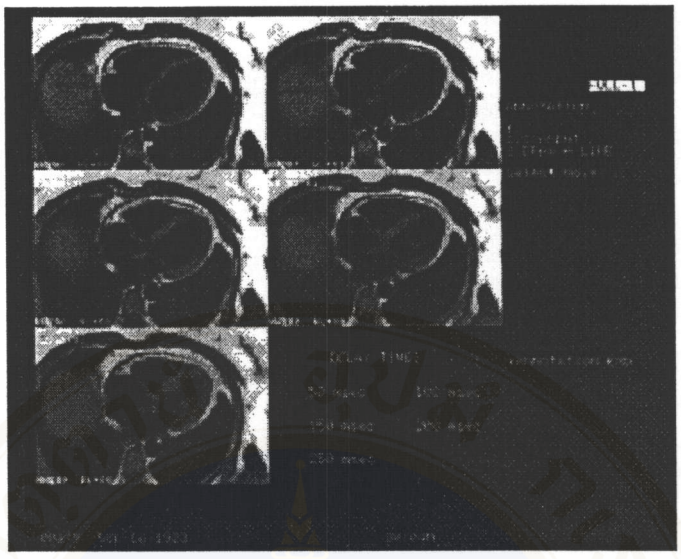

Figure 10-28 – Multi-phase images at one anatomic location provide information about the function of the heart. Demonstrated are five phases of the left ventricle from early systolic (50 ms delay time) to end systolic (250 ms delay time) contraction (36).

10.5.3 Blood and CSF Flow Artifacts (1, 2, 6, 23, 35, 36, 54, 55, 56)

Arterial blood and CSF flow are both driven by the cardiac cycle. Therefore, it makes sense that gating to the cardiac cycle is the most effective way of suppressing the ghosting artifacts that can be produced by flow. Although ghosting may occur in any direction, these artifacts are usually most conspicuous in the phase-encoded direction, when the blood flows perpendicular to the imaging plane. Flow artifacts are most prominent in the first and last slices in an axial study, for example, the most superior and most inferior slices. This occurs because the inflow of unsaturated (fresh) spins between successive excitations serves as a "flow-related enhancement" i.e., it enhances signal, thereby enhancing this artifact.

10.5.3.1 Flow Compensation or Gradient Moment Nulling (GMN) (1, 2, 6, 35, 36)

Flow Compensation or Gradient Moment Nulling (GMN) is a reduction technique to diminish artifacts caused by moving protons. Flow artifacts are caused by the modulation of the phase either coherence or incoherence of the magnetization in each pixel induced by the movement of protons. That is true nor only for such physical movement as respiration and cardiac contraction, but also for the flow of such liquids as blood and CSF. In fact, flow artifacts are the most troublesome of all, because of the involved velocities and total displacement. Flow incoherence can manifest itself as a loss of brightness in areas of high velocity. Nevertheless, an even more disturbing effect is the appearance of a fuzzy replica of flow in the phase direction (similar to the duplication of the thorax caused by respiratory motion). They are caused by body fluids which velocities and magnetic amplitudes vary with the cardiac cycle.

There are two types of flow modulation:

1. Pure amplitude modulation caused by protons entering or exiting a slice the in-out flow effect
2. Phase modulation caused by imperfect rephasing of flowing protons between their excitation and signal sampling Phase modulation can be effectively minimized with flow compensation (Flow Comp). Gradient waveforms are simply added to rephase both moving and stationary spins at the time of sampling (figure 10-29).

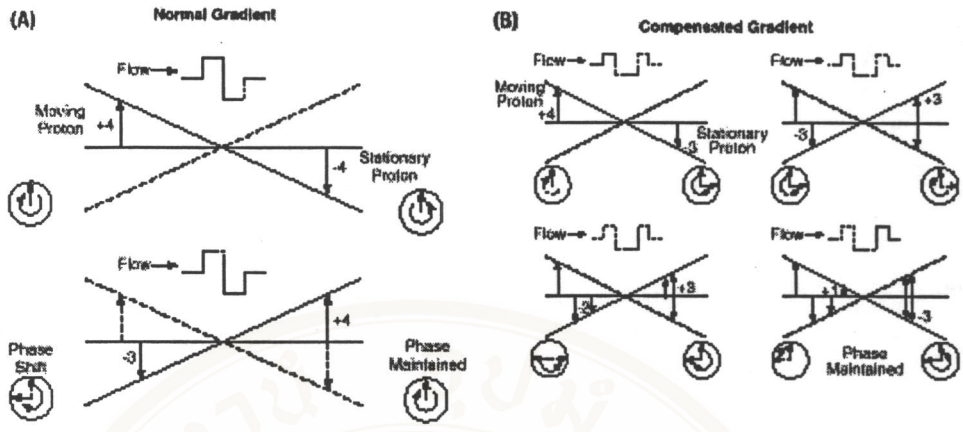

figure 10-29 – Effect of flow compensation on phase modulation (36).

The disadvantage of flow compensation is that an increment in the minimum echo will delay the additional gradient pulses (figure 10-30 and figure 10-31). The scenario is discussed about effectiveness only for flow with a constant velocity. Although it is possible to correct for higher order motion, like acceleration, there exists a penalty of increased minimum TE. Just as first order moment nulling requires additional gradient interaction and therefore, time, higher order moment nulling imposes an even greater time penalty. Maximum artifact reduction benefits can be obtained by using flow compensation, presaturation and gating techniques. Flow compensation is most effective with in-plane flow motion. Presaturation pulses are effective on flow perpendicular to the imaging plane.

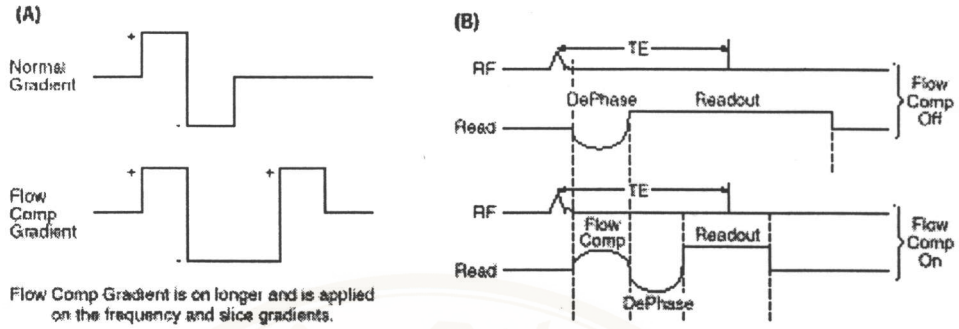

Figure 10-30. In (A), the Flow Compensation is on longer and applied to the frequency and slice gradients. This can result in some gradient stress (thus, fewer slices) and a wider bandwidth (reduced signal-to-noise). In (B), note that Flow Compensation requires additional gradient time. The TE is unchanged and the readout window is shortened resulting in a wider bandwidth. This may result in a decrease in SNR (36).

Figure 10-31- Flow compensation helps to reduce in-plane flow motion artifacts such as those, which arise from CSF in sagittal imaging. Application of additional gradients corrects for velocity changes, which occur during the acquisition pulse sequence (36).

10.5.3.2 Presaturation (1, 2, 6, 36)

Vascular flow motion can be minimized with a capability called spatial presaturation (P-SAT). A 90-degree pulse is applied to saturate the nuclei outside the imaging volume and to nullify signal from flowing spins entering the imaged slice between successive excitations. If they do not provide a readable signal, they cannot create an artifact (figure 10-32).

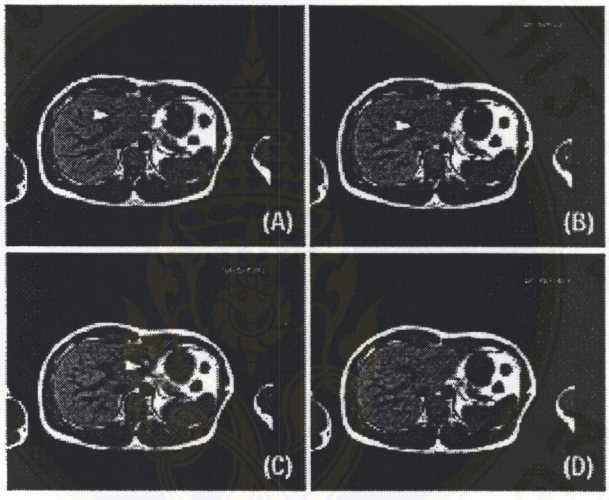

Figure 10-32. Impact of presaturation on flow artifacts. An image acquired using conventional techniques (A) shows flow artifacts from the major abdominal vessels – e.g., the IVC and descending aorta. Presaturation pulses applied in the direction of the head eliminates arterial artifacts (B), since the blood moving from the heart in the caudal direction has been saturated. Similarly, presaturation in the foot direction eliminates venous flow motion artifacts (C). Presaturation pulses applied in both directions suppress both venous and arterial flow artifacts (D) (36).

Presaturation pulses are 80-mm thick "slabs" that can be applied in any of the six orthogonal directions including head, foot, anterior, posterior, left, or right view in any combination. These slabs are fixed at 20 mm outside the FOV in the selected directions (figure 10-33). The crucial locations, however, are those parallel to the

imaging plane for example, head and foot in axial images, and anterior and posterior views in coronal images.

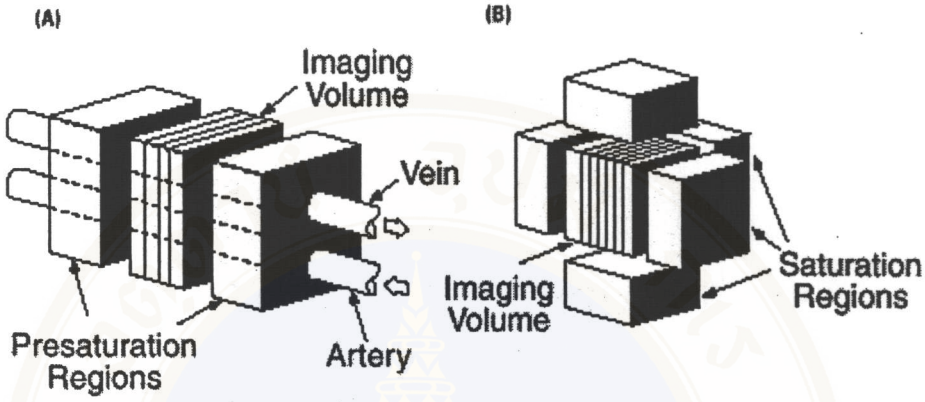

Figure 10-33 – Principle of spatial presaturation: (A) Saturation volumes on either side of the imaging slab; (B) saturation on all three axes (36).

Furthermore, since most vessels run between head and foot, P-SAT is most effective (and most needed) in axial images, particularly in the abdomen, neck and extremities. Not only does P-SAT eliminate these phase artifacts, it also provides intraluminal signal void, to help distinguish between patent and obstructed vessels. Two disadvantages are associated with P-SAT: First, the application of the presaturation pulses and subsequent gradient spoiler pulses requires time; the number of slices per TR will therefore be somewhat reduced. Second, if ECG gating is used, the minimum delay time will increase when P-SAT is prescribed. The severity of these compromises will depend on the number of chosen presaturation pulse directions. It makes sense, then, to select only the SAT planes that are necessary for the study at hand. For example, in head studies (imaging to the apex) only a foot SAT

pulse is used, do not bother saturating air above the head since it will not improve image quality.

10.5.3.3 Swapping Phase and Frequency (1, 2, 6, 36)

Since flow results in motion artifacts in the phase-encoding direction, it is important for the user to understand the MR Max Plus default directions for phase and frequency encoding. They are presented in table 10-2.

PLANE	PHASE ENCODING	FREQUENCY ENCODING
Axial	Anterior / Posterior	Right / Left
Sagittal	Anterior / Posterior	Head / Foot
Coronal	Right / Left	Head / Foot

Table 10-2 – Phase and frequency encoding gradients: defaults for squared matrices

When the area of interest is obscured by motion in the phase-encoding gradient, the swapping of the phase and frequency directions can be extremely helpful. The images in figure 10-34 illustrate this capability. If the thoracic spine image (10-34A) is acquired by the system's phase and frequency defaults, respiratory and cardiac motion will interfere with the area of interest. Once phase and frequency has been swapped (figure 10-34B), this ghosting artifact is effectively eliminated. Noted, however, that we will introduced the new problem (aliasing) if we put phase in the direction of the long-axis of the body. To eliminate this wraparound, No phase wrap in combination with swapping phase and frequency is used (figure 10-34C). In

addition, if a reduced asymmetrical matrix is used in the phase encoding direction, it may also be desirable to use the rectangular pixel option to assure full FOV coverage and prevent wraparound (figure 10.34D and figure 10.34E). In addition, if a reduced asymmetrical matrix is used in the phase encoding direction, it may also be desirable to use the rectangular pixel option to assure full FOV coverage and prevent wraparound (figure 10.34D and figure 10.34E).

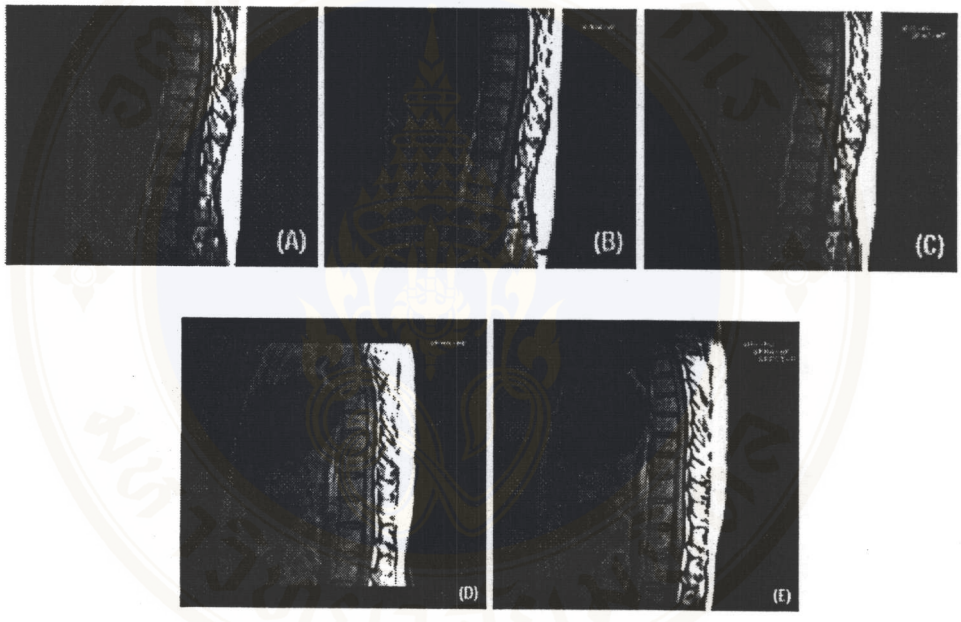

Figure 10-34ABC. Swapping phase and frequency. Motion and flow artifacts are common in thoracic spine images acquired using the system default for phase and frequency directions (A). These artifacts can be moved perpendicular to the area of interest by swapping phase and frequency (B); however, phase wraparound can result. No Phase Wrap may be applied to eliminate this wraparound (C), The figure DE, illustrate when we is reduced matrix used in the phase direction, only part of the FOV will be displayed (D). The remedy: using the rectangular pixel option to assure full FOV coverage (E) (36).

10.6 Flow artifacts in Magnetic resonance imaging

10.6.1 High-velocity signal loss (1, 2, 6, 23, 35, 56, 57, 58)

Flow void represents signal intensity loss from moving spins. The decreased signal intensity can be caused by time-of-flight and phase effects. Time-of-flight effects that contribute to decrease vascular signal are washout and saturation. With spin echo, imaging, washout or high velocity signal loss occurs when spin is not exposed to both initial 90^0 pulse and subsequent 180^0 refocusing pulse. Spin flowing into the slice after before the 180^0 refocusing pulse will not emit a signal. For flow perpendicular to the imaging plane at the constant velocity (v), the fraction of washout is given by

$$(TE/2)(v/D)$$

Where TE is echo time and D is slice thickness. For a given velocity, washout effects will increase with a longer TE and thinner slice. When $(v)(TE/2)>D$, washout is complete and the signal will be zero.

Saturation effects can decrease intravascular signal by reducing flow-related enhancement. As in this case, presaturation RF pulses outside the imaging volume can be used to accentuate vascular flow voids. Factors that reduce flow-related enhancement will result intravascular signal loss; these factors include an increase in the repetition time (TR), a short T1 of stationary tissue, a longer T1 of flowing blood, and the use of multislice imaging to allow saturation in center slice.

Phase effects also reduce vascular signal. Intravoxel spatial variations of velocity and acceleration that promote phase dispersion as flow occurs along field gradients will decrease signal intensity. Turbulence that increases random motion will

also decrease vascular signal intensity because of the resultant loss of phase coherence.

10.6.2 Flow-related enhancement and effect of presaturation radiofrequency pulses (1, 2, 6, 23, 35, 56, 57, 58)

Flow-related enhancement represents a relative increase in intravascular signal from unsaturated blood when compared with the partially saturated background tissues.

By increasing intravascular signal intensity, flow-related enhancement competes with washout effects and make ghost artifacts worse. Both flow-related enhancement and associated ghosting can reduced by applying presaturation RF pulse outside the acquisition volume. The presaturation RF pulses are designed to eliminate the magnetization from inflowing spins so that they do not contribute to signal intensity. This reduction in signal accentuates vascular flow-void and decreases ghost artifact.

10.6.3 Intravascular signal: spin-echo versus gradient-recalled echo imaging (1, 2, 6, 23, 35, 56, 57, 58)

Flow-void with routine spin-echo imaging helps to establish vascular patency. The absence of intravascular signal is caused by moving spins and spin dephasing With slice-selective spin-echo pulse sequences, two competing time of flight phenomena contribute to the final intravascular signal intensity. Washout effects counterbalance flow-related enhancement. When washout dominates, intravascular signal decreases and is manifested by flow-void.

Washout means that, for through-plane flow, moving protons do not receive both the 90^0 and 180^0 RF pulses that are required to produce a signal. Factors that decrease the likelihood that moving spins are irradiated by both RF pulses include a decrease in slice thickness and increase in the TE. With a thin slice, moving protons remain within the image plane for a shorter period of time. With a longer TE, spins are more likely to flow from or washout of the selected slice during the interpulse interval.

Saturation effects that oppose flow-related enhancement will promote intravascular signal loss and accentuate flow-void. The application of presaturation RF pulses outside the imaging volume will increase the saturation of inflowing spins and decrease the signal intensity from flow-related enhancement. Increased saturation of flowing blood will occur with longer TR and a relative in T1 relaxation of blood compared with adjacent stationary tissue.

Phase effects can contribute to decreased intravascular signal intensity. Spatial variations in velocity and acceleration across a vessel lumen result Intravoxel phase shift variations, since flow occurs in the presence of field gradients. The resultant phase shifts promote loss of phase coherence and decrease in signal intensity. Turbulent flow can have a complex effect on intravascular signal intensity. Turbulence will promote signal loss when increased random motion accentuates spin dephasing.

Times of flight washout effects that contribute to flow-void are feature of spin-echo sequence with slice selective 90^0 and 180^0 pulses. Gradient echo sequences are structured such that flow voids are decreased and flow related enhancement is

accentuated. Gradient echo imaging increases intravascular signal intensity with improved sensitivity to flow.

There are two important features of gradient echo scanning that reduce intravascular signal loss. First, gradient echoes refocusing gradients are not slice selective. This reduced signal loss from washout effects. Second, gradient echo images typically are acquired with TEs that are shorter than those used with spin-echo imaging. The shorter TE minimizes signal loss from spin dephasing pior the readout.

10.6.4 Laminar flow and Even-echo rephasing (1, 2, 6, 23, 35, 56, 57, 58)

Paradoxical enhancement or signal increased within patent vascular structures is observed on the even-echo image of symmetric multiecho spin-echo pulse sequence. Even echo rephasing is usually observed with slow laminar flow in the presence of linear gradient. Unlike adjacent stationary spins, phase angles that accumulate from larminar flow in linear gradient are not corrected at the odd echo in the standard spin echo pulse sequence. These uncorrected phase changes result in signal loss from dephasing. However, at even echoes, the quadratically acquired phase changes are reversed, resulting in rephasing and increased signal intensity. When compared with stationary background tissue, which loses signal intensity at longer TE, intravascular rephasing results in greater signal intensity than expected on second and subsequent even echoes. This produces a paradoxical increase in brightness of vessels compared with the remainder of the image, which loses overall brightness.

10.6.5 Flow-related spatial misregistration (1, 2, 6, 23, 35, 56, 57, 58)

Two conditions are necessary to be observed for spatial misregistration of signal from vascular flow. First, there must be flow-related increase in signal intensity. This can be from flow-related enhancement, even-echo rephasing, or the application of flow compensation gradient. Second, there must be obliquely oriented through-plane or in-plane flow. Flow-related bright signal is spatially misregistered because of fluid motion between the phase and frequency-encoding steps during 2 DFT localization.

At the beginning of the pulse sequence, spin location is assigned as a function of phase, In the time interval between phase-and frequency-encoding steps, the spin will move downstream. When the read-out gradient is applied, the frequency assignment is determined by its new position. The signal generated from this moving spin will therefor be registered as function of the earlier phase assignment and the later frequency assignment resulting in phase and frequency coordinates that are outside the true anatomical vessel location. Spatial mismapping causes the signal intensity from flowing spins to be added to the signal of the adjacent stationary tissue. This results in a bright line or dot that is adjacent to the true vessel location. The true vessel lumen is displayed as a signal void, because few spins are accurately mapped to the lumen.

Spatial misregistration artifacts can have a variable appearance, on depending on the mechanism generation flow-related bright signal. With flow-related enhancement and even echo rephasing, greater displacement away from the true vessel lumen is expected with longer TE, since there is a greater time interval between phase-and frequency-encoding steps. This TE dependence, however, is not usually observed

with flow compensation gradients. The distance that the spatially misregistered signal is displaced from the vessel lumen will be determined by flow velocity and the angle of orientation of the vessel with the phase-encoding axis. The width of the displace is determined by the flow profile.

Spatial misregistration artifact is commonly encountered in clinical MRI imaging because of the routine use of flow compensation gradients. Important clinical information can be derived by analyzing the spatial misregistration artifact. The presence of this artifact helps to confirm vessel patency. Simple analysis of the position and distance of displaced bright signal can give the direction of flow and an estimate of mean velocity.

10.6.6 Flowing blood versus station tissue (1, 2, 6, 23, 35, 56, 57, 58)

A definite flow-void or flow related enhancement establishes vessel patency. These time-of-flight effects can produce sufficient contrast to distinguish between flowing blood and adjacent static tissue. With some acquisition, however, differentiating flow from stationary tissue or thrombus can be difficult.

A signal void is a common feature of high-velocity blood flow with routine spin-echo imaging. Flow void is maximized by selecting a thin slice, long TE, and a plane perpendicular to flow direction. Supplementary RF pulses for spatial presaturation can also be used to produce flow-void. The effectiveness of presaturation depends on many variables, such as the proximity of the presaturation band to the selected slice.

A signal void is not always generated by spin-echo imaging despite vessel patency. This tends to occur with show or recalculating flow. Mechanisms that

contribute to increased intravascular signal include entry phenomenon, even echo rephasing and pseudogating. The bright signal that results from these type of flow-related enhancement can make it difficult to distinguish flowing blood from subacute thrombus and soft tissue.

10.6.7 Artifacts in 2D Time-of-flight (TOF) (1, 2, 6, 58)

Artifacts may occur in 2D TOF methods whenever there is uneven weighting of the acquired data. For example, if a purely sinusoidal variation is superimposed on the signal two distinct ghost image are created one on each side of the main object. Differences in saturation produced by variation in blood velocity can lead to uneven weighting of the acquired data. The variation due to saturation may be reduces by reducing the tip angle, which in turn reduces the degree of saturation.

Respiration also can lead to saturation induced artifacts in 2D TOF images. One such artifacts is bright bands in nonvascular tissue in the MIP images. This results when fresh, fully magnetized nonvascular spins are brought into the images slice by respiration. These fully magnetized nonvascular spins give rise to a large signal and appear bright in the image. Respiration essentially causes in-flow refreshment of nonvascular tissues during acquisition of some of the slices, which gives rise to bright bands in nonvascular tissues in 2D TOF images acquired in regions affected by respiration. Respiration may also dark bands within a vessel.

Another artifacts that can appear in a 2D TOF image is thrombus mimicking flowing blood. It is well known that thrombus can have a short T1 and appear bright in 2D TOF image. When this is suspected, two methods can be used to determine whether a vessel signal is due to thrombus or flow. Placing a saturation pulse

upstream of the direction of suspected blood flow would suppress the inflow refreshment and the vessel would have a low signal if it contained the flowing blood, whereas it would have a low signal is approximately proportional to blood velocity and would provide a direct determination of the flow state.

10.6.8 Artifact in the Three-Dimension Multiple Overlapping Thin Slap Angiography (MOTSA) (1, 2, 6, 62)

One of the problems of the MOTSA approach is discontinuity in the image at the junction of the slabs. The discontinuities are due to the fall-off of the excitation profile at the edged of the slabs, and also differences in the a mount of blood saturation at the slab entrance and exit. This is so-called venetian blind artifact at the slab junctions may be reduced by overlapping the slabs to create a more uniform MIP image. The penalty for doing this, in the case of a 50 % slab overlap, is a factor of two increase in scan time for the same spatial resolution and coverage. A spatially varying RF pulse, may be used to reduce the venetian blind artifact.

10.6.9 Staircase artifact (1, 2, 6, 62)

This artifact occurs in M2D inflow technique and might be seen in the projections of the slices. The staircase artifact can be reduced by using a slice gap with a negative value. Normally an overlap factor of 25-30 % is sufficient, e.g. 4 mm slice with 1 mm overlap.

10.6.10 Zebra stripe artifact (1, 2, 6, 62)

This artifact some time occurs when using Region Suppression Technique (REST) in combination with 3D turbo spin echo (3D-TSE). Changing the number of REST slabs of decreasing the TSE factor reduces the artifacts.

10.6.11 REST artifact (1, 2, 6, 35, 62)

This artifact can be seen when two free REST slabs intersected each other are used. Interference between the REST slaps can cause an artifact. This can be voided by applying the REST slabs such that do not overlap.

10.6.12 Aliasing artifact in PC MRA occurred when choose the VENC incorrectly (1, 2, 6, 62)

VENC stands for velocity encoding, which is a parameter that must be specified by operator to perform a PC MRA technique. VENC, measured in centimeters per second (cm/sec), should be chosen to encompass the highest velocities likely to be countered within the vessel of interest. The VENC parameter adjusts the strength of the bipolar gradient so that the maximum velocity selected corresponds to 180^0 phase shift in the data.

The VENC setting is critical for proper performance of the MRA pulse sequence but often can only be estimated since its optimum value is generally not know in advance. If VENC is chosen too high, the range of flow imaged will encompass only a limited number of degrees of phase shift. The signal-to-noise ratio of the image is adversely affected, and vessels with show flow may be difficult to see.

If VENC is picked too small, velocity aliasing may occur with faster flows not being appropriated represented. For example, if the chosen value of VENC is 50 cm/ sec, the bipolar gradient is adjusted so that a flow of 25 cm/sec is assigned a phase of 90^0 , whereas a flow 50 cm/sec is assigned 180^0. If the actual vessel velocity is 75 cm/sec, this flow is represented by a phase shift of 270^0, which the computer cannot distinguish from a phase shift of -90^0. Instead of representing the 75 cm/sec flow as its actual velocity, the computer will assign it a flow of 25 cm/sec in the opposite direction. Proper estimation of VENC is thus critical for successful PC MRA.

10.7 Pulse sequence-related artifacts

10.7.1 Inversion Recovery Bounce Point (1, 2, 6)

The timing diagram of inversion recovery (IR) sequence consists of 180 degree pulse followed with 90 degree pulse. The first pulse inverts all of the signals in the slice and recovery the period of beginning TI. The faster relaxing spins lead the pack and some point pass through zero on their way to regaining the full positive alignment. the slowest relaxing signals are still point in the negative direction. Any two tissues with different spin-relaxation times, T1, will be such a state for a period between their respective zero-crossings. The readout part of the sequence is now supplied.

10.7.2 SPIR artifact (1, 2, 6)

Water suppression instead of fat or no suppression, sometimes occur in scans made with SPIR. This is due to disturbances in magnetic field homogeneity, because of the patient or coil interference. If SPIR is not possible for fat suppression, use IR

or IR-TSE with short T1 (STIR). STIR sequences provide good fat suppression. STIR sequences are not useful in combination with contrast agents.

In some cases, the use of pads made out special material may help. Noted that by putting the pad between surface coil and patient, the SNR is adversely affected (larger coil-patient distance)

10.7.3 Artifacts is echo planar imaging (EPI) (1, 2, 6, 36, 37)

There are two main type of EPI techniques including single shot EPI and multishot EPI. Earlier single shot EPI techniques use a constant phase-encode-gradient. Newer techniques use a blipped phase-encoded gradient as referred to blipped EPI.

10.7.3.1 N/2 Ghost Artifacts (1, 2, 6, 36, 37)

Even with blipped EPI, phase errors may result from multiple positive and negative passes through k-space (i.e. alternating polarity of the readout gradient). Ghost artifacts that are not caused by motion as in CSF but by eddy currents, imperfect gradients, field nonumiformities or mismatch between the time of the odd and even echoes appeared along the phase axis in the main image. Since the ghosts are derived from half the data (even or odd), they are called N/2 ghosts. The way to reduce N/2 ghosts is to minimize the eddy current by the proper tuning of the gradient.

10.7.3.2 Susceptibility artifacts in EPI (1, 2, 6, 36, 37, 62)

Diamagnetic susceptibility effects in EPI may result in variations in frequencies and phase errors. This effect is reduced for multishort EPI because phase errors have less time to build up. An advantage of nultishot EPI over fast spin echo is that it has contrast much closer to convention spin echo, so it has greater sensitivity to magnetic susceptibility effects such as hemorrhage compared with FSE. The ways for minimizing the susceptibility artifacts in EPI are using proper shimming, TE shortening, or multishot echo.

10.7.3.3 Chemical shift artifacts in EPI (1, 2, 6, 36, 37, 62)

Because of the presence of phase error propagation along the phase-encode axis, chemical shift artifacts in EPI occur along the phase-encode axis rather than along the frequency-encode axis seen in conventional spin echo. These artifacts are much more pronounced than with conventional spin echo, so an effective fat suppression technique is necessary. The way for minimizing these artifacts is to apply fat suppression technique.

CHAPTER XI

CONCLUSION AND RECOMMENDATION FOR FUTURE RESEARCH

Artifacts can occur in MR images for a number of reasons, degrading the image quality and some time hindering diagnosis. They may be caused by technical problems and data handing or by physiological effects from the patient. Since most artifacts can be reduced, it is important to recognize them, and to know what can be done to prevent them.

This thesis can be summarized MRI artifact based on its sources and can be divided in to 3 groups. First, it is occurred from the instrument. Second it is occurred from the data acquisitions and pulse sequence imaging. Third, it is occurred from the patient's physiologic motion.

Whereas artifacts that occurred from the instrument can not be found due to the development in imaging technology, MRI artifacts usually have cause from the data acquisitions such as aliasing, chemical shift, turncation, magnetic susceptibility etc. and the patient's motion. Therefor, if we consider the reduction techniques in MR imaging we would consider mainly for these last 2 causes.

The techniques for elimination or reduction all 3 causes of these MR artifacts roughly include 1). using the appropriate hardware for instrument-related artifacts 2). the suitable software for data acquisition-related artifacts and 3). the gating for motion artifacts

Some artifacts can be reduced or eliminated completely by the appropriate techniques. However, at present there are still some problems about these reduction techniques that required the future development for better correction or improvement. These certain directions are as followings. First, the hardware development mainly of the coils to produce the optimal ones (surface, elliptical or special procedure-targeted) for spatial resolution improvement. Second, the software development of artificial intelligence for allowing unerring selection of optimal sequence such as echo-planar imaging (EPI) for the given clinical condition. Third, the software development of increased scan speed for reducing the scanning time to a few seconds which would examine some organs with the better quality. Finally, the development method to elimination and reduction for motion artifacts such as gating.

REFERENCES

1. Edelman RR, Zlatkin MB, Hesselink JR. Clinical magnetic resonance imaging.(vol 2). USA: W.B. Sauanders company, 1996.

2. Stark DD, Bradly WG. Magnetic resonance imaging. 2 nd (vol. 2). New York: Mosby Yearbook; 1992.

3. Elizabeth P, Oaks S, and Brown R, Lufkin RB, Solomon M, Walach V, Ruszkowski J, and Hanafee W. Artifacts in MR imaging: mechanisms and clinical significance. [Abstract]. Radiology 1985; 157:397

4. Petterson H, Allsion D. The encyclopedia of medical imaging. In: Von Shculthe FK'Physics, technique and procedures.Sweden: NICER, 1998.

5. Bellon EM, Haackc EM, Coleman PE. MR artifacts: a review.AJR 1986;47: 1271-81.

6. Stark DD, Bradly WG. Magnetic resonance imaging. New York: Mosby Yearbook, 1988.

7. Markisz JA, Aquillia M. Technical magnetic resonance imaging. USA: Yearboo, 1992.

8. Solia KP, Viamonte M and Starewicz PM. Chemical shift Misregistration effect in magnetic resonance imaging. Radiology 1984; 153: 819-20

9. Ludeke KM, Roschman P and Tischler R. Susceptibility artifacts in NMR imaging. Magnetic resonance imaging 1985; 3:329-43.

10. Haacke EM, Tkach JA, Parrish TB. Reduction of T2* dephasing in gradient field echo imaging. Radiology 1989; 170: 457-62.

11. Kim JK, Kucharczyk W and Henkelman RM. Carvernous Hemagiomas: dipolar susecptibility artifacts at MR imaging. Radiology 1993; 187: 753-41.

12. Sakurai K, Fujita N and Harada K. Magnetic susceptibility artifact in spin echo MR-imaging of the pituitary gland AJR 1992; 13:1301-08.

13. Macgawon CK, Wood ML. Phase-encode reodering to minimize errors causes by motion. Magnetic resonance medicine 1996;35:391-398.

14. Wood ML, Henkelman RM. MR imaging artifacts from periodic motion. Medical physics 1985; 12: 143-56.

15. Schultz CL, Alfidi RJ, Nelson AD and Kopiwaxdo SY. Effect of motion on two-dimensional Fourier transforms imaging. Radiology 1986; 152: 1177-21.

16. Haacke EM, Patrick JL. Reducing motion artifacts in two-dimension Fourier transform imaging. Magnetic resonance imaging 1986; 4: 359-76.

17. Pattany PM, Phillips J, Chiu LC and Lipcamon JD. Motion artifact suppression techniques(MAST) for MR imaging Comput assistant tomography 1987; 118: 369-77.

18. Ehaman RL, Felmlee JP. Flow artifact reduction in MRI: a review of the role of gradient moment knelling and spatial prostration Magnetic resonance medicine 1990; 14: 293-307.

19. Lars TC, Kelly WM, Ehman RL and Wehrli FW. Spatial misrgistration of vascular flow during MR imaging of CNS: causer and clinical significance. AJR 1990; 155: 1117-24.

20. Edelman RR, Atkinson DJ, Silver MS, Loaiza FL and Warren WS. RRODO pulse-sequence: a new means of eliminating Motion flow, and wraparound artifacts. Radiology 1988;166: 231-36

21. Roo TKF, Hayes CE. Phase-correction method for reduction of Bo instability artifacts. JMRI 1993; 3: 676-81.

22. Wood ML, Henkelman RM. Truncation artifact in MR imaging magnetic resonance Medicine. 1985; 2:517-21.

23. Emternet. Email addresses Ball@uflt.Health.ufl.edu.[computer program]. Website/Internet/Mritutor/Artifact.html, internet/uc/Artifact. html,1998.

24. Elster AD. Question and answer in magnetic resonance imaging. St Louis: Mossby yearbook.1994.

25. Stephen JR, Wood ML. Categorical course in physics: The basic physic of MR imaging. North America: RANA, 1997.

26. Lufkin RB. The MRI manual. USA: Yearbook publisher, 1990.

27. Arena L,Morehouse HT,Safix J. MR imaging artifacts that stimulant disease: how to recognize and eliminate them. Radiographic 1995; 15: 1373-94.

28. Peggy W, Freimarck R. MRI for technologist New York: McGraw Hill 1995.

29. Carolyn K, MRI workbook for technologist. New York: Ravan Press 1992.

30. มานัส มงคลสุข. พื้นฐานทางฟิสิกส์ของ CT และ MRI. กรุงเทพ: ไพศาลศิลป์ การพิมพ์, 2532.

31. Buhong SC. Magnetic resonance imaging: physic and biological Principles St.Lious: Mosby company, 1988.

32. Elizabeth P. Oaks S, Brown R, Lufkin RB, Solomon M, Walach V, Ruszkowski j, and Hanafee W. Artifacts in MR imaging mechanisms and clinical significance. [abstract]. Radiology 1985;157:397.

33. Young WS. Magnetic resonance imaging basic principle. New York; Raven press, 1984.

34. Henkelman RM, Bronskill MJ. Artifacts in magnetic resonance imaging Rev. Magnetic resonance medicine, 1987; 2:1-126.

35. Hendrick RE, Russ PD, Simon JH. MRI; Principle and artifacts. New York Raven press 1993.

36. Signa Advantage Customer 5.4 EPIC software reference manual. GE Medical system, General electric company, 1994.

37. Basic Principles of MR imaging 2 nd edition Phillip Medical system.

38. Hornar JP. (www.cis.rit.edu). The basics of MRI. Email to Professor Hornark (jphsch@ rit.edu.) [Accessed 1999 July 30].

39. Hashemi R.H, Bradley W.G. MRI the basics. William & Wilkins, 1997.

40. Marcus ML, Schelbert HR, Shorton DJ, Wolf GL. Cardiac Imaging W.B. Saunders company,1991.

41. Manfield P, Morris PG. NMR imaging in Biomedicine. Academic Press, New York, 1982.

42. Lauffer RB. Magnetic resonance contrast media: Principle and Progress Magnetic Resonance Quarterly (6) 2: 65-84, 1990.

43. Hufman L, Kraner DM, Crooks LE, Ortendahl DA. Measuring signal to noise ratios in MR imaging. Radiology 1989; 173: 265-267.

44. Wehrli FW, Macfall JR, Prost JH. Impact of the choice of operating parameters on MR images. Magnetic resonance imaging. 2nd ed. Philadelphia: WB Saunders, 1988:73-86.

45. Hendick RE, Raff U. Image contrast and noise. In: Stark DD, Bragley WG. Eds. Magnetic resonance imaging 2nd ed. St.Louis; Mosby Year Book Inc.,1992:109-144.

46. Laakman RW, Kaufman B, Han JS, et al. MR imaging in patients with metallic implants. Radiology 1985;157:711-714.

47. Wesbey G, Edelman RR, and Harris R. Artifacts in MR imaging: descriptions, cause, and solutions. In:Edelman RR, Hesselink J.eds. Clinical magnetic resonance imaging. Philadelphia: WB Saunders, 1990.

48. Czervonke LF, Daniels DF, Wehrli FW, et al. Magnetic susceptibility artifact in gradient –recalled echo MR imaging. AJR 1988;9:1149-1155.

49. Ehman RL. MR imaging with surface coils. Radiology 1985;157:549-550.

50. Kulkarni MV, Patton JA, Price RR. Technical considerations for the use of surface coils in MRI. AJR 1986;147:377-378.

51. Brateman L. Chemical shift imaging: a review. AJR 1986;146:971-980.

52. Simon JH, Szumowski J. Chemical shift imaging with paramagnetic contrast material enhancement for improved lesion depiction Radiology 1989; 171:539-543

53. Clark JA II, Kelley WM. Common artifacts encountered in magnetic resonance imaging. Raiol Clin No Amer 1988;26:893-920.

54. Bradley WG JR, Walunch V. Blood flow magnetic resonance imaging. Radiology 1985;154:443-450.

55. Larson TC III, Kelly WM, Ehman RL, et al. spatial misregistration of vascular flow during MR imaging of the CNS: cause and clinical significance. AJNR 1990;11:1041-1048.

56. Axel L. Blood flow effects in magnetic resonance imaging. AJR 1984;143: 1157-1166.

57. Von Schulthess GK, Higgind CB. Blood flow imaging with MR: spin –phase phenomenon. Radiology 1985;157:687-695.

58. Nishimura DG. Time-of-flight MR angiography. Magnetic resonance medicine. 1990;14:194-201.

59. Anderson CM, Saloner D, Tsuruda JS, et.al. Artifacts in maximum-intensity-projection display of MR angiograms. AJR 1990;154:623-629.

60. Edelman RR, Mattle HP, Wallner B, et.al. Extracranial carotid arteries: evaluation with black blood MR angiography. Radiology 1990;177:45-50.

61. Basic Physics of MR imaging: Application guide gyro scan NT: Volume one Phillip Medical system 1997.

62. Dumoulin CL, Hart HR. Magnetic resonance angiography. Radiology 1986;161: 717-720.

APPENDIX A

DEFINITION

180-DEGREE-PULSE: An RF pulse that rotates the net magnetization by an angle of 180^0 degree.

90-DEGREE-PULSE: A pulse that rotated the magnetization vector 90 degree from a reference axis often, that of the static magnetic field, in which case transverse magnetization occurs.

2D-Fourier TRANSFORM: A technique used to reconstruct raw image data into two dimensional images, composed of pixels with brightness proportional to the intensity of the MR signal from the corresponding protons; data acquisition technique in which a thin slice is excited, followed by frequency and phase encoding to produce a 2D image.

2D GRADIENT ECHO SEQUENTIAL: Formerly called GRASS, this fast scan technique reverses gradient polarity to rephase protons and form echoes. Permits the use of short TRs and flip angles of less than 90 degrees to excite only a portion of the longitudinal magnetization. unsaturated spins: Spins whose net magnetization equals their fully aligned magnetization, because they have not been exposed to an RF pulse within a period of several T1.

3D acquisition: A gradient echo pulse sequence that permits the acquisition of high resolution, thin slice images. Valuable for reformatting information into other planes. The slab selects and the encodes along the slice-select axis in addition to phase and frequency.

3D Fourier transform: An acquisition method in which a thick slice, or slab, is excited, followed by in-plane spatial resolution using phase and frequency encoding. Slice thickness is resolved by phase encoding along the slice-selection direction. The technique permits thin contiguous slices to be obtained. Since signal from the entire slab is repeatedly sampled, SNR is improved over conventional 2D imaging. 90-degree pulse is followed by the acquisition of multiple echoes.

ACQUISITION: 1) A collection of data. A scan may require one or several acquisitions, depending upon the parameters prescribed.

2) Slice Location

ALGORITHM: A step-by-step process used to solve a problem. In MR, a mathematical sequence used to convert the acquired data.

ALIASING: (1) in standard imaging, an artifactual phenomenon created when fewer than two samples are digitized per period. Occurs when the field of view (FOV) is smaller than the anatomy being imaged; anatomy outside the FOV is folded back into the image. Also called *wraparound*

(2) In phase contrast vascular imaging. The phenomenon created when the signal from faster flowing vessels appear in an image as a slower speed or as flow in the opposite direction.

ALPHA PULSE: The initial RF excitation pulse in a pulse sequence. In a sequence using a 90-degree and a 180-degree pulse, the 90 is the alpha pulse; subsequent pulse (s) are also called refocusing pulses.

ANGIOGRAPHY: An MR angiography technique that employs conventional cardiac-or peripheral-gating imaging technology, and relies on velocity-induced phase shift to distinguish flowing blood from surrounding tissues.

ANGUAR FREQUENCY: Frequency of oscillation or rotation, in radians, frequency in Hertz.

AP: 1) Anterior-posterior orientation

2) Array Processor.

APODIZATION: A process where the time domain signal is mathematically manipulated (e.g., multiplied by a decaying exponential function).

ARRAY PROCESSOR: A fast numerical processor used for image reconstruction and display features such as magnification and reformation.

ARTIFACT: An image error. Three major forms of artifacts can occur in MR imaging, resulting in poor image quality: geometric distortion, inhomogeneous signal intensity and spurious signal.

ASYMMETRIC ECHOES: An echo whose peak, at TE, is not centered in the sampling window. Also called fraction echo or partial echo.

AVERAGE VELOCITY: Flow Q (expressed in cm 3 /sec) divided by the cross-sectional area A (expressed in cm 2) of a vessel: V = Q/A (cm/sec); ½ V maximum for laminar flow.

AXIAL PLANE: A plane that divides the body into head (superior) and feet (inferior) aspects. Also called the *transverse* plane.

BO: (B-sum zero) The symbol that indicates the static magnetic field.

B1: (B-sub one) the symbol for the magnetic field created by RF energy. In MR, B_1 is perpendicular to B_0

BALANCED MATRIX: In ECG gated scanning, an acquisition in which the number of slice locations equals the number of cardiac phases selected.

BANDWIDTH (BW): The range within a band of frequencies. An image's receiver bandwidth determines how many frequencies will be encompassed in that image. The bandwidth chosen by the system depend on the TE, matrix and FOV that you select.

BASELINE: The noise floor of a spectrum; the signal that is produced if there is no sample. Baseline distortions and baseline rolls are a common source of error in spectral quantification.

BEATS PER MINUTE (BPM): The average heart rate as shown on the cardiac monitor.

BELLOWS: A device placed on a patient to monitor breathing during studies employing respiratory compensation.

CARDLAC GATING: See Gating.

CARDIAC PHASE IMAGES: Images demonstrating different times or phases within a cardiac cycle within a cardiac cycle.

CHEMICAL SHIFT IMAGING (CSI): See spectroscopic imaging. first-order phase correction: A phasing process in which the amount of phase correction applied increases linearly across the spectrum.

CONTRAST AGENT: A pharmaceutical that changes the relaxation time of tissues, thereby increasing their conspicuity in an image. Often administered intravenously to improve the signal-to-noise or contrast-to-noise ratio.

CONTRAST-TO-NOISE RATIO (CNR): The amount of contrast in an image versus the amount of noise; determines the resolution of an image.

CRYOSTAT: The apparatus that maintains the low constant temperature necessary for superconducting magnet operation. The cryostat consists of two concentric cylindrical containers housed in an outer vacuum-tight vessel. The windings that create the magnetic field are in the innermost container, which is filled with liquid helium.

DELAY AFTER TRIGGER: In gating, the time between the occurrence of the triggering pulse and the actual onset of the acquisition.

DENSITY: Camera control, which regulates exposure time as you film images.

DEWARS: Large vacuum containers that store the cryogen.

DIASTOLE: The period between the end of the T-wave and the beginning of the R-wave in the cardiac cycle. Also called *ventricular filling.*

ECHO SPACE: The time between each echo in the Fast Spin Echo sequence, in which a 90-degree pulse is followed by the acquisition of multiple echoes.

ECHO TIME: See TE.

ECHO TRAIN LENGTH: The number of echoes selected (by the operator) in the Fast Spin Echo. It is annotated as TE.

EFFECTIVE R-R INTERVAL (RR): The inverse of BPM (Beats Per Minute) measured in msec: RR=60,000 divided by BPM.

EFFECTIVE TR: The "average" repetition time, or TR, in cardiac gating. Measured as the number of RR intervals between successive excitations of a particular slice location e.g., RR, 2xRR, 3xRR, 4xRR.

EXTREMITY COIL: A quadrature receive coil, or linear transmit/receive coil, used for imaging the knee.

FAST SCAN F1 (FS): Pulse sequence that uses pulses of 1 to 179 degrees to excite the protons of interest, and then rephases them by means of gradients rather than conventional RF pulses.

FAT SUPPRESSION: An IR technique used to suppress fat hydrogen signal.

FAT/WATER IMAGING: An imaging sequence that lets you suppress signal from.

FAT/WATER SUPPRESSION (Chem SAT): An imaging enhancement that lets you suppress signal from either fat or water by applying a frequency-selective saturation pulse.

FERROMAGNETIC: A substance, such as iron, that is attracted to a magnet.

FID: See free induction decay.

FIELD OF VIEW (FOV): The area (expressed in centimeters) of the anatomy being imaged, a function of acquisition matrix times pixel size.

FLIP ANGLE: Refers to the angle applied to the RF pulse of a spin echo sequence.

FILP ANGLE: Rotational angle of the magnetization vector produced by an RF pulse.

FLOW COMP: An imaging enhancement that uses the system's gradients to put flowing protons into phase with stationary protons, thereby reducing flow artifacts.

FLOW EDDY: See *vortex flow.*

FLOW ENCODING: A technique used in MR to measure or display motion such as blood

FLOW SEPARATION: The separation of the central streamline of flow from the wall

FLOW: A measure of the volume of displacement per unit of time, expressed

FOURIER TRANSFORM:A mathematical procedure used to interconvert functions of conjugate pairs of variables. In MR, Fourier transforms usually convert functions of time (i.e.,FIDs or spin echoes) to functions of frequency (spectra or images).

FOV CENTER: The center of the image, ideally located at the magnet's isocenter; when it is not, the FOV is said to be offset, or off-center.

FOV: Acquisition field of view.

FRACTIONAL ECHO: A capability that instructs the system to collect just part of the data it.

FRACTIONAL NEX: A capability that instructs the system to use about half or exactly

FREE INDUCTION DECAY (FID): The measurable magnetic resonance signal that occurs as the transverse magnetization (produced by the application of the 90^0 pulse) decays toward zero.

FREQUENCY ENCODING GRADIENT (G x): Also known as the *readout* gradient, it causes a frequency relationship to occur among the spins at various locations on the x-axis. While this gradient is turned on, the echo is sampled.

FREQUENCY: (1) the scanning direction associated with the frequency gradient. Usually corresponds to the long axis of the image. (2) The number of cycles or completed alternations per unit of time, measured in Hertz (Hz).

G x G y G z : Symbols for the MR gradients. Subscripts indicate the spatial direction of each: Gx = frequency, Gy = phase, Gz = slice select.

GAIN, 90/180: The RF 90^0 gain is a prescan option, used to optimize the transmit power of the 90 pulse. The 180^0 gain prescan option optimizes the transmit gain of the 180^0 rephasing pulse.

GATING: A technique for imaging rapidly moving anatomy such as the heart, by using such equipment as a peripheral photopulse sensor or standard electrocardiograph to trigger data acquisition. In cardiac or peripheral gating, slice excitation is timed to the cardiac cycle.

GAUSS (G): A unit in the measurement of magnetic field strength. The internationally accepted unit is the Tesla (T)-1 Tesla = 10,000 gauss. As a comparison, the earth's magnetic field is approximately .5 gauss.

GRADIENT COILS: Coils designed to alter the main magnetic field so that it will be stronger in some locations than in others. The three gradient coils are used primarily to spatially encode slice information.

GRADIENT ECHO (GRE): An MR signal produced by using an initial RF pulse and a gradient pulse to refocus spins. Unlike spin echo, it does not use a 180-degree pulse to refocus.

GRADIENT ECHO: A scan sequence, FS (F1), that uses the gradients to recall or rephase the spin rather than 180^0 RF pulse.

GRADIENT MOMENT NULLING: Application of gradients to correct phase errors caused be velocity, acceleration or other motion. First-order gradient nulling is the same as flow compensation.

GRADIENT MOMENT: In MR angiography, the first moment describes the effect of a gradient on the phase of a spin with constant velocity ; the second moment, its effect on spin experiencing acceleration; the third moment, its effect on spin experiencing jerk.

GRADIEN ECHO REFOCUED: See *gradient echo.*

GRADIENTS:(1) the magnetic fields that are added to, or subtracted from, the main field to make it stronger in some locations than others. (2) Waveforms, generated by the pulse control module, which instruct the gradient amplifiers and coils inside the magnet how much to modify the static magnetic field by adding or subtracting field strength.

GRADIENTS: 1) Waveforms, generated by the system, which instruct the gradient coils (located inside the magnet enclosure) how much to modify the static magnetic field by adding or subtracting field strength.

GRASS: Gradient-Recalled Acquisition in the Steady State. A fast scan (gradient echo) pulse sequence that uses pulses of 1 to 180 degrees to excite the protons of interest, and then rephases them by means of gradients rather than conventional RF

GRASS: Gradient-Recalled Acquisition in the Steady State. A fast scan gradient

GRASS: See 2D gradient echo sequential.

Gx, Gy, and Gz: symbols for MR gradients. Subscripts indicate the spatial direction of the gradient.

GYROMAGNETIC RATIO (γ): The ratio of the magnetic moment to a particle's angular

HALF ECHO: A capability that instructs the system to collect just over half (55 %) of the data it normally would. Shortens TE in early echoes, reducing susceptibility and flow artifacts and improving SNR.

HARDWARE: The physical parts of the MR system (circuit boards and their components as well as nuts, bolts, motors, etc.)

HERTZ (Hz): Unit of frequency. 1 Hz = 1 cycle/second.

HOMOGENEITY: Uniformity of the static magnetic field, an important quality of the magnet.

IMAGE ACQUISITION TIME: Scanning time, a function of TR time NEX times the images depends on T2*. $1/T2^* = 1/T2 + {}_{delta}B0$ B0 is a measure of inhomogeneities γ is gyromagnetic ratio

IMAGINARY IMAGE: Images created from Fourier components that are 90 degrees out of phase with a reference signal in the receiver or demodulator.

INHOMOGENEITY: Lack of uniformity in the static magnetic field (B 0) or the RF field (B 1).

INTERLEAVED ACCQUISITION: The collection of data from a single slice; one phase encode performed for one slice per TR. All phase encodes are completed for one slice before exciting the next slice.

INTERLEAVED SPACING: Selection of slice spacing that uses a concatenated (multi- pass)

INTERLEAVING: The process of collecting data from every other slice during the first acquisition, and then going back to acquire the rest in a second acquisition. Minimizes cross talk artifacts but doubles scan time for a series.

INTERPULSE TIME: Times between successive RF pulses used in pulse sequences. Particularly important in inversion recovery are the inversion time (TI) and the recovery time (TR). The time between a 90^0 pulse and subsequent 180^0 pulses to produce a spin echo will be approximately one-half the spin echo time (TE), also called TAU or TE2.

INTERSCAN SPACING: The amount of space left between slices, used to minimize cross-talk artifacts such as saturation. Also referred to as *skip.*

INTRAVOXEL-SPIN PHASE DISPERSION: A loss of phase coherence and, therefore, signal intensity. This can occur when a wide spectrum of flow velocity exists, when high orders of motion like acceleration are present, or when there are minor variation in magnetic field homogeneity.

INVERSION RECOVERY (IR): A pulse sequence that inverts the magnetization and then measures the recovery rate as the nuclei return to equilibrium. This rate of recovery depends on T1.

INVERSION TIME: See T1.

IR: Inversion Recovery. A pulse sequence that inverts the magnetization by a 180-degree RF pulse and then applies a 90- degree pulse followed by a 180-degree refocusing pulse. A pulse sequence that provides T1 discrimination.

IR-PREPARATION: The application of a 180-degree inversion (IR) pulse and *prep time*, Prior to the application of the excitation pulse. Produces T1 –weighted image

ISOCENTER: The point within the magnet at which the three gradient planes cross.

ISOMETRIC CONTRACTION: The time immediately after the R-wave when the heart prepares for contraction but does not change in volume.

ISOTROPIC VOXEL: Voxels that are close to equal in all three dimensions phase-frequency- and slice-select provide better quality images.

JERK: A change in acceleration over time: acceleration time. Can cause dephasing in MR vascular image

K-SPACE: The amount of space that must be filled with information that can be mathematically manipulated in order to form an image. Can also be thought of as the inter-section of one phase-encoded axis and one frequency-encoded axis.

LARMINAR FLOW: Flow occurring in layers; a flow profile with maximum velocity flow in the center of the vessel and the slowest flow along the vessel wall.

LARMOR EQUATION: Expression of the proportional relationship between the precessional frequency of a nuclear magnetic moment

LARMOR FREQUENCY: The resonant frequency of a given substance. systems use this phenomenon to determine the spatial locations of protons, since changing the field strength via precisely controlled gradients also changes the larmor frequency of the proton being imaged (see gyromagnetic ratio).

LONGITUDINAL MAGNETIZATION (M 0 or M z): The state the protons are in when they are aligned with the magnet bore when they are not affected by RF.

LONGITUDINAL MAGNETIZATION (Mz): The part of the macroscopic magnetization vector that parallels the static magnetic field. After the RF excitation Mz it's to return to its equilibrium value Mo as a function of T1 time of the tissue. Longitudinal relaxation time.

LONGITUDINAL MAGNETIZATION: The state the protons are in when they are aligned with the magnet bore when RF does not affect them.

M0: The equilibrium value of a magnetization, running in the direction of the static magnetic field.

MAGNETIC FIELD (H): The region surrounding a magnet which produces a magnetizing force on a body within it.

MAGNETIC FIELDGRADIENT: Device for varying the strength of the static magnetic field at different spatial locations. This is used for slice selection and determining the spatial locations of the protons being imaged. Also used for velocity encoding, flow compensation, and in place of RF pulses during gradient echo acquisitions to rephase spins. Commonly measured in Gauss-per-centimeter.

MAGNETIC MOMENT: A measure of the magnitude and direction of an object's magnetic properties that cause it to align with the static magnetic field and create its own magnetic field.

MAGNETIC RESONANCE (MR): Absorption or emission of electromagnetic energy by nuclei in a static magnetic field after excitation by a suitable RF pulse.

MAGNETIC RESONANCE IMAGING (MRI): Creation of images using the magnetic resonance phenomenon. The current application involves imaging the distribution of hydrogen nuclei (protons) in the body. The image brightness in a given region usually depends jointly on the spin density and the relaxation times. Image brightness is also affected by motion such as blood flow.

MAGNETIC RESONANCE SIGNAL: Electromagnetic signal (in the radio frequency range) produced by the precession of the transverse magnetization of the spins. The rotation of the transverse magnetization induces a voltage in the coil. The receiver amplifies this voltage.

MAGNETIC SUSCEPTIBILITY: The measure of the ability of a substance to become magnetized or to distort a magnetic field; includes the effect of diamagnetic. paramagnetic, and ferromagnetic material.

MAGNETIC RECONSTRUCTION: Reconstruction technique yielding modulus images representing the actual magnitude of magnetization within each voxel, regardless of its phase.

MATRIX: An array of numbers usually arranged in two dimensions; rows and columns. Acquisition matrix refers to the number of phase-and frequency-encoding views used to acquire data; reconstruction matrix refers to the number of pixels used to reconstruct the image.

MAXIMUM INTENSITYPROJECTION (MIP): A technique for producing multiple projection images from a volume of image data (i.e.,3D volume or a stack of 2D slices); the volume of image data is processed along a selected angle and the pixel with the highest signal intensity is projected onto a two-dimensional image.

MISREGISTRATION: Artifacts caused by imprecise mapping of the spatial locations of acquired signals, often caused by motion or aliasing.

MODULUS IMAGE: An image demonstrating the actual magnitude of the magnetization of each voxel, create from real and imaginary image.

MOMENTS: Position/time derivatives that define the motion-induced phase shifts occurring in the presence of the magnetic gradient fields.

MR CONTRAST AGENT: A pharmaceutical that reduces the relaxation times of tissues, thereby changing their appearance in an image. Often administered intravenously to improve signal-to-noise ratio.

MR EXPREIMENT: A designation for the total number of pulses applied within one TR.

MULTIPLE ECHO (ME): A pulse sequence consisting of a 90^0 pulse followed by multiple 180^0 pulses.

MULTIPLE ECHO IMAGING: A magnetic resonance imaging technique in which the spin-echo magnetic resonance signal, rather than the free induction decay (FID), is used to produce images.

MULTIPLE PLANE IMAGING: The acquisition of multiple slices of patient data through a single scan prescription.

MULTI-SLICE SCAN MODE: Scan mode that allows you to take multiple slices at a time.

MULTI-SLICE, MULTI-PHASE: A cardiac gating pulse sequence that produces images at multiple heart locations and several different cardiac phases at each location.

MULTI-SLICE, SINGLE-PHASE: A cardiac gating pulse sequence that produces images at multiple heart locations, each at a different phase of the cardiac cycle.

My: see transverse magnetization.

NARROW BANDWIDTH: Reduces the range of frequencies "read" by the system, resulting in less noise being real along with the signal. This increases the SNR.

NATURAL FREQUENCY: All objects have a certain natural frequency at which they vibrate. For example, when the open G-string of a tuned guitar is plucked, it will

NEX: Number of excitations. The number of times a pulse sequence is repeated in a

NEX: See Number of Excitations.

NO PHASE WRAP: An imaging option designed to minimize wraparound artifacts in the phase direction when the anatomy imaged is larger than the FOV.

NUMBER OF EXCITATIONS (NEX): The number of times a pulse sequence will be repeated in a given acquisition. (See Acquisition.)

NYQUIST THEOREM: For a complex set of frequencies to be accurately deciphered, they muse be sampled at a rate at least two times the highest frequency. In MR, this technique is called *oversampling.*

OBLIQUE IMAGING: Scanning that produces images in non-orthogonal planes.

OFFCENTER FOV: A field-of-view that is not centered at isocenter.

OFFSET: To prescribe or display an image whose center is not at isocenter.

ORTHOGONAL PLANES: Planes that are perpendicular to one another for example, axial, sagittal and coronal planes.

PARAMAGNETIC: Possessing a positive magnetic susceptibility; the opposite of diamagnetic. Paramagnetic substances align themselves with an external magnetic parameters are equal, a larger gyromagnetic ratio yields a higher Larmor frequency

PARAMETERS: Values of all image variables such as pulse sequence, start and end locations, X, Y, and Z coordinates, magnetic factor, and algorithm.

PARAMETERS: Values of all scanning variables such as pulse sequence, TR, TE, FOV, plus the various imaging options.

PARTIAL VOLUME EFFECT: Occurs when a piece of anatomy fills only a portion of a voxel. This can result in images that are less than ideal.

PHASE COHERENCE: Agreement in phase of two signals of identical or similar frequency. Loss of phase coherence of spins within a voxel decreases MR signal because of a decrease in the macroscopic transverse magnetization.

PHASE CONTRAST (PC) ANGIOGRAPHY: A 2D or 3D imaging technique that relies on velocity-induced phase shifts to distinguish flowing blood from stationary tissues. Two or more acquisitions with opposite polarity of the bipolar flow-encoding gradients are subtracted to produce an image of the vasculature.

PHASE ENCODING GRADIENT (Gy): This gradient affects the rate of precession of the spins that were excited by the slice select gradient; it changes the phase relationship of the spins.

PHASE ENCODING CENTRIC: Acquisition in which amplitudes of the phase encoding gradient begin at the lowest level (minimum negative or minimum positive) and alternate polarity as they increase out to maxi-mum negative and maximum positive.

PHASE ENCODING , SEQUENTIAL: Acquisition in which amplitudes of the phase encoding gradient begin at maximum polarity (positive or negative) and increment to the minimum of that same polarity. Then, polarity changes and the gradient amplitudes increment from the minimum out to the maximum.

PHASE ENCODING: The act of localizing an MR signal by applying a gradient to alter the phase spin before signal readout.

PHASE IMAGE: Computer-generated image in which pixel intensity is proportional to the amount of the phase shifts within it voxel. Created from real and imaginary images

PHASE TIME: The duration of one operator defined phase of the cardiac cycle.

PHASE , AND PHASE ANGLE: The position of a spin relative to a fixed reference point

PHASE: (1) The scanning direction associated with the phase gradient, usually corresponding to the image's short axis. (2) The angular position in a precession of a spinning proton (3) Image acquired at the same slice location but at a different temporal phase.

PHASE: A distinguishable period of time within a cardiac cycle systole, for example. Also the scanning direction associated with the phase encoding gradient, usually corresponding to the image axis.

PHASE ARRAY: Multiple coils and receivers whose individual signals are combined to create one image with improve SNR and increased FOV capability.

PHASE-ENCODING STEPS: The number of times that data are sampled in the phase gradient direction

PIXEL: Picture element. The pixel projects the voxel, or volume element, on the display plane.

PLUG FLOW: Flow in which all components are moving at the same velocity.

PRECESSION: A wobbling motion of a proton about the magnetic field, occurring at the Larmor frequency. Causes the spins to a certain path.

PREPARATION TIME: (More commonly *prep time*.) The time, following the application of the preparation pulse, during which tissue magnetization occurs this allow contrast to evolve at which time acquisition being.

PRESATURATION: AN imaging enhancement designed to minimize artifacts created by fast flowing blood. An RF pulse applied together with a gradient pulse.

PRESCAN: A procedure that allows you to achieve optimal 90^0 and 180^0 transmit gains and receive gain settings for each scan. This "fine tunes" the system, prior to an acquisition, to optimize image quality.

PROJECTION DEPHASING GRADIENT: A gradient applied to diminish signal from stationary in thick-slab 2D PC angiography.

PROJECTION-RECONSTRUCTIONIMAGE: Technique that employs CT-like reconstruction method to create images from a set projection profiles, obtained with the gradients aligned at different angles to the region of interest.

PROTOCOL: (1) A selection of imaging parameters. (2) A prescription programmed in to the system by user for fast, easy exam setup.

P-SAT (Pre-Saturation): An imaging enhancement designed to minimize artifacts created by fast-flowing blood.

PSD: Pulse sequence database.

PULSE LENGTH DURATION: The duration of a pulse, expressed in milliseconds.

PULSE SEQUENCE: Series of RF pulses, used in conjunction with gradient magnetic fields to produce magnetic resonance images.

PULSE, $90/180^0$: The 90^0 pulse is the excitation pulse; the 180^0 is the spin-echo, or rephasing, pulse

QUENCH: Condition where a superconducting magnet boils off liquid helium. In this condition, the static magnetic field is removed. A very loud but brief sound results when the cryogen boil off. Once the magnet is quenched, it can take a significant amount of time and material to return it to the super-conducting state.

RADIO FREQUENCY (RF): Frequency, intermediate between audio and infrared frequencies, used in magnetic resonance systems to excite to resonance.

RAW DATA: Scan data before reconstruction, which may contain information of value to service engineers in determining the cause of certain scanning problems.

READOUT GRADIENT: A gradient first applied when an MR signal is collected. used for frequency encoding.

READOUT GRADIENT: See frequency-encoding gradient.

REAL IMAGE: An image created from Fourier components that are in phase with a reference signal. The real component from which the image is generated is the part that is in phase with the reference signal.

RECEIVE BANDWIDTH/VARIABLE BANDWIDTH (VB): An imaging option that lets you vary the receiver bandwidth to increase SNR or decrease acquisition time.

RECEIVE GAIN: Part of the prescan process, it controls the level of the receive signal. A number on your image screen that indicates the amplitude, or strength, of the received signal represents it.

RECONSTRUCTION TIME: The time it takes from the start of reconstruction to the end of reconstruction.

RECONSTRUCTION: Process of creating a displayable image from scan data.

RECTANGULAR FOV: An imaging enhancement that lets you achieve 256x256 or 512x512 resolution in the time it normally takes to achieve 256x128 or 512x256 resolution, respectively.

REFOCUSING PULSE: Any pulse applied subsequent to the initial excitation (alpha) pulse. In spin echo it is an RF (180^0) pulse. In gradient echo sequences, refocusing is done with gradient pulses (also called *rephasing* gradients).

REFOCUSING: Reestablishment of phase coherence via gradient or RF pulse (see *echo rephasing and gradient moment nulling*)

RELAXATION TIME: Time required for the nuclei to revert to their original state in the magnetic field after the RF pulse is turned off. Also called T1.

RELAXATION: The emission of energy that causes the nuclei to shift from a high-energy state back to a low-energy state. The opposite of resonance.

RELAXATION: The emission of energy that causes the nuclei to shift from a high-energy

REPETITION TIME: See TR.

REPHASING GRADIENT: Gradient applied in the opposite direction of a recent selective excitation pulse, in order to correct for gradient-induced phase errors. This rephases out-of phase spin and form a spin echo

RESONANCE: A condition established when the frequency of an applied electromagnetic

RESONANCE: An energy transition that results when an object is subjected to a frequency the same as its own. In MR, applying an RF pulse at the same frequency as the precessing nuclei induces resonance. The energy associated with this RF pulse causes a shift of those nuclei from the low energy

PESPIRATORY COMPENSATION: An imaging enhancement where the phase encoding is modified to minimize ghosting caused by respiratory motion.

REYNOLD'S NUMBER (Re): A value, used to predict vessel turbulence, that is determined by dividing viscosity into the product of density, velocity and vessel diameter. Reynold's numbers above 2000 indicate unstable hemodynamics; those above 2500 usually indicate turbulent blood flow within a vessel.

RF COILS: The hardware (body, head, and surface coils) responsible for exciting the tissue of interest with radio frequency pulses and receiving the MR signal.

RF PULSE: (radio frequency) the frequency used in magnetic resonance systems to excite nuclei to resonance.

ROTATING FRAME OF REFERENCE: A frame of reference rotating around the B0 axis at the nuclear precessional (Larmor) Frequency.

RPD: Relative proton density.

R-R INTERVAL: Length of one cardiac cycle; from one R-wave to the next.

R-WAVE: The part of the cardiac QRS complex that usually has the greatest amplitude. It is electrically the most significant. There is one R-wave per heartbeat.

S/N: See Signal-to-Noise Ratio.

SAGITTAL PLANE: A longitudinal plane dividing the right side of the body from the left.

SAR: Specific Absorption Rate. The amount of RF energy a patient is permitted to absorb at a given time, as determined by a formula that utilizes patient weight.

SAT: See presaturation.

SATURATED PROTON: Protons that have recently been excited by an RF pulse and, therefore, create almost no transverse magnetization upon subsequent excitations. For example, flowing protons that are excited in one slice (i.e., saturation pulse) may not be fully relaxed by the time they reach the next slice; the application of another RF pulse will not produce significant signal from these protons (see saturation pulse).

SATURATION PULSE: A slice-selective RF pulse applied, often followed by a dephasing gradient, to saturate spins and therefore minimize their signal. Used, for example, to minimize signal from flowing blood.

SATURATION: Occurs when the TR is too short to allow total relaxation and the net magnetization vector is pushed beyond the transverse plane.

SATURATION: Repeated application of radio-frequency pulses in a time that is short compared to the T1 of the tissue, producing incomplete realignment of the net magnetization with the static magnetic field.

SCAN DATA: A digitized signal i.e., raw data as it exists before reconstruction.

SCAN FOV: Scan field of view. This is the data collection area for the anatomy being scanned.

SCAN RANGE: The area of anatomy scanned in one acquisition.

SCAN TIME: Amount of time needed to acquire data. (TR X NEX X Phase Encodes) 60,000

SCAN: The act of collecting image data. A plane of the body scanned to produce MR image.

SHIM COILS: Superconducting magnet coils used to compensate for inhomogeneities (imperfections) in the main magnetic field. Inhomogeneities can be caused by imperfections in the magnet or by the effects of ferromagnetic objects in the surrounding environment.

SHIMMING: Correction of inhomogeneity in the main magnetic field.

SIGNAL: Usually refers to the MR signal, which is the electromagnetic energy released by the hydrogen nuclei in the tissue being scanned. When used in the context of peripheral gating, signal refers to the sensor's response to the patient's arterial pulse, as measured in the capillary bed.

SIGNAL-TO-NOISE RATIO (SNR, S/N): The ratio of signal amplitude to noise, i.e., the amplitude of signal emitted by the patient's pro-tons, divided by the amount of patient noise and electronic noise inherent in any electronic instrument.

SINGLE SLICE MODE: Scan mode that allows you to take a single slice at a time.

SLICE SELECTION GRADIENT (Gz): Its application causes the spins at various locations along the z axis to precess at selected frequencies (in only one slice). Those spins whose frequencies match that of the applied RF bandwidth will be excited. Where this occurs, transverse magnetization is created.

SLICE SELECT: The scanning direction associated with the system's slice-select gradient. Usually corresponds to the direction of the scanning range.

SLICE: Location within selected anatomy.

SOFTWARE: The computer language program that is stored magnetically on the system disk. Software is a changeable person/computer interface that gives

SPATIAL ENCODING: A method by which data are collected in order to formulate a three-dimensional image in a two-dimensional plane.

SPATIAL RESOLUTION: That distance between two points at which the points can be distinguished as separate and distinct. Defines the clarity of any object that can be seen in ban image.

SPRECTRAL PRESATURATION: Applying presaturation pulses to suppress spins that precess at a specific frequency (as opposed to sup-pressing spins at a spatial location).

SPRECTRUM: A plot that shows the amount of energy absorbed as a function of frequency. In MR, energy is absorbed while nuclear magnetic moments reorient in a magnetic field. The resonant frequencies at which absorption occurs are dependent upon the chemical environment at each nucleus.

SPGR (Spoiled GRASS): A gradient echo pulse sequence designed for acquiring T1-weighted images in 2D or 3D (Volume) mode.

SPIN ECHO IMAGING: A magnetic resonance imaging technique in which the spin-echo magnetic resonance signal, rather than the free induction decay (FID), is used.

SPIN ECHO IMAGING: A magnetic resonance imaging technique in which the spin-echo magnetic resonance signal, rather than the free induction decay (FID), is use. This produces images that may depend strongly on T2.

SPIN ECHO: An MR signal generated from a pair of RF pulses (most often a ninety-degree pulse and a 180-degree pulse).

SPIN: The intrinsic angular momentum of a proton, a fixed value that is also responsible for its magnetic moment, Since pairs of neutrons or protons align and cancel out their spins, only nuclei with odd numbers of either particle can have a net nonzero rotational component, expressed by a nuclear spin number I.

SPIN-DENSITY WEIGHTED: Referring to the type of image produced, this is another name for *proton-density weighted.*

SPOILER PULSE: The application of a gradient to minimize or eliminate residual signal by dephasing the spins.

STEADY STATE PRECESSION: A condition achieved by repeatedly exciting an MR sample with phase coherent RF pulse at repetition rate (TR) that is shorter than T2.

SUPERCONDUCTING MAGNET: A magnet that uses cryogen to achieve a powerful magnetic field with minimal power requirements.

SURFACE COIL: An RF coil that is placed on the surface of the region of interest to be imaged, for a higher signal-to-noise ratio.

SYSTOLE: The period between the R-wave and the end of the T-wave. Also known as *ventricular contraction.*

T: See Tesla.

T1 RELAXATION: The process by which nuclear magnetization returns to its equilibrium value in a magnetic field. It is characterized by the T1 relaxation time.

T1: The characteristic time constant for the magnetization to return to the longitudinal axis after being excited by an RF pulse. Also called *spin lattice* or longitudinal relaxation time.

T2 RELAXATION: The process by which an MR signal loses its coherence and becomes undectable. It is characteristized by the relaxation time.

T2* (T-two-star): The characteristic time constant for loss of transverse magnetization and MR signal due to local field inhomogeneities. Normally referred to when referencing gradient echo images.

T2*: The characteristic time constant for loss of transverse magnetization and MR signal due to T2 and local field inhomogeneities. Since such inhomogeneities are not compensated for by gradient reversal, contrast in gradient-echo

T2: The characteristic time constant for loss of the phase coherence of spins, caused by their interaction, and the resultant loss in the transverse-magnetization MR signal.

TAU: One half of the TE, measured in milliseconds. Tau is the length of time

TE: Echo time. The time between the center of the excitation pulse and the peak of the echo, which usually occurs at the center of the readout (see asymmetric echo).

TE: Echo time. The time between the middle of the excitation pulse (90^0) and the middle of the echo the moment the system is collecting signal data (i.e., half echo doesn't have echo center at readout window center).

TE1: The time from the middle of the first excitation pulse to the middle of the first readout in an asymmetrical spin echo (VEMP) pulse sequence.

TE2: The time from the middle of the excitation

TEMPORAL RESOLUTION: The shortest time that can be used to distinguish events in, for example, the cardiac cycle.

TESLA (T): The internationally accepted unit of magnetic field measurement. One Tesla is equal to 10,000 gauss.

TESLA (T): The internationally accepted unit of magnetic field strength measurement. One Tesla is equal to 10,000 Gauss.

TI: Inversion time. The time between the center of the first (180^0) inverting pulse and the beginning of the second (90^0) refocusing pulse in an IR sequence.

TILTED SCAN: Any scan angled in one or two directions from an orthogonal plane.

TIME DOMAIN SIGNAL: A signal acquired as a function of time. Typically, time domain signal are acquired in MR studies and the Fourier transform to produced either spectra or image. Echoes and FIDS are time domain signal.

TIME OF FLIGHT ANGIOGRAPHY: 2D or 3D imaging technique that relies primarily on flow-related enhancement to distinguish moving from stationary spins in creating MR angiograms. Blood that flows into the slice does not experience RF pulses and, therefore, appears brighter than stationary tissue.

TISSUE PREPARATION: A technique to help optimize contrast in fast gradient echo images where TRS can be extremely short. Prior to the alpha pulse, one or more RF pulses are applied to the tissue, followed by prep time, during with contrast between the tissue is allow to evolve. Specific preparation method are IR-

TR: Repetition time. The time between successive excitations of a slice i.e., the time from the beginning of one pulse sequence to the beginning of the next. In conventional imaging, it is a fixed value equal to the time available for spin

relaxation. In cardiac gating, it varies from beat to beat by a few milliseconds or more, depending upon the patient's heart rate

TRANSVERESE MAGNETIZATION (M xy): Occurs when the initial RF pulse is applied. It is the part of the magnetization vector that is perpendicular to the static magnetic field (B 0) also called B1. The detectable MR signal is created when the transverse magnetization precesses at the Larmor frequency. After the RF pulse is turned off, this signal decays on a scale of T2*.

TRIGGER DELAY: See *Delay after Trigger*.

TRIGGER: In cardiac gating, signal sent by the hardware to activate data acquisition after the QRS complex is sensed.

TURBULENCE: In a flowing fluid, velocity components that fluctuate randomly, causing spin dephasing and signal loss.

VARIABLE BANDWIDTH: An imaging option that lets you choose one of three pre-set bandwidths wide, medium or narrow which will set a maximum chemical shift artifact of approximately one, two or three millimeters, respectively. The object is to decrease chemical shift at the expense of SNR.

VARIABLE ECHO (VE): A pulse sequence consisting of a 90^0 pulse followed by two 180^0 pulses spaced at variable intervals called TE1 and TE2.

VASCULAR MR IMAGING: Magnetic resonance imaging of the vascular system. Two of the most promising techniques rely on flow-related enhancement (time-of-flight angiography) and velocity-induced phase shifts (phase contrast angiography) to distinguish flowing from stationary tissues. vascular occlusive disease: Narrowing of the vessel lumen due to a pathologic process such as atherosclerotic disease.

VECTOR: A mathematical quantity possessing both magnitude and direction, expressed by an arrow whose length indicates the magnitude.

VELOCITY: Displacement per unit of time, measured in cm/sec; a vector quantity which has magnitude (cm/sec) and direction (S/I,A/P,R/L).

VENC: Aliasing velocity or velocity encoding.

VICOSITY: The resistance of blood flow due to the friction of blood elements in the moving stream.

VOLUME IMAGING: An acquisition technique in which signal is collected from an entire volume rather than individual slice. Permits reconstruction of extremely thin slice, and usually enhance SNR.

VOLUME: The acquiring of 3D data from a group of slices rather than in a slice-by-slice 2D mode.

VORTEX FLOW: Localized, slowly swirling or stagnant blood. Often the result of sudden deceleration distal to area of stenosis.

VOXEL (Volume Element): A three dimensional volume.

VOXEL: Volume element a three-dimensional region of an imaged object that is represented in two dimensions by a pixel.

VOXEL: Volume element. Three-dimensional area of a scan represented in two dimensions by a pixel and in the third by slice thickness.

W/L: Width/Level. See Window Width and Window Level.

WATER SUPPRESSION: The suppression of the water signal in an MR spectrum, usually by a specialized excitation sequence. zero-order phase correction: A phasing process in which all the peaks in a spectrum are corrected by the same amount.

X and Y COORDINATES: Image display locations of a point on a two-dimensional grid.

X AND Y COORDINATE: Locations of a point on a two-dimensional grid. The image center is at (0,0).

ZERO-ORDER ZERO PHASE CORRECTION: A phasing process in which all the peaks in a spectrum are corrected by same amount.

ΔKY: Indicates the change (delta) in k-space along the y axis.

APPENDIX B

FOURIER TRANSFORM

The measured MR signal represents the sum of the signals from the innumerable individual nuclei within a signal slice. This composite signal varies continuously in amplitude as a function of time. However, the positions of nuclei are encoded in the frequency content of the signal. To extract the individual frequency components (frequency domain) from the time – varying signal (temporal domain) , the computer employs a mathematics operation, the FT (figure B-1). The FT perform an operation for the computer in decoding MR signals analogous to that of the basilar membrane of the human cochlea in processing sound. Somewhat like the human ear deciphering the individual notes of a chord played on harp, the FT isolates the number of that is, the FT tells us what frequencies are simultaneously present in the signal.

The FT is applied to each frequency – encoded line of data to extract the frequency content of the signal and thereby determine the density of spins along the x-axis.

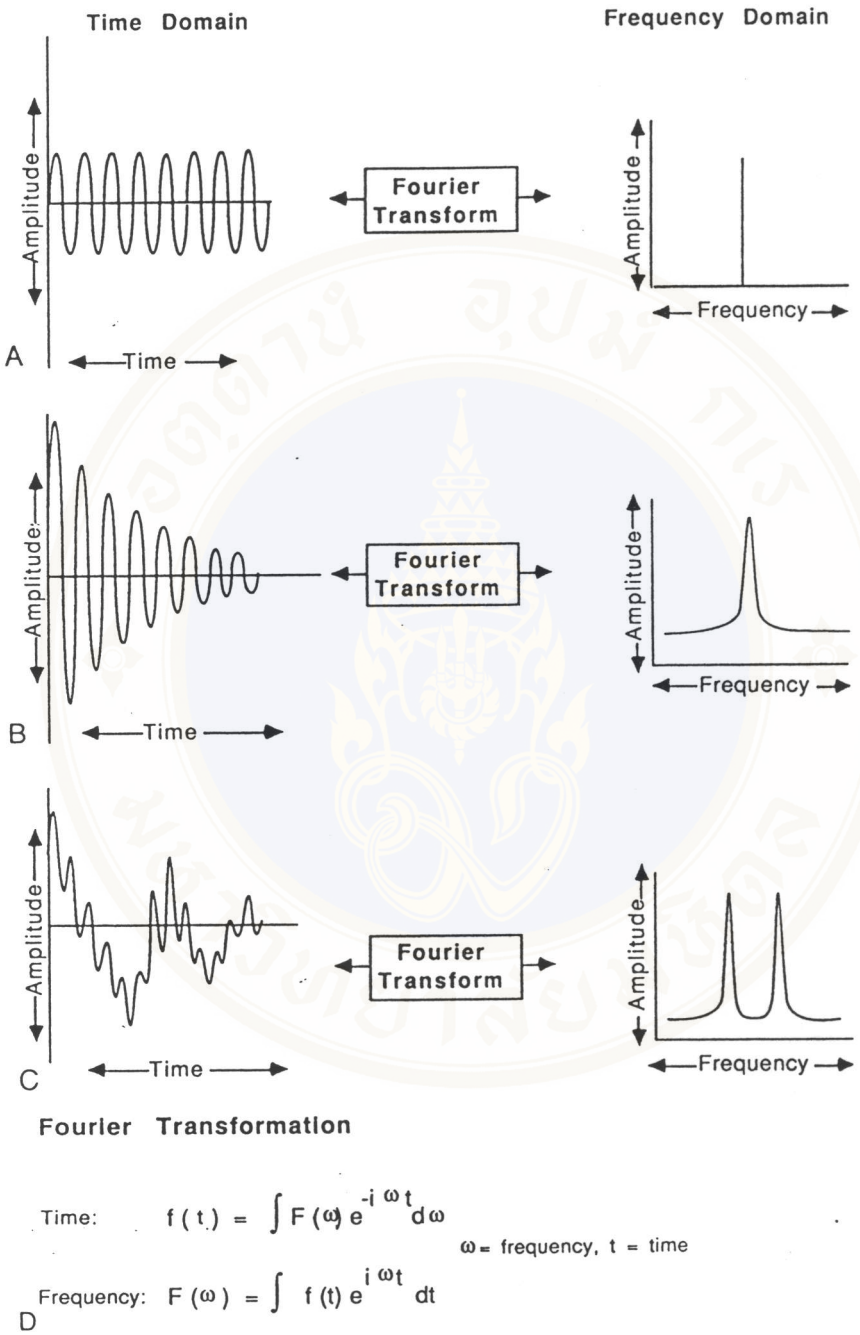

Figure B-1 Fourier transform. A, FT of sine wave yields a single frequency. B, FT of an MR signal from a single proton. C. FT of an MR signal from two spins in different positions. D. Mathematical notation for the FT.

APPENDIX C

K-SPACE

K-space is the Fourier Transform (FT) (space) of standard two-dimension (2D) or three-dimension (3D) image (space) and is extensively used when discussing data acquisition strategies in MR imaging. The concept of K-space is useful, because in MR imaging the acquired data actually represent the Fourier transformation of the imaged object rather than the object itself.

The imaging trick in MR is that different spatial position are mapped into different MR frequencies (frequency-encoding, phase-encoding) (figure C-1)(x to w) Rather than recording individual resonance frequencies the MR scanner record time dependent radio-frequency bursts (w less than or not equal to t),data which are related to the frequency domain data by an inverse Fourier transformation. Just as the spatial positions can be mapped into frequencies, temporal information can be mapped in to k-information (t to k). Hence, MR is said to acquire data in K-space. A Fourier transformation will convert k-space data to image data (k to x). Because an image is at least a 2D space, we speak of k-space, which is a plane for 2D MR imaging and a 3D MR imaging.

It is difficult to gain an intuitive feeling as to how imaging data might look in k-space, but extended image features are imaged into the center and point-like objects are mapped into extended regions in k-space. This translates in to the frequently expressed statement that the contrast of an image is mapped into the center of k-space

while high-resolution fine detail structures are represented in its peripheral regions. Hence, K-space has to be mapped extensively to enable the reconstruction of a high-resolution image. Like scanning TV-image line by line, k-space can be sampled line by line and a Fourier transform of it will then result in the desired image. Typically in MR imaging, data point in k-space are indeed sampled line by line. In the figure C-2 on the left a k-space trajectory is shown for standard pulse sequence, on the right for an echo planar imaging (EPI) sequence. Many other strategies, however, have been devised to sampled data point in k-space. Data point on k-space line can be space at equal distance (linear sampling) or at variable distance (nonlinear sampling). The best known strategies is use, not following the schemes indicated in the figure c-2, are interleaved echo-planar imaging, the Mosaic techniques and spiral scanning characterized by spiral k-space trajectory (spiral scanning) In order to optimize image acquisition, strategies have also been devised to sample only fraction of k-space such as in partial Fourier technique. More frequently sampling of the central k-space region than the periphery will provide rapid update of contrast changes in an image, i.e. after injection contrast media, but less frequent updates of subtle high resolution changes in an image (keyhole imaging). Finally, limited sampling of k-space may become very useful in instrument visualization in interventional MR imaging.

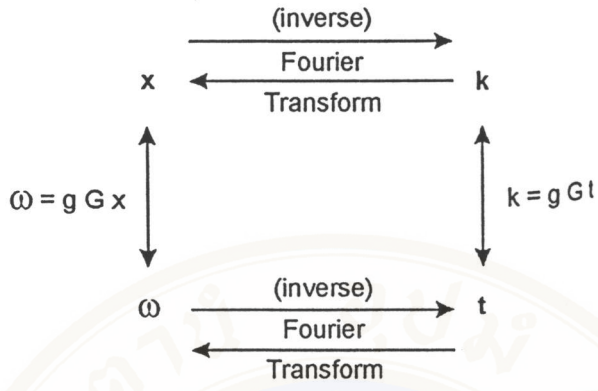

Figure C-1 Relation of variables in Fourier transform imaging in the k-space.

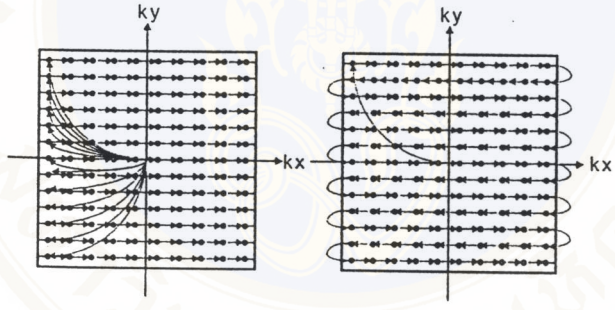

Figure C-2 the K-space trajectories in standard and single shot echo-planar imaging.

APPENDIX D

IMAGES EXAMPLE

Images example of these artifacts with a little descriptions can be shown in order to extend understanding the causes or sources of artifacts in MR imaging

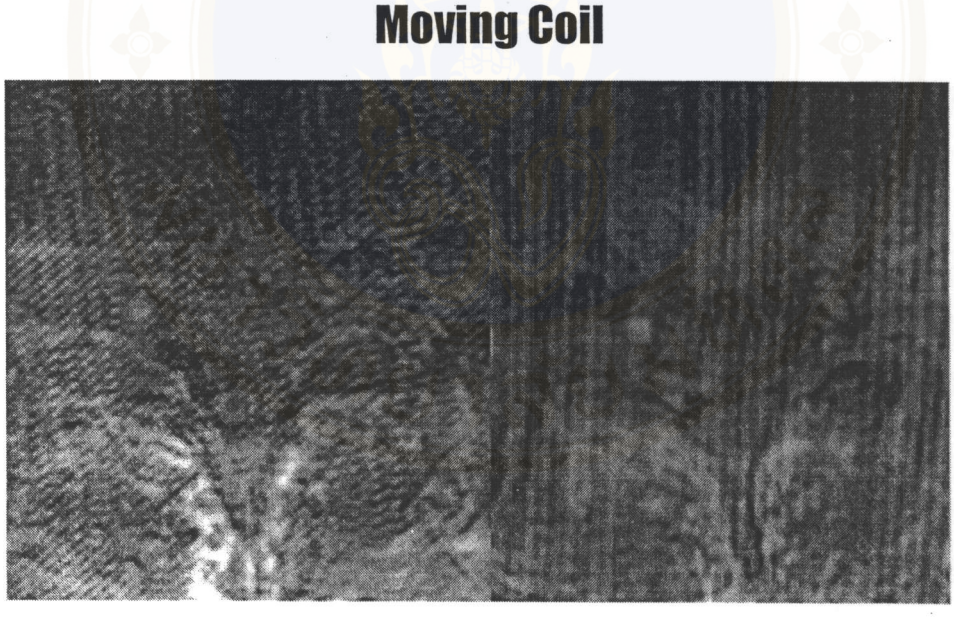

Figure D-1 The patient moved while attached to the posterior neck coil, moving coil (23).

Dentalwork

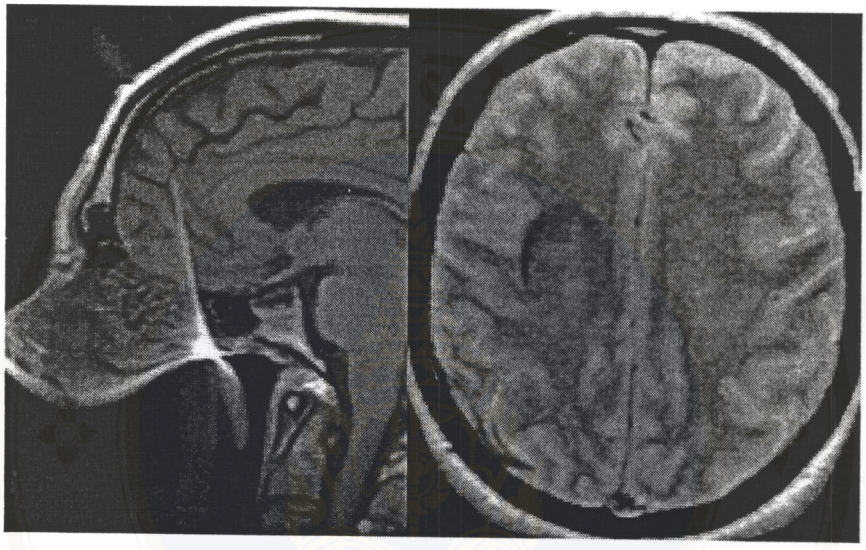

Figure D-2 Some metal dental work can cause an associated artifact distant from the source.

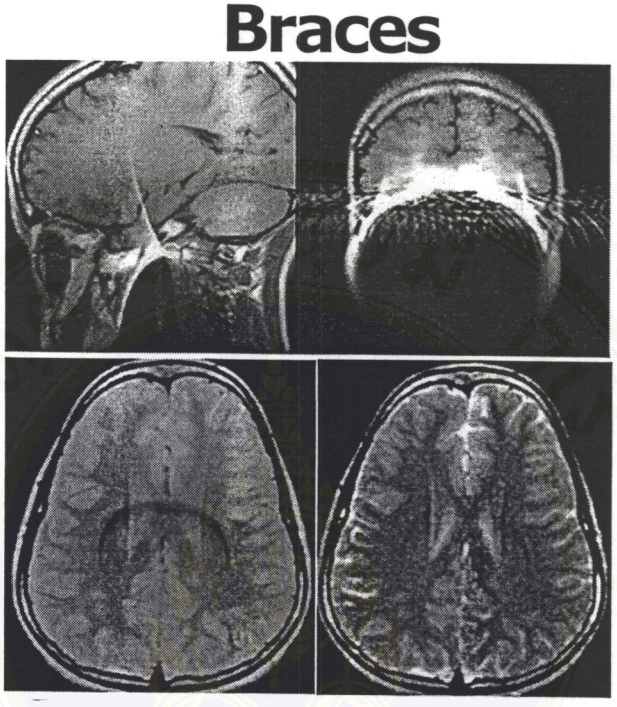

Figure D-3 Brace may cause an artifact distant from the source. The axial proton density (left bottom) and T2-weighted (eight bottom) image exhibit horseshoe shaped artifacts Note it much subtle on the T2 image (23).

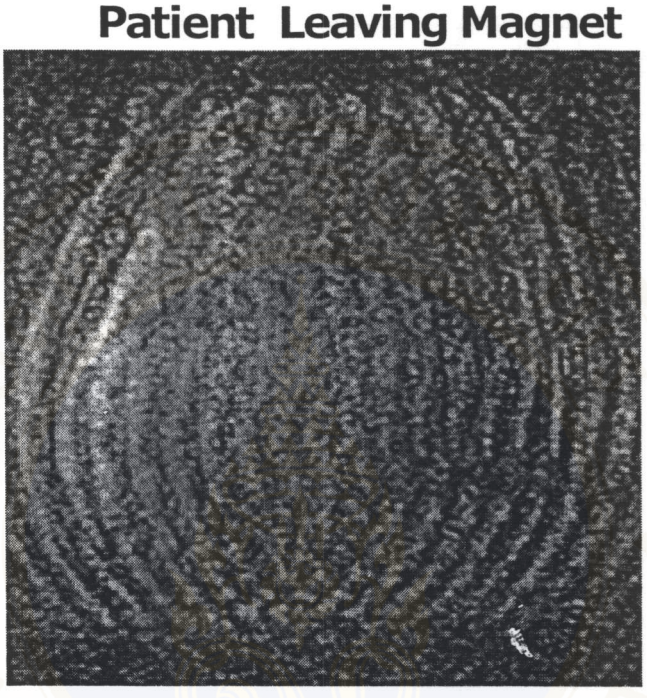

Figure D-4 Patient moving magnet. This case the patient pushed the head coil out of position in the middle of the scanning sequence He was in hurry to leave (23).

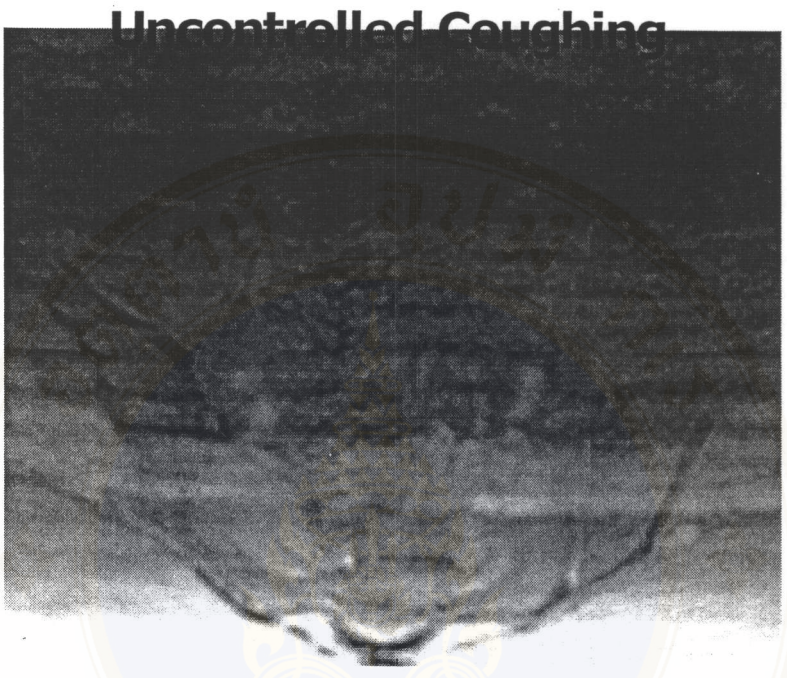

Figure D-5 Uncontrolled coughing. The patient had a left of uncontrolled coughing during this axial T1-weighted lumbar spine scan (23).

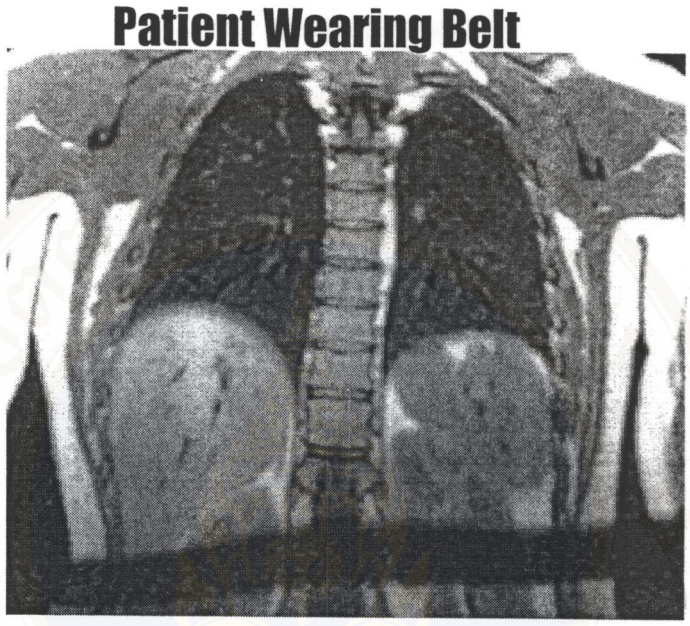

Figure D-6 Patient wearing belt. The patient was a metal-studded belt during this coronal T1-weighted abdominal scan (23).

Phased Array Coil Malfunction

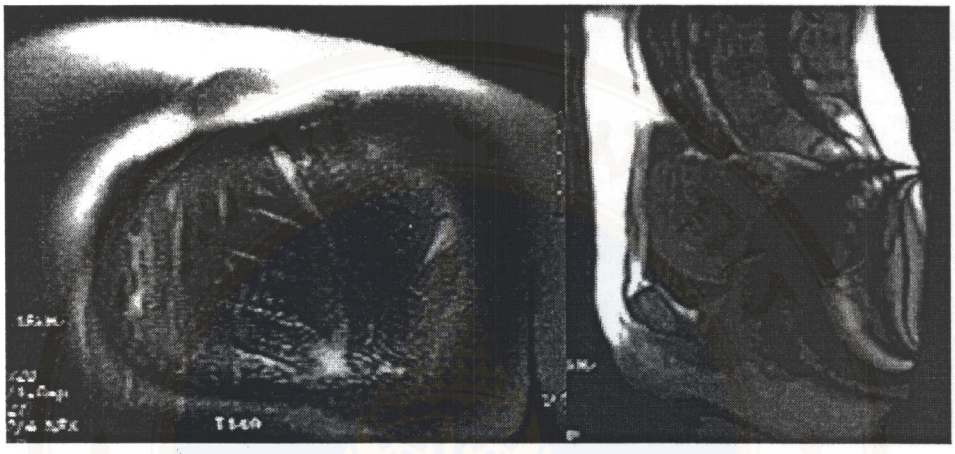

Figure D-7 One coil of a phased array multi-coil (pelvic array in this case) is out of phase with the other coils This results in bands of phase addition and cancellation, demonstrated here coronally, in the chest, and in the pelvis (23).

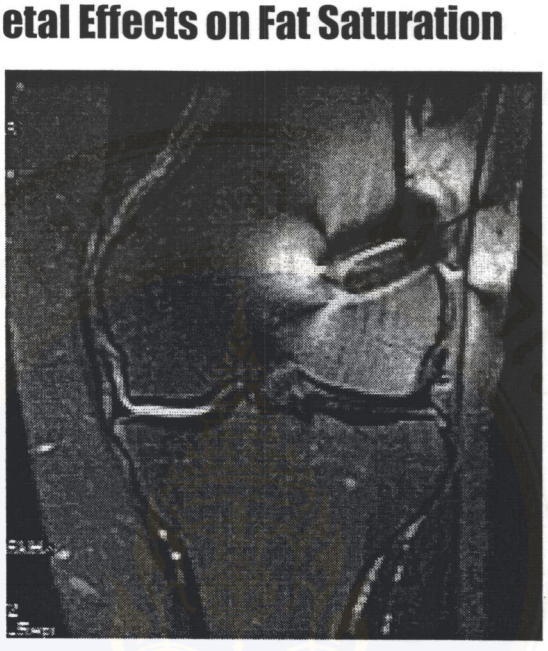

Figure D-8 This T2-weighted, Fast spin echo, Fat Saturated image shows how poor Fat Saturation can be in region of Metallic Prosthesis. This is caused by an alteration in the local magnetic field resulting in change to the precessional frequencies, rendering the chemical saturation pulses ineffective.

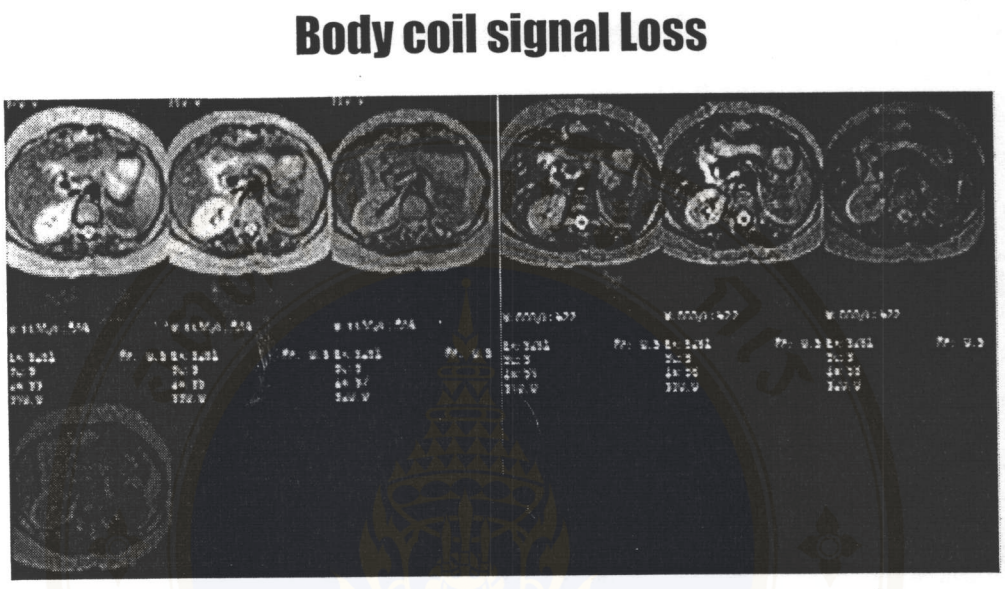

Figure D-9 During this Dual Echo Axial T2 weighted, spin echo scan of the abdomen as we got progressively lower in the abdomen we had increasing signal loss (23).

Patient Motion During Filling of Edges of K - Space

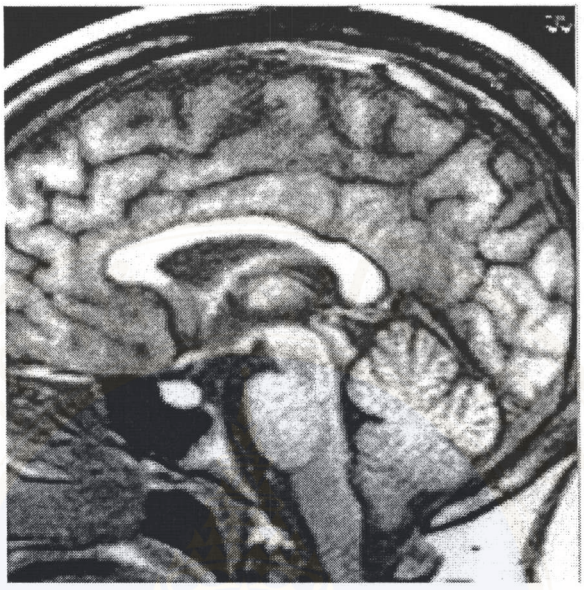

Figure D-10 The fine lines on this image (seen near the vertex and in the brainstem) were caused by the patient moving in the last few of the scan. Only the outside edges of K-space were being filled and as a result the artifact does not overly compromise the image.(23).

Cross – slice excitation due to intersecting Slices

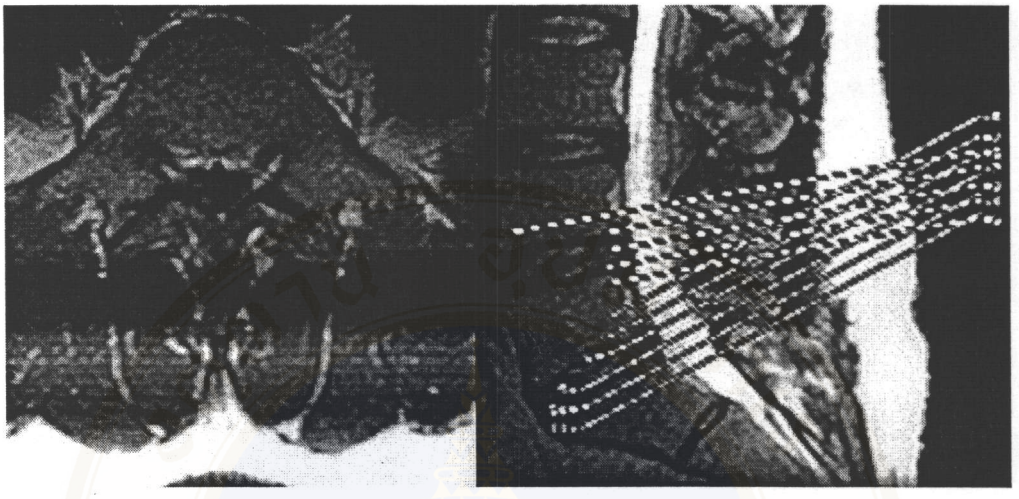

Figure D-11 The dark bands visible on the T1-weighted Spin –echo axial image are due to intersection of the axial image through the image. these are acquired in multi-planar fashion and thus cause pre-excitation (saturation) of the protons in the area where the slice intersect. The sagittal image illustrates where the slice were obtained and how they intersect posteriorly.

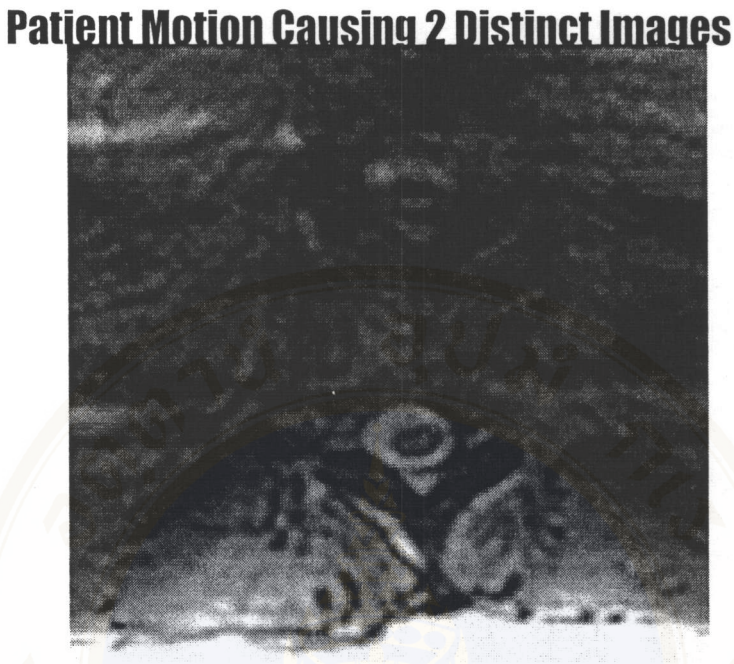

Figure D-12 the two distinct spinal columns are the result of patient movement Artifacts from patient movement are widely varied due to a dependence on when during k-space filling the motion occurs (23).

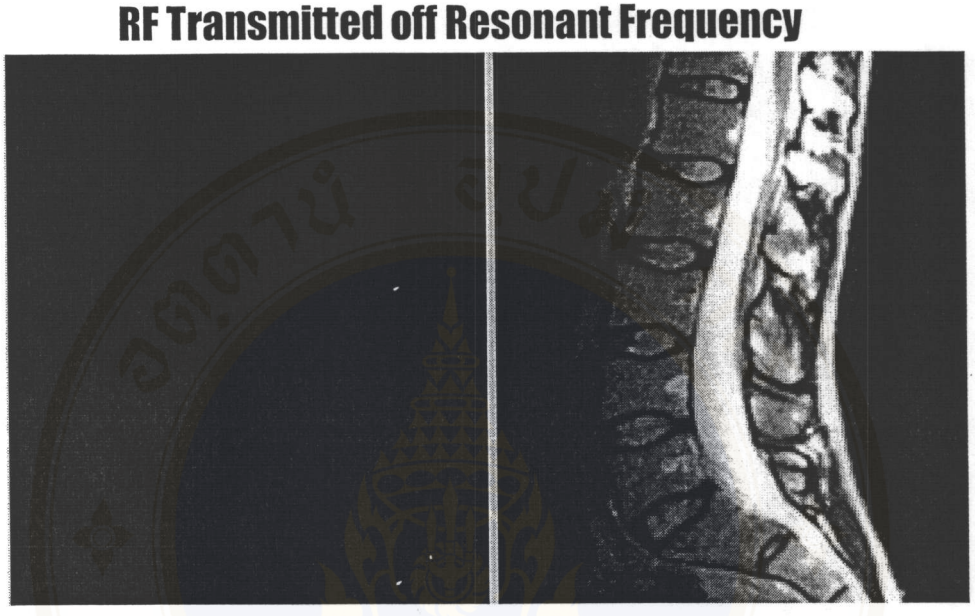

Figure D-13 Scanned off resonant frequency, The image on the left was obtained when the RF-transmitted into the patient was 10,000 Hz lower than the resonant frequency of the protons. This resulted in no protons being excited, thus no signal return. When scanned at the correct resonant frequency the image on the right was obtained.

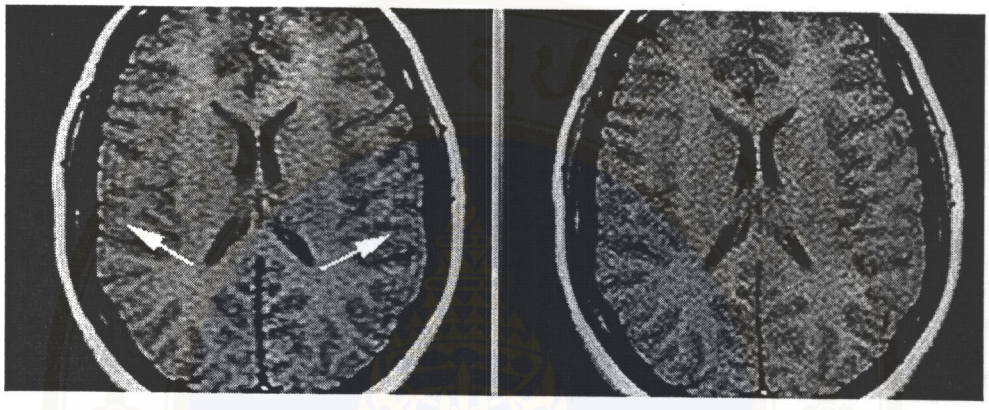

Figure D-14 Truncation artifact, The fine line visible in the image on the left are due to the high spatial frequencies. Sharp edged borders between areas of high contrast are represented by high spatial frequency data. If not enough samples are taken (i.e. 128 phase encodes) these areas cannot be accurately represented. This result in a ring type of artifact following these borders in the phase direction (R to L in this image) These problem can be easily fixed by taking more sample such as the age on the right with 256 phase encodes (23).

Cardiac Motion

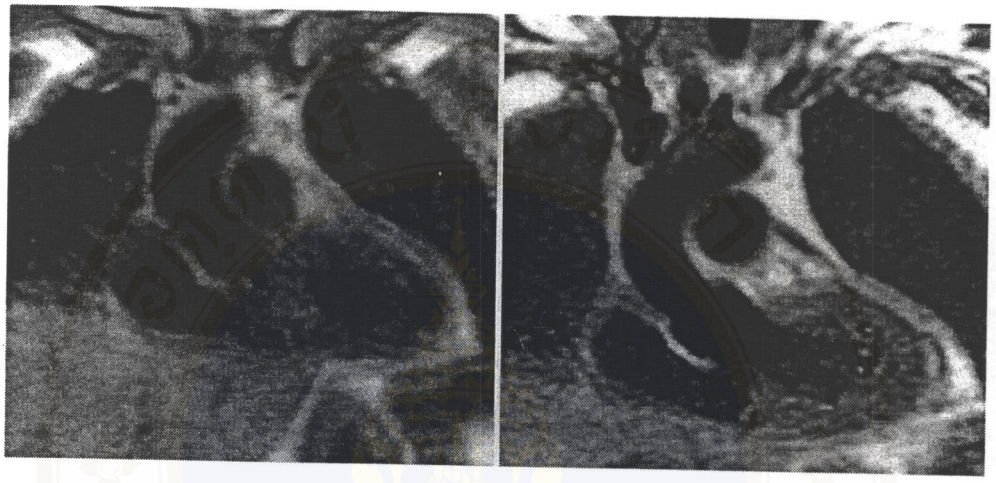

Figure D-15 Cardiac motion, The image on the left was acquired without and form of motion compensation techniques for cardiac motion although respiratory motion was compensated for. Notice the blurring of the cardiac structures. The image on the right was obtained using cardiac gating. The imaging sequence is triggered by the R-wave and data collection occurs during the same potion of the cardiac cycle for each TR period. This effectively eliminates cardiac motion (23).

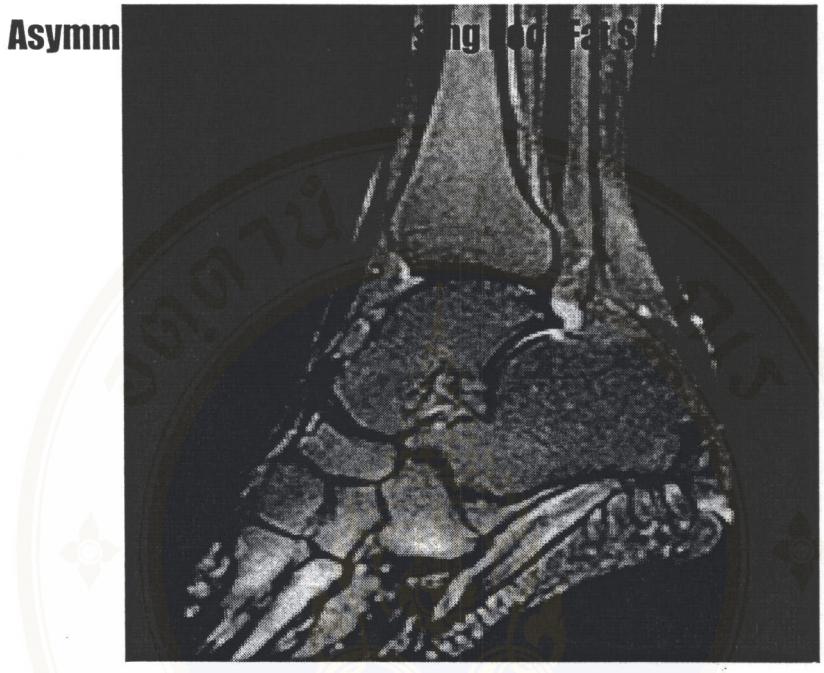

Figure D-16 Inhomogeneous Fat suppression, The image of ankle exhibits poor fat suppression due to asymmetric volume of this body part. The volume of the alters the magnetic field felt by the protons in the foot to a different degree than the smaller volume of the lower leg effecting the protons there. There is only a small band of tissue where the fat protons are precessing at frequency expected resulting in frequency selective fat saturation working only in that area. This can be corrected for by creating a more symmetric volume being imaged with water bags (23).

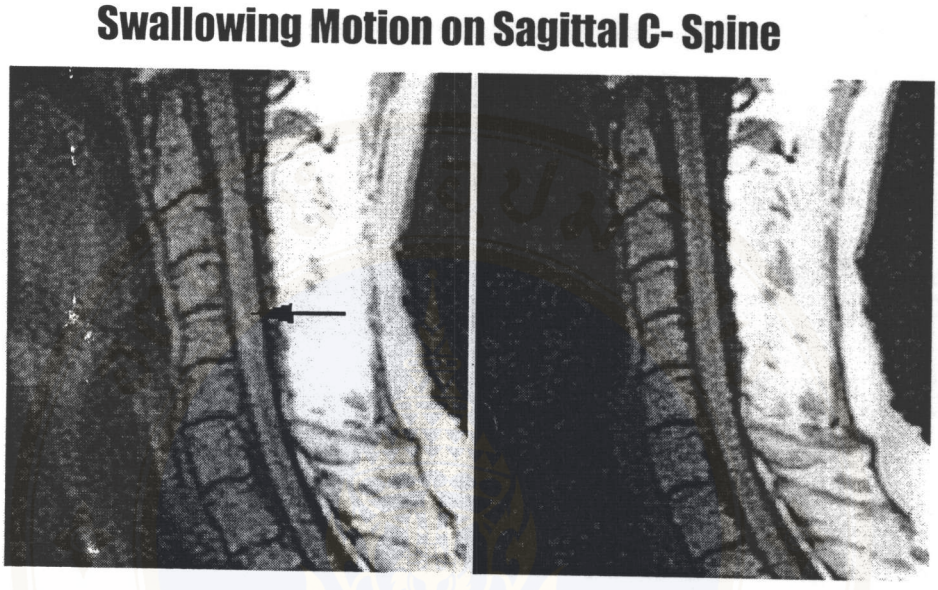

Figure D-17 swallowing motion. Any type of patient motion during a scan will cause artifacts to propagate in the phase direction (A to P in this case) The image on the left demonstrates the artifact generated by the patient swallowing while data was being obtained. Note the area of increased signal intensity in spinal cord. Applying presaturation RF pulses to anatomy that was generating the artifacts eliminated this artifact. Note how the anterior neck is well saturated and the absence of any artifacts in the image on the right (23).

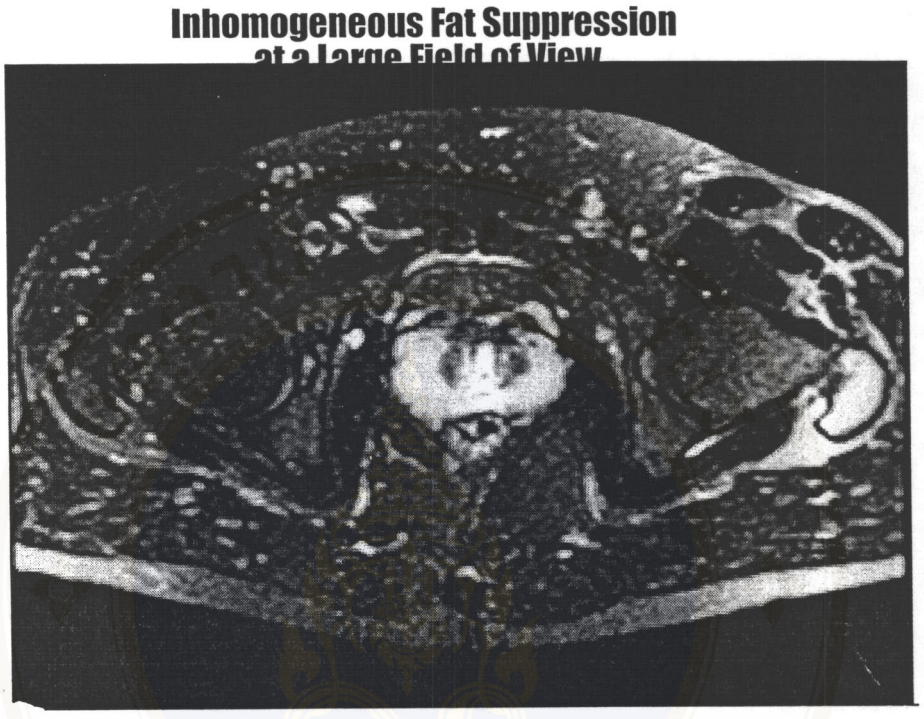

Figure D-18 Inhomogeneous fat saturation across large field of view. Frequency specific fat saturation pulse become less effective when the field of view is increased. The magnetic field homogeneity decrease as more tissue is imaged. As a result the precessional frequencies change across the imaging volume. Thus fat is precessing at the imaging volume. Thus fat is precessing at the expected frequency only in the center of imaging volume. It is best to use smaller field of views when applying fat saturation pulses.

Respiratory Motion in the Abdomen

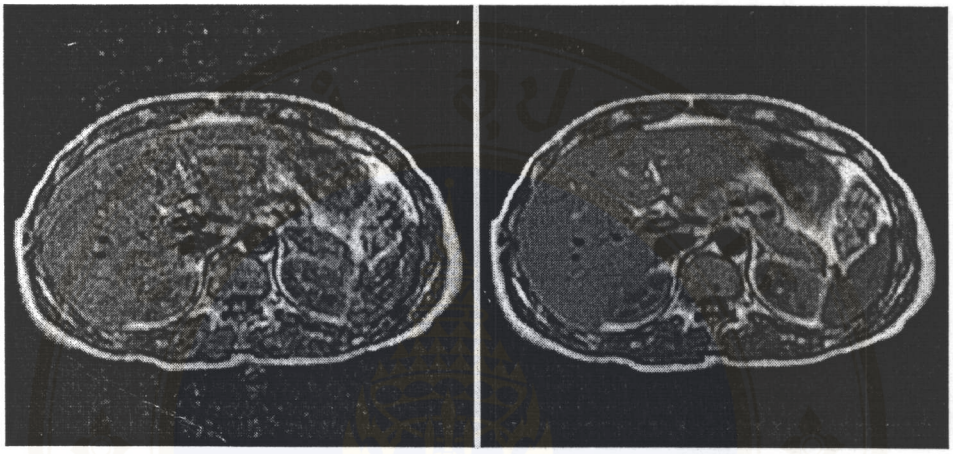

Figure D-19 the image on the left exhibits respiratory motion as blurring of the structures as well as motion-induced ghosting. By using multiple average motion can be reduced in the same way that multiple averages increase the signal to noise ratio. Noticeable motion averaging is seen when four average are obtained, six techniques and average is often as good as respiratory compensation higher averages will continue to improve image quality. The image on the right was obtained with 16 average

Partial Volume Averaging

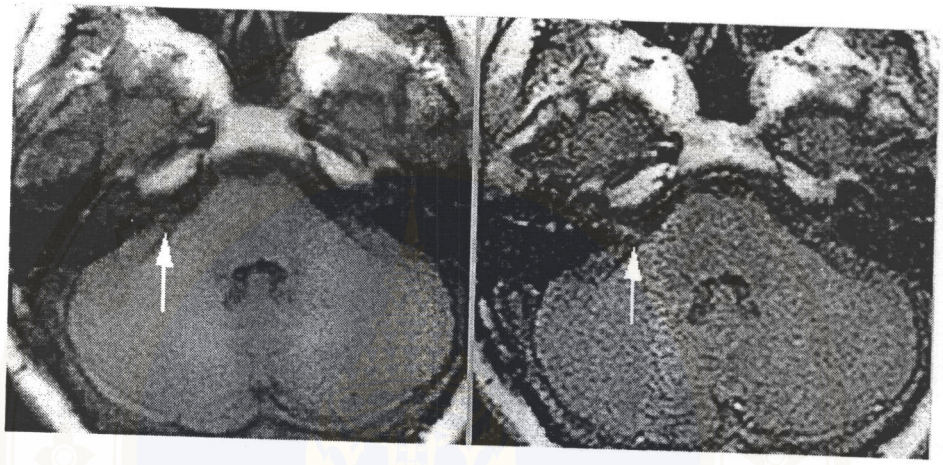

Figure D-20 These two axial T1-weighted image of the head were obtained at exactly the same location, yet the second image shows the VII and VIII cranial nerves while the first does not. The reason for the vanishing nerve is explained by partial volume averaging. The first slice was obtained with a thickness of 10 mm while the second was at a thickness of 3 mm. When a small structure is entirely contained within the slice thickness within the slice thickness with other tissue of differing signal intensity then the resulting signal displayed on the image is a combination of these two intensities. This may cause the small structure, to disappear. If the slice is the same thickness or thinner than the small structure, only that structures signal intensity is displayed on the image.

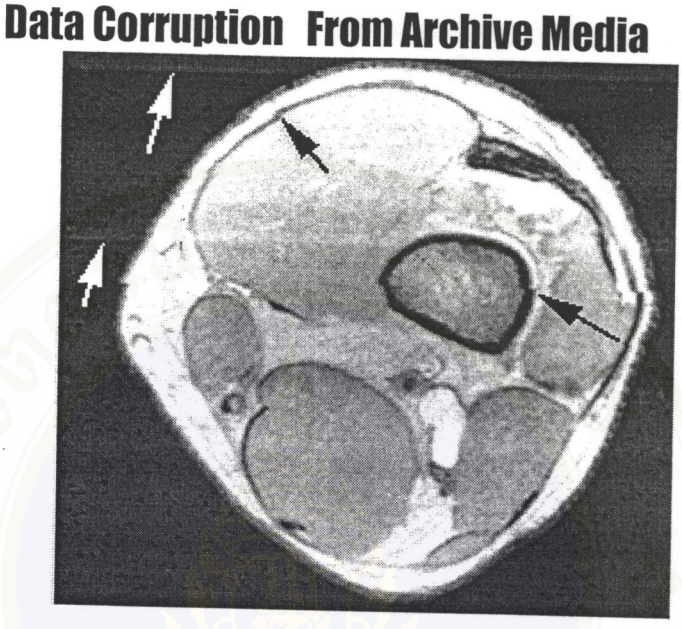

Figure D-21 Data corruption during read of optical disc, Although not actually an MRI artifact, these image appeared on MRI image on an MRI image. This appeared when data being read off an optical disc became corrupted. Note the two effect seen here. The white arrows indicate band arrows indicate areas where the intensity has been incorrectly interpreted while the back arrows indicate area where the horizontal position of the pixels has been incorrectly displayed. It is important to be able to differentiate between artifacts caused during an MRI scan from those caused by the associated hardware of an imaging system.

BIOGRAPHY

NAME	Mr Paitoon Maprakob
DATE OF BIRTH	3 Agust 1967
PLACE OF BRITH	Uttaradit, Thailand
INSTITUTIONS ATTENEDED	Mahidol University,1997-2000: Bachelor of Communication Arts (Public relation) Sukhothaithammathirat,1988-1991 Bachelor of Science (Radiological Technology) Mahidol University, 1995-1996: Master of Science (Radiological Science)
POSITION HELD & OFFICE	1986-Present, Dept of Radiology, Buddhachinaraj Hospital, Pittsanulok. Position : Radiological technologist